Nucleosynthesis

Bradley S. Meyer
Clemson University

Ernst Zinner
Washington University

Primitive meteorites contain nano- to micrometer-sized dust grains with large isotopic anomalies relative to the average solar system composition. These large anomalies convincingly demonstrate that the dust grains condensed in the outflow from their parent stars and survived destruction in the interstellar medium and solar-system processing to retain memory of the astrophysical setting of their formation. In addition to the dust grains, certain primitive refractory inclusions in meteorites also show isotopic anomalies, which suggests that the inclusions formed in the solar system from large collections of anomalous dust. Finally, the inferred presence of short-lived radioisotopes in the early solar nebula yields important clues about the circumstances of the Sun's birth. We review these topics in cosmochemistry and their implications for our ideas about stellar nucleosynthesis.

1. INTRODUCTION AND HISTORY

Today it is well established that all elements from C on up were made by stellar nucleosynthesis. After the Big Bang the universe consisted only of H and He and trace amounts of Li, Be, and B, and it was not until the formation of the first stars that the heavier elements came into existence. There exists some evidence now (e.g., *Umeda and Nomoto,* 2003) that the earliest stars, which started out with essentially only H and He, were very heavy. Such stars run through their evolution relatively rapidly (in millions of years) and produce nearly all the heavier elements by various nuclear processes in their hot interiors. They end their lives in gigantic explosions as supernovae that expel the newly synthesized elements in their ejecta into the interstellar medium (ISM), where they are mixed with interstellar gas. The next generation of stars incorporated these elements during their formation and the material in our galaxy underwent several such cycles before our solar system (SS) formed. In contrast to massive stars that become supernovae (SNe), stars with a mass less than ~8 $M_\odot$ experience a different history. They take hundreds of millions to billions of years to burn the H and He in their interior into C and O and in their late stages lose their outer envelopes in the form of stellar winds and planetary nebulae, thereby leaving behind a C-O white dwarf (WD) star that does not undergo further nuclear processes. The stellar wind and planetary nebula material are enriched in certain nuclei that were produced in hot shells on top of the WD.

When the SS formed it incorporated material from many different stellar sources: supernovae, late-type stars, and novae. This material was mixed extremely well so that the SS as a whole has a very uniform elemental and isotopic composition. Differences in elemental abundances among different chondrite groups are considered to reflect variations in the environment where their parent asteroids formed (*Palme,* 2000). However, major elemental differentiation occurred through planet formation and geological processes taking place on larger planetary bodies. Thus, terrestrial rocks have elemental compositions that are quite different from the overall mix from which the whole SS was made. In contrast, primitive meteorites to a large extent preserve the original composition of the SS. They originate from small asteroids that did not experience any planetary differentiation. Their elemental abundances agree very well with that of the Sun except for the volatile elements H, C, N, and O, the noble gases, and Li (*Anders and Grevesse,* 1989; *Grevesse et al.,* 1996). Since geological processes do not affect isotopic ratios very much (they introduce only some mass-dependent fractionation), the isotopic compositions of solar materials from different planetary bodies (Earth, Moon, Mars, and the parent bodies of different types of meteorites) are essentially identical. An exception are isotopic anomalies in certain elements that are due to the decay of radioactive isotopes. Some of these radioisotopes were short-lived, i.e., they existed only early in the SS and evidence for their decay products are found in early-formed SS solids.

Although stellar nucleosynthesis had been proposed before (*Hoyle,* 1946), in the early 1950s it was far from clear that most elements are synthesized in stars. The first observational evidence for stellar nucleosynthesis came from the discovery of the unstable element Tc in the spectra of S-stars (*Merrill,* 1952). A few years later in their classical papers, *Burbidge et al.* (1957) and *Cameron* (1957) established the theoretical framework for stellar nucleosynthesis. They proposed a scheme of eight nucleosynthetic processes taking place in different stellar sources under different con-

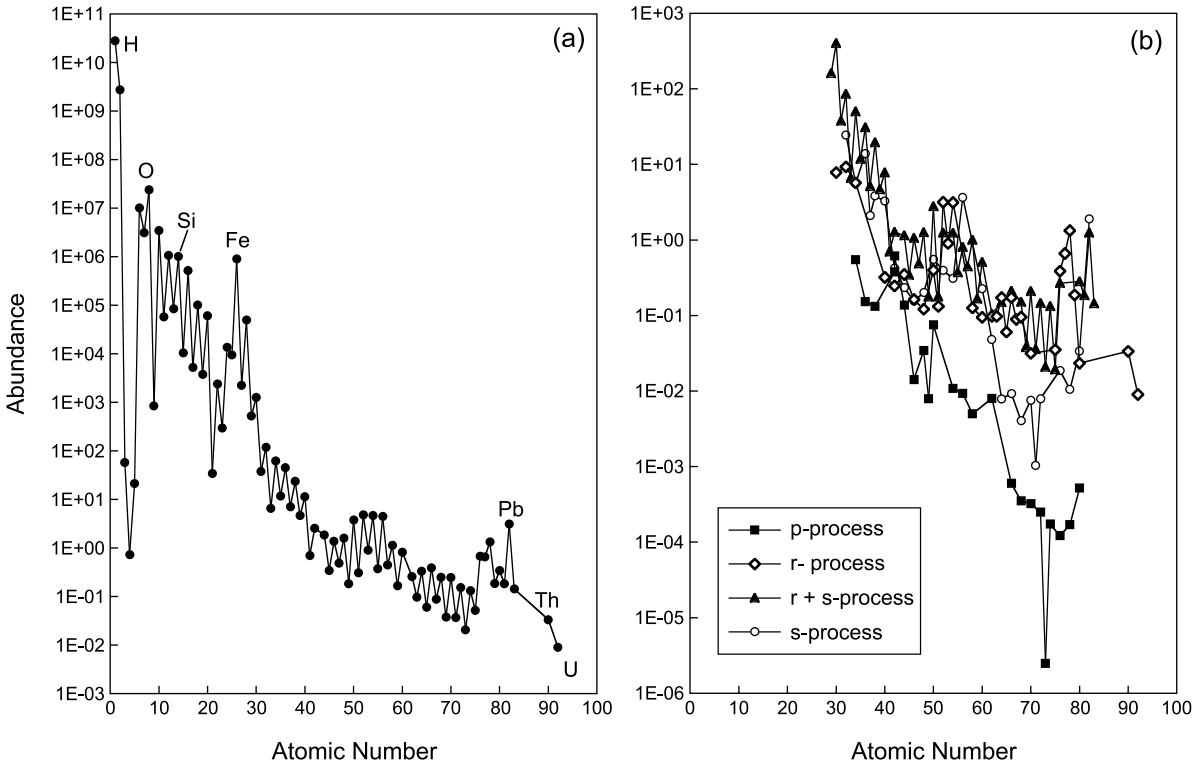

Fig. 1. **(a)** Abundances of the elements in the solar system (*Anders and Grevesse,* 1989). **(b)** Abundances of the nuclides of a given element produced by the p-, r-, and s-process, respectively.

ditions. One important motivation for this work was to explain regularities in the abundance of the nuclides in the SS (Fig. 1) as obtained by the study of meteorites (*Suess and Urey,* 1956). (For a table of the solar system abundances of the nuclides and a brief description of their principal nucleosynthesis production processes, the reader is invited to visit the Web site *http://nucleo.ces.clemson.edu/pages/solar_abundances/.*) While the SS represents only a grand average of many distinct stellar sources, the SS (sometimes also termed cosmic) abundances of the elements and isotopes (*Cameron,* 1973; *Anders and Grevesse,* 1989; *Grevesse et al.,* 1996; *Lodders,* 2003) became an important reference for astronomers. They remained the touchstone for testing models of stellar nucleosynthesis as two generations of nuclear astrophysicists tried to reproduce them (e.g., *Käppeler et al.,* 1989; *Timmes et al.,* 1995). The complete homogenization of all presolar material in a hot solar nebula (*Cameron,* 1962) seemed to be confirmed by the observation that the isotopic compositions of SS materials, including primitive meteorites, are very uniform. The prevalent view was that all solids had been vaporized and thus had lost all memory of their stellar sources, and that the solids we find now in primitive meteorites were produced by condensation from a well-mixed gas (*Grossman,* 1972).

The first hints that not all presolar material had been homogenized and some components found in primitive meteorites preserved a record of their presolar history came in the form of isotopic anomalies, i.e., deviations from the SS ratios, in the element H (*Boato,* 1954) and the noble gases Xe (*Reynolds,* 1960a) and Ne (*Black and Pepin,* 1969). However, these early signs were largely ignored, and it was not until the discovery of an ^{16}O excess (*Clayton et al.,* 1973), an isotopic anomaly in a major rock-forming element, in refractory inclusions (Ca-Al-rich inclusions, or CAIs) that the idea of the survival of presolar isotopic signatures was widely accepted. This discovery was followed by the discovery of anomalies in elements such as Ca, Ti, Cr, Fe, Zn, Sr, Ba, Nd, and Sm (for an overview see *Lee,* 1979, 1988; *Wasserburg,* 1987; *Clayton et al.,* 1988). Important was the realization that certain isotopic patterns represented distinct nucleosynthetic components. For example, Ba, Nd, and Sm in the FUN inclusion EK1-4-1 from the Allende meteorite (*McCulloch and Wasserburg,* 1978a,b) show an r-process signature and thus provided direct evidence for the distinct origin of the r- and s-process nuclides (see also *Begemann,* 1993). Another example is the correlated excesses and depletions of the neutron-rich (n-rich) isotopes ^{48}Ca and ^{50}Ti in the FUN inclusions EK1-4-1 and C-1 and in hibonite grains (*Lee et al.,* 1978; *Niederer et al.,* 1980; *Fahey et al.,* 1985; *Zinner et al.,* 1986) that indicate a separate nucleosynthetic process for the production of the n-rich isotopes of the Fe-peak elements. While some of these isotopic anomalies can be fairly large — ^{50}Ti excesses in hibonite grains range up to almost 30% (*Ireland,* 1990) — it has to be emphasized that the solids exhibiting these anomalies are of SS origin and only incorporated certain presolar components. This is

not only evidenced by the size of the effects that are generally much smaller than those expected for bona fide stellar material (*Begemann,* 1993), but also by the fact that other elements (e.g., O, Mg, Si) in CAIs carrying isotopic anomalies in certain elements have essentially normal isotopic compositions.

In addition to isotopic anomalies of nucleosynthetic origin, solids from primitive meteorites show isotopic effects due to the decay of short-lived, now extinct radioisotopes. The first evidence for the presence of a short-lived isotope at the time of SS formation came from excess ^{129}Xe (*Reynolds,* 1960b) and its correlation with ^{127}I (*Jeffery and Reynolds,* 1961), indicating the decay of ^{129}I ($T_{1/2}$ = 16 m.y.). Another relatively long-lived radionuclide, ^{244}Pu ($T_{1/2}$ = 82 m.y.), was identified from excesses in the heavy Xe isotopes resulting from fission (*Rowe and Kuroda,* 1965) and subsequently from fission tracks (*Wasserburg et al.,* 1969). While the observed abundances of these two radioisotopes could be attributed to their steady-state production in the galaxy, the later discovery of evidence for isotopes with much shorter half-lives indicated that the time between their nucleosynthetic production and the formation of the first SS objects could not have been much longer than 1 m.y. This made it necessary to invoke a stellar event (a supernova or an asymptotic giant branch, or AGB, star) shortly preceding SS formation and possibly even triggering it (*Cameron and Truran,* 1977). These short-lived isotopes include ^{26}Al ($T_{1/2}$ = 0.73 m.y.) (*Lee et al.,* 1976, 1977), ^{53}Mn ($T_{1/2}$ = 3.7 m.y.) (*Birck and Allègre,* 1985), ^{60}Fe ($T_{1/2}$ = 1.5 m.y.) (*Shukolyukov and Lugmair,* 1993), and ^{41}Ca ($T_{1/2}$ = 0.1 m.y.) (*Srinivasan et al.,* 1994). Short-lived isotopes contain several types of important information. They not only can serve as chronometers for early solar system (ESS) history (see *Chaussidon and Gounelle,* 2006), but their abundances at the time of SS formation provide information about their nucleosynthetic production, throughout the galaxy as well as in a late stellar event, and possibly even about the mechanism of SS formation.

While the previously discussed types of isotopic anomalies (anomalies of nuclear origin and from the decay of short-lived radionuclides) are carried by solids that themselves formed in the SS, primitive meteorites contain also grains that are of presolar origin. These grains condensed in the outflows of late-type stars and supernova and nova ejecta and thus represent true stardust. Their stellar origin is indicated by their isotopic compositions, which are completely different from those of the SS and, for some elements, cover extremely wide ranges. They can be located in and extracted from their parent meteorites and studied in detail in the laboratory. The finding of an anomalous Ne component in meteorites (*Black and Pepin,* 1969) prompted *Black* (1972) to propose presolar solid carriers, but it took another 15 years until presolar grains were isolated and identified by E. Anders and colleagues at the University of Chicago. These scientists were led by the presence of anomalous ("exotic") noble gas components in Ne and Xe to subject primitive meteorites to increasingly harsher chemical dissolution and physical separation procedures in order to track the gases' solid carriers (*Amari et al.,* 1994). This approach, termed "burning down the haystack to find the needle," resulted in the discovery of presolar diamond, the carrier of Xe-HL (*Lewis et al.,* 1987); silicon carbide (SiC), the carrier of Ne-E(H) and Xe-S (*Bernatowicz et al.,* 1987; *Tang and Anders,* 1988b); and graphite, the carrier of Ne-E(L) (*Amari et al.,* 1990). Subsequently, other presolar grain types, not tagged by exotic noble gases, were identified by isotopic analysis of individual grains in the ion microprobe. These types include silicon nitride (Si_3N_4); oxides such as corundum, spinel, and hibonite; and silicates. With the exception of diamonds, which are too small to be analyzed as single grains, the presolar grains were found to be anomalous in *all* their isotopic ratios and it is this feature that identifies them as samples of stellar material. Their isotopic compositions thus provide direct information on nucleosynthetic processes in their stellar sources.

Besides isotopic anomalies of nucleosynthetic origin, meteorites and especially interplanetary dust particles contain isotopic signatures that are apparently caused by chemical processes. These include D and ^{15}N excesses that indicate an origin in dense molecular clouds (but possibly also in the solar nebula) where ion-molecule reactions at low temperature can lead to large isotopic fractionation effects (*Messenger and Walker,* 1997; *Messenger,* 2000). It is ironic that the ^{16}O enrichments in CAIs, which led to the acceptance of the existence of presolar material in meteorites and for which a nucleosynthetic origin has been invoked (*Clayton,* 1978), might actually be of chemical origin (*Thiemens and Heidenreich,* 1983; *Clayton,* 2002). These effects are covered in *Robert* (2006) and *Nuth et al.* (2006). In addition to these anomalies, there are also possible isotopic effects of irradiation in the SS such as the production of short-lived ^{10}Be (*McKeegan et al.,* 2000). These are discussed in *Robert* (2006). There are also all kinds of isotopic variations in meteorites such as isotopic anomalies of N in iron meteorites (*Murty and Marti,* 1994), for which an unambiguous explanation has not been found. We will not treat them here.

In this chapter we will provide a general introduction to nucleosynthesis and stellar evolution, followed by the discussion of nuclear anomalies in CAIs and other materials, short-lived isotopes in the ESS, and presolar grains. Since the first edition of *Meteorites and the Early Solar System* (*Kerridge and Matthews,* 1988), these last two topics have seen significant advances, and the study of presolar grains in particular is essentially a completely new field. They will therefore receive most of our attention.

2. REVIEW OF NUCLEOSYNTHESIS AND STELLAR EVOLUTION

Stars live most of their lives in hydrostatic equilibrium, the stable configuration in which the stellar pressure supports the star against its self-gravity. These stable states, however, belie the constant struggle stars endure to maintain this equilibrium: The light that we see from their sur-

faces carries away energy and lessens the internal pressure, and the star must replenish this lost energy. By the turn of the twentieth century, it was becoming clear that no then-known energy source could account for the age and luminosity of the Sun. Work by Helmholtz, Lord Kelvin, and others showed that energy radiated by gravitational collapse could only sustain the Sun's luminosity for some tens of millions of years. This clearly conflicted with geological data, which indicated an age of billions of years for Earth. Rutherford's work on nuclear transmutations suggested a resolution of this problem, namely, that the centers of stars were intense furnaces in which nuclear reactions converted rest mass energy of nuclei into heat to replenish the energy lost from the star by radiation and maintain the star's balance between gravity and pressure. By 1939, Bethe and collaborators (*Bethe and Critchfield,* 1938; *Bethe,* 1939) had worked out the reactions responsible for energy generation by H burning in stars in general and in the Sun in particular, and the connection between stars and nuclear reactions had been firmly established.

In 1946, Hoyle turned this early attention on the role of nuclear reactions in stellar energy generation to their consequences for genesis of the chemical elements (*Hoyle,* 1946). This work led to the classic papers of the 1950s that laid out the essential framework of stellar nucleosynthesis (*Hoyle,* 1954; *Burbidge et al.,* 1957; *Cameron,* 1957). In particular, *Burbidge et al.* (1957), in their seminal paper known as *B²FH*, classified and named the principal processes by which nuclei form in stars, and because their terminology has proven so useful, we largely continue to use it today. In what follows, we review the basics of stellar evolution and nucleosynthesis as we currently understand them. The goal is to set the stage for our discussion of extinct radioisotopes and isotopic effects in presolar grains and primitive SS minerals. For the sake of brevity, our review must necessarily only touch on the key points. The interested reader may turn to any number of recent reviews for further information (e.g., *Wallerstein et al.,* 1997; *Busso et al.,* 1999; *Woosley et al.,* 2002).

2.1. The Main Stages of Hydrostatic Stellar Evolution and Nucleosynthesis

In their hydrostatic phases, stars consume nuclear fuel to replenish energy lost by radiation. The evolution proceeds through a sequence of burning stages as the ashes from the previous stage serve as the fuel for the subsequent phase. Because the temperature is usually highest in the stellar core, a stellar burning phase first occurs there. Once the fuel is exhausted, the star contracts until burning of that same fuel commences in a shell surrounding the core. Continued contraction ignites the next burning phase in the core. This process repeats itself and each progressive nuclear burning cycle occurs at higher temperature and on a shorter timescale than the previous one. Finally, the core becomes sufficiently dense that pressure from the degenerate electrons can support the star or nuclear reactions can no longer release energy. We now summarize the principal hydrostatic burning stages.

2.1.1. Hydrogen burning. The initial nuclear fuel available to stars is H, and we know that *H burning*, in which four H nuclei are converted into He, is the principal energy source in main sequence stars. In the Sun, this proceeds via the PP chains (see Table 1) in which the p + p reaction produces a deuteron via a weak decay. Deuterium subsequently captures a proton to make ^{3}He, which, in the principal PP chain (PPI), captures another ^{3}He to make ^{4}He and two protons. In stars of somewhat higher mass, core temperatures are greater and the burning proceeds by the CNO bicycle in which the burning is catalyzed by capture of protons by isotopes of C, N, and O. In these cycles, the ^{14}N(p,γ)^{15}O reaction is typically the slowest of these reactions at H-burning temperatures, thus CNO-burning material is characteristically enriched in ^{14}N. It is also worth noting for the presolar grains that, at the typical temperatures of CNO burning (some tens of millions of degrees Kelvin), the nuclear flows tend to enhance the ^{13}C/^{12}C and ^{17}O/^{16}O abundance ratios over their starting values. Material processed by core H burning is convectively mixed to the stellar surface in the in so-called dredge-up processes during later burning stages.

Our basic understanding of the key reaction sequences in H burning has remained largely unchanged since *B²FH*, although we now have a better understanding of the related side reactions in H burning that generate the neutrinos seen in Earth-based detectors and that make isotopes such as ^{17}O and ^{26}Al. The most significant advances since 1957, however, have been in experimental nuclear physics, which have led to improvements in our knowledge of the rates for many of the nuclear reactions involved and their consequences for predicted neutrino fluxes from the Sun and other stars. Interestingly, the reactions occurring in the center of the Sun take place at lower energies than are easily measured in laboratories on Earth. This is due to low count rates and to atomic interactions in the targets that mask the effects of the reaction; thus, in most cases, experimental data must be extrapolated down to energies appropriate for the centers of stars. In order to counter some of these difficulties, experimentalists are moving some of their experiments underground to reduce background due to cosmic rays (*Bonetti et al.,* 1999).

2.1.2. Helium burning. After the star has consumed the H in its core, it contracts and heats. It will begin burning H in a shell. Once the core gets hot enough, it will begin *He burning,* which produces ^{12}C from ^{4}He in the triple-α process and ^{16}O via ^{12}C(α,γ)^{16}O. Core He burning in stars typically occurs at about (1–3) × 10^{8} K. *B²FH* envisioned He burning also producing ^{20}Ne and possibly ^{24}Mg, but we now know that C burning is largely responsible for ^{20}Ne and C and Ne burning for ^{24}Mg. Interestingly, the ^{12}C(α,γ)^{16}O reaction remains rather uncertain, and this uncertainty strongly affects stellar evolution models because of the reaction's importance in determining the central ^{12}C and ^{16}O abundances, which, in turn, strongly affect the subsequent evolution of

TABLE 1. Principal burning stages in hydrostatic stellar evolution.

Stage	Key Reactions	Important Products	Notes
Hydrogen	PPI: $^{1}H + {}^{1}H \rightarrow {}^{2}H + \gamma$ $^{2}H + {}^{1}H \rightarrow {}^{3}He + \gamma$ $^{3}He + {}^{3}He \rightarrow {}^{4}He + 2{}^{1}H$	^{4}He	In the solar interior, PP chain percentages are PPI (85%), PPII (15%), PPIII (0.02%). The percentages are expected to be somewhat different in other stars.
	PPII: $^{3}He + {}^{4}He \rightarrow {}^{7}Be + \gamma$ $^{7}Be + e^{-} \rightarrow {}^{7}Li + \nu$ $^{7}Li + {}^{1}H \rightarrow {}^{4}He + {}^{4}He$	^{4}He	
	PPIII: $^{3}He + {}^{4}He \rightarrow {}^{7}Be + \gamma$ $^{7}Be + {}^{1}H \rightarrow {}^{8}B + \gamma$ $^{8}B \rightarrow 2{}^{4}He + e^{+} + \nu$	^{4}He	
	CN cycle: $^{12}C + {}^{1}H \rightarrow {}^{13}N + \gamma$ $^{13}N \rightarrow {}^{13}C + e^{+} + \nu$ $^{13}C + {}^{1}H \rightarrow {}^{14}N + \gamma$ $^{14}N + {}^{1}H \rightarrow {}^{15}O + \gamma$ $^{15}O \rightarrow {}^{15}N + e^{+} + \nu$ $^{15}N + {}^{1}H \rightarrow {}^{12}C + {}^{4}He$	^{4}He, ^{14}N, ^{26}Al	Together, the CN and NO cycles comprise the CNO bicycle. During shell burning of H in the CN and NO cycles temperatures are high enough to produce ^{26}Al via $^{25}Mg + {}^{1}H \rightarrow {}^{26}Al + \gamma$
	NO cycle: $^{15}N + {}^{1}H \rightarrow {}^{16}O + \gamma$ $^{16}O + {}^{1}H \rightarrow {}^{17}F + \gamma$ $^{17}F \rightarrow {}^{17}O + e^{+} + \nu$ $^{17}O + {}^{1}H \rightarrow {}^{15}N + {}^{4}He$	^{4}He, ^{14}N, ^{17}O, ^{26}Al	The NO cycle operates at higher temperature than the CN cycle and provides a leakage out of the CN cycle.
Helium	$^{4}He + {}^{4}He + {}^{4}He \rightarrow {}^{12}C + \gamma$ $^{12}C + {}^{4}He \rightarrow {}^{16}O + {}^{4}He$ $^{14}N + {}^{4}He \rightarrow {}^{18}F + \gamma$ $^{18}F \rightarrow {}^{18}O + e^{+} + \nu$ $^{18}O + {}^{4}He \rightarrow {}^{22}Ne + \gamma$ $^{22}Ne + {}^{4}He \rightarrow {}^{25}Mg + n$	^{12}C, ^{16}O, ^{18}O, ^{22}Ne ^{25}Mg, s-process isotopes	End burning stage of stars under 8 $M_{\odot}$.
Carbon	$^{12}C + {}^{12}C \rightarrow {}^{24}Mg^{*}$ $^{24}Mg^{*} \rightarrow {}^{20}Ne + {}^{4}He$ $\rightarrow {}^{23}Na + {}^{1}H$ $\rightarrow {}^{24}Mg + \gamma$	^{20}Ne, ^{23}Na, ^{24}Mg	End burning stage of stars in mass range 8–10 $M_{\odot}$.
Neon	$^{20}Ne + \gamma \rightarrow {}^{16}O + {}^{4}He$ $^{20}Ne + {}^{4}He \rightarrow {}^{24}Mg + \gamma$	^{16}O, ^{24}Mg	
Oxygen	$^{16}O + {}^{16}O \rightarrow {}^{32}S^{*}$ $^{32}S^{*} \rightarrow {}^{28}Si + {}^{4}He$ $\rightarrow {}^{31}P + {}^{1}H$ $\rightarrow {}^{32}S + \gamma$	^{28}Si, ^{31}P, ^{32}S	QSE clusters develop
Silicon	$^{28}Si + {}^{28}Si \rightarrow {}^{54}Fe + 2{}^{1}H$ $^{28}Si + {}^{28}Si \rightarrow {}^{56}Ni$ $^{56}Ni \rightarrow {}^{56}Co + e^{+} + \nu$ $^{56}Co \rightarrow {}^{56}Fe + e^{+} + \nu$	Fe-peak isotopes ^{56}Fe, ^{54}Fe	$^{28}Si + {}^{28}Si$ are effective reactions. The true character of silicon burning is a QSE shift from ^{28}Si to iron isotopes.

the star through advanced burning stages. Determining the $^{12}C(\alpha,\gamma)^{16}O$ reaction rate is a subject of intense experimental study (*Kunz et al.,* 2002).

After He is exhausted in the core, the star will begin He burning in a shell outside the He-exhausted core. In stars of mass greater than about 8 $M_{\odot}$, this proceeds in a relatively quiescent fashion. For lower-mass stars, however, which undergo He-shell burning during their ascent of the asymptotic giant branch (AGB) in the Hertzsprung-Russell diagram, the densities will be high enough that electron de-

generacy provides a significant component of the overall pressure. This means that the He shells will undergo periodic shell flashes, which drive convection and mix the material in the shell with the overlying stellar envelope.

Helium burning is the end stage of burning for stars of mass below 8 $M_\odot$. The strong pressure from degenerate electrons means that the star can support itself against gravity without having to continue nuclear fusion reactions in its core. As shell burning continues on top of the degenerate C/O core, strong stellar winds also occur and drive off mass in the planetary nebula phase. Once the envelope of the star is completely lost, a degenerate C/O WD is left behind to cool and fade away. The star may brighten again if accretion from a companion star drives explosive H burning on the surface, which we see as a *nova.* If enough mass has accreted, the C and O may burn explosively and completely disrupt the star. We believe such explosions are the outbursts we see as *Type Ia supernovae.*

From the SS abundances, we know that two main neutron-capture processes are responsible for most of the elements heavier than Fe. These are the s- and r-processes, each of which contributed about one-half the SS's supply of the heavy nuclei (see Fig. 1b). It is during He burning that neutron-liberating reactions can occur and drive the s-process of nucleosynthesis. The s in s-process denotes the fact that neutron densities are sufficiently low to make neutron captures *slow* compared to β decays. This means that the nuclear flow is always near stable nuclei, in contrast to the r-process, in which the neutron density is high and neutron captures are typically much more *rapid* than β decays (see below).

The s-process has two principal components, the weak and main components. The weak component is the dominant producer of s-process isotopes up to mass number A = 90. It occurs primarily during core He burning in massive stars. Here, ^{14}N left over from H burning reacts with two α particles to form ^{22}Ne. The reaction ^{22}Ne(α,n)^{25}Mg liberates neutrons that then may be captured by preexisting seed nuclei.

The main component of the s-process occurs during H- and He-shell burning in the AGB phase of a low-mass star. In this phase, the star has developed an inert C/O core from previous He burning. Most of the time H burning proceeds relatively quiescently in a shell at the base of the H envelope. As the He ashes from this burning build up, however, the temperature and density in the He intershell between the H envelope and C/O core rise and the He ignites in a thermal pulse. This drives a convective mixing of the He intershell and temporarily extinguishes the H burning above the He intershell. After the brief pulse has occurred, the C and O ashes settle onto the core, thereby increasing its mass, and the H-burning zone reignites. Dredge-up transports matter from inner to outer stellar layers after the pulse and carries the products of shell burning into the envelope where they may be observed. This process repeats itself roughly every 1000 to 10,000 yr. In this way, the star progressively grows its C/O core and enriches its envelope with heavy elements. The reader is referred to Fig. 5 in the review by *Busso et al.* (1999) and the attendant discussion for more details of this rich phase of a low-mass star's life.

It is in the He intershell that the main component of the s-process most probably occurs. The essential idea is that protons leak down into the shell from the H-rich overlying zones by a process that is still not well understood since an entropy gradient exists between the He and H layers that should prevent such mixing. A "^{13}C pocket" forms as these protons are captured by abundant ^{12}C. Once the shell heats up sufficiently, the reaction ^{13}C(α,n)^{16}O occurs. The neutrons thus liberated are captured by preexisting nuclei. When the thermal pulse occurs, the ^{22}Ne(α,n)^{25}Mg reaction marginally ignites, which gives a high-temperature but short-duration burst of neutrons. Careful recent work has shown that the He shell is radiative (i.e., the heat transfer to the star's outer layers occurs through radiation; this is in contrast to convective transfer) in the phase in which the ^{13}C is burning but convective during the burning of the ^{22}Ne (*Straniero et al.,* 1995; *Gallino et al.,* 1998; *Busso et al.,* 1999). The isotopic ratios of presolar SiC grains confirm this double-neutron-exposure picture (see sections 5.4.1 and 5.4.2).

2.1.3. Carbon burning. Upon exhaustion of He, a star will next begin to burn C at a temperature near (0.8–1) × 10^9 K by the reaction $^{12}C + {}^{12}C \rightarrow {}^{24}Mg^*$, where ^{24}Mg* is an excited nucleus of ^{24}Mg. The ^{24}Mg* mostly decays into ^{20}Ne and an α particle; thus, C burning is the major producer of ^{20}Ne in the universe. Light particles released during C burning can also be captured by heavier species, thereby altering their abundances (e.g., *The et al.,* 2000).

Once C is exhausted in the core, shell C burning develops. The amount of ^{12}C left over from He burning strongly affects the nature of the shell C burning (e.g., *Imbriani et al.,* 2001; *El Eid et al.,* 2004) which also affects the later stellar burning stages. For stars in the roughly 8–10 $M_\odot$ range, degeneracy pressure dominates thermal pressure after C burning, and, after the star loses its envelope, an O/Ne/Mg WD is left behind.

2.1.4. Neon burning. The abundant ^{20}Ne remaining after C burning is the next nuclear fuel in the star's life. As *B^2FH* recognized, ^{20}Ne burns in the following sequence. First, a ^{20}Ne nucleus disintegrates via ^{20}Ne(γ,α)^{16}O. This is an endothermic reaction; however, another ^{20}Ne nucleus may capture the α particle thus liberated in an exothermic reaction to produce ^{24}Mg: ^{20}Ne(α,γ)^{24}Mg. The net exothermic reaction in *Ne burning* is thus $^{20}Ne + {}^{20}Ne \rightarrow {}^{16}O + {}^{24}Mg$, and it is the major producer of ^{24}Mg. Neon burning typically occurs at a temperature near 1.5 × 10^9 K.

2.1.5. Oxygen burning. As a star contracts and heats to temperatures in excess of about 1.8 × 10^9 K, O burns by the reaction $^{16}O + {}^{16}O \rightarrow {}^{32}S^*$, where ^{32}S* is an excited nucleus of ^{32}S. The ^{32}S* predominantly decays into ^{28}Si and an α particle, though deexcitation to ^{32}S also occurs; thus, ^{28}Si and ^{32}S are the principal products of *O burning*.

Upon exhaustion of O in the core, the star begins burning O in a shell. At this point, the structure of the massive star is quite complex: The O-burning shell is surrounded by Ne-,

C-, He-, and H-burning shells, and all the shells are typically convective. Oxygen-shell burning is the first of these phases in which the nuclear burning timescales become comparable to the convective timescales, and the standard treatment of convective burning breaks down. Detailed models show that the burning is rather inhomogeneous as convective blobs burn before they have a chance to mix turbulently with their surroundings (*Bazan and Arnett,* 1998). Realistic treatment of this multidimensional burning still lies at the frontiers of computational astrophysics, and we must await further advances to see all the implications for nucleosynthesis.

2.1.6. Silicon burning. At the end of O burning, the matter is dominated by ^{28}Si and ^{32}S. It is also slightly neutron rich due to weak interactions that occurred during O burning. As the star contracts further, *Si burning* is the next stage in the star's life. The mechanism for Si burning is more complicated than that for the previous stages because the high charges of the Si and S isotopes prevent them from interacting directly. In Si burning, disintegration reactions break some of the nuclei down to lighter nuclei and neutrons, protons, and α particles. The remaining nuclei capture these light particles to produce heavier isotopes (up to Fe and Ni). At the conditions present in Si burning, the nuclear reactions are sufficiently fast that nuclei begin to form equilibrium clusters, i.e., subsets of isotopes in equilibrium under exchange of light particles. As the temperature and density rise, the clusters merge into larger clusters until a full quasi-statistical equilibrium (QSE) develops. A full QSE is the condition in which all nuclear species heavier than C are in equilibrium under exchange of light particles (*Bodansky et al.,* 1968; *Meyer et al.,* 1998a). At still higher temperatures, even the three-body reactions that assemble heavy nuclei from light ones, namely, ^{4}He + ^{4}He + ^{4}He $\rightarrow$ ^{12}C and ^{4}He + ^{4}He + n $\rightarrow$ ^{9}Be followed by ^{9}Be + ^{4}He $\rightarrow$ ^{12}C + n, become fast enough to establish a full nuclear statistical equilibrium (NSE), the condition in which all nuclear species are in equilibrium under exchange of light particles. In such equilibria, nuclei with strong nuclear binding win out in the struggle for abundance. These are typically the Fe and Ni isotopes. Further nuclear reactions will not release binding energy; hence, when the star has developed an Fe core, it has reached the end of its hydrostatic equilibrium.

Table 1 summarizes the main hydrostatic stages of stellar evolution and some of the key products. We now turn our attention to explosive burning.

2.2. Explosive Nuclear Burning

Explosive burning occurs at higher temperatures and on shorter timescales than the corresponding hydrostatic burning phases. For our purposes, the explosive events we consider are either (1) thermonuclear, in which the nuclear reactions themselves deposit energy too quickly for the system to readjust itself hydrodynamically and allow the burning to take place in a steady fashion; or (2) gravitational, in which part of the star falls down a gravitational well and transfers energy to the remaining layers, which may be ejected. Novae and Type Ia supernovae are of the first type; core-collapse (Type II, Ib, Ic) supernovae are of the second type.

2.2.1. Novae. When WD stars accrete material from a companion star, which is usually a main-sequence star, that accreted matter can ignite under degenerate conditions and burn explosively. The resulting outburst is visible as a *nova.* The accreted matter is mostly a mix of H and He, so the burning is typically explosive H burning, which means that the important products, such as ^{15}N, ^{22}Na, and ^{26}Al, are from proton captures on CNO nuclei. The burning is usually sufficiently energetic to drive some matter out of the gravitational well of the WD and into interstellar space. Moreover, the burning can drive some mixing, which may draw underlying WD matter into the ejecta. The composition of the WD (i.e., whether it is a C/O or O/Ne/Mg WD) may be reflected in the outflow from the star.

2.2.2. Type Ia supernovae. The classification Type I for supernovae is observational and indicates that the ejecta show little H in their spectra. We are now confident that Type Ia supernovae are thermonuclear disruptions of WD stars. If a C/O WD has accreted enough mass, the pressure and temperature can rise high enough to cause the C and O making up the star to fuse. This happens under highly degenerate conditions, so the pressure is insensitive to changes in temperature. Energy deposition increases the temperature further, leading to an increased rate for the nuclear reactions and energy generation; thus, a thermonuclear runaway occurs. This eventually leads to the disruption of the entire star. Because the temperatures become high enough in the explosion to drive the C and O into Fe and Ni isotopes, Type Ia supernovae are prodigious producers of ^{56}Fe and other Fe-peak isotopes. Furthermore, because they are fairly uniform in their light curve characteristics, they have become preferred standard candles in astronomy (*Phillips,* 2003). Observation of these standard candles has led to the astonishing conclusion that the expansion of our universe is in fact accelerating (*Riess et al.,* 1998; *Perlmutter et al.,* 1999).

The literature frequently discusses Type Ia as either deflagrations or detonations. The difference between these two types of events is that in deflagrations the burning front is subsonic while in detonations it is supersonic. Because the flame is subsonic in a deflagration, the matter ahead of the front has a chance to adjust itself before the flame arrives; therefore deflagrations tend to have lower temperatures than detonations. This allows deflagrations to burn less of their matter into Fe, which leaves more Si and S in the ejecta. Detonations, on the other hand, burn more matter into Fe. Spectroscopy on Type Ia supernovae thus yields insights into the nature of the burning front in the explosion. Such spectroscopy has suggested that a plausible scenario for Type Ia events is that of a deflagration turning into a detonation. Recent work has demonstrated the complicated manner in which such a transition may occur (*Plewa et al.,* 2004).

It is also possible that massive WD stars undergo accretion-induced collapse (AIC) directly to a neutron star and

explode in a core-collapse supernova (see the next section). Because of the lack of H in their spectra, these would be Type I (perhaps Type Ic) supernovae. Some nucleosynthetic constraints exist on this scenario (e.g., *Woosley and Baron,* 1992), but more work clearly needs to be done. There is interesting speculation that such explosions could be the site of r-process nucleosynthesis (*Qian and Wasserburg,* 2003).

2.2.3. Core-collapse supernovae. Massive stars die in the second type of explosion, the gravitational explosion mentioned above. The literature often refers to such supernovae as Type II, Ib, or Ic, which are spectral classifications based on the light curve (*Filippenko,* 1997). Since the core of the star has already evolved to Fe, no further useful fuel remains. A combination of disintegrations and electron captures initiate the sudden collapse of the core. The inner part of the core collapses subsonically, thus when it reaches nuclear matter density, the pressure rises dramatically due to nucleon-nucleon interactions and causes the collapse to halt and the core to "bounce." The outer part of the collapsing core, on the other hand, falls in supersonically; thus, it does not receive the signal from the inner core to cease collapsing and it crashes onto the inner core. This highly nonadiabatic process generates a shock, which works its way out through the remainder of the star, expelling these layers into the interstellar medium. Current SN models show that the energy lost by the shock in traversing the outer part of the Fe core causes it to stall. The outward motion must be regenerated.

Left behind the shock is an extremely dense proto-neutron star at temperatures of tens of billions of degrees. This star cools over a timescale of seconds by emission of neutrinos, which are the only particles that can escape the dense core. The current thinking is that these neutrinos deposit energy behind the stalled shock and thereby provide the push to revive its outward motion (e.g., *Colgate and White,* 1966; *Bethe and Wilson,* 1985; *Burrows,* 2000).

As the shock traverses the outer layers of the star, it compresses and heats them. This initiates explosive burning in these stellar shells, thereby modifying the composition established by the previous hydrostatic burning. The different presupernova and explosive burning phases give rise to widely varying compositions in the ejecta. The reader may find it useful to keep in mind the "onion-skin" picture, such as that in Fig. 1 of *Meyer et al.* (1995), although the true nature of the ejecta is probably more complicated.

We now discuss some of the particular explosive burning phases in the shells. For detailed output from modern stellar models, we recommend that the interested reader visit *http://www.nucleosynthesis.org* and *http://www.ces.clemson.edu/physics/nucleo/pages/cugce*.

2.2.4. Explosive silicon burning. Shock heating of the Si-rich layer drives explosive Si burning. In the innermost regions, the heating is sufficient for the matter to achieve NSE. The dominant products are Fe and Ni isotopes; however, the expansion and cooling is sufficiently rapid to leave a large abundance of free α particles. This expansion is thus known as the *α-rich freezeout* from NSE. Some reassembly of the free α does occur in the late stages of the freeze-out, which makes abundant ^{44}Ti, among other interesting isotopes.

In the outer layers of the Si shell, the matter is less heated from shock passage. The nuclear burning does not achieve full NSE, though it can reach QSE. This is a principal site for production of the short-lived radioisotope ^{53}Mn.

2.2.5. Explosive oxygen burning. Explosive burning in the O-rich layer occurs at even lower temperatures than explosive Si burning. Nevertheless, in the inner regions QSE clusters develop and significant production of isotopes such as ^{40}Ca, ^{44}Ti, and ^{48}Ti occurs. It is also in these regions that the γ process occurs, which is thought to be responsible for many of the p-process isotopes (see below).

2.2.6. Explosive helium burning. Explosive burning in the C-rich zone is not a significant modifier of nuclear abundances except in the innermost layers. The reason is that the outer layers do not achieve high enough temperatures to do much burning by the main C-burning channels, and the preexisting abundances of light particles are too low for other reaction channels to play much of a role. The situation changes in the inner zones of the He-burning shell, however, where there are abundant ^{4}He nuclei as well as a large supply of ^{22}Ne. The sudden heating of this zone causes the ^{22}Ne(α,n)^{25}Mg reaction to release a burst of neutrons, which can be captured by preexisting nuclei and drive an "n-process" (*Blake and Schramm,* 1976). In this way, the n-process is intermediate between the s-process, in which the β-decay rates typically dominate the neutron-capture rates, and the standard r-process, in which neutron captures are more rapid than β decays and certainly fast enough to establish an (n,γ)–(γ,n) equilibrium.

Some researchers in the 1970s and 1980s studied the possibility that the r-process nuclei were in fact produced in an n-process occurring in the He-burning shell (*Hillebrandt et al.,* 1976; *Truran et al.,* 1978; *Thielemann et al.,* 1979). Subsequent work showed that the ^{13}C and ^{22}Ne abundances required to explain the r-process yields were too large (*Blake et al.,* 1981), and thinking on the site of the r-process has returned to matter ejected from the SN core or from neutron star-neutron star collisions (see section 2.3). Nevertheless, the work on the He-shell n-process showed that interesting quantities of the isotopes ^{26}Al and ^{60}Fe could realistically be produced, a point that identified this site as important for cosmochemistry. This was bolstered by independent and contemporaneous efforts to understand the Xe-isotopic patterns in meteoritic nanodiamonds in terms of a "neutron burst" (*Heymann and Dziczkaniec,* 1980; *Heymann,* 1983).

Interest in this nucleosynthetic process is reviving, motivated by the measurements of ^{95,97}Mo excesses in presolar SiC grains of type X (see section 5.6.1) (*Pellin et al.,* 1999, 2000b), which show the signature of a neutron burst (*Meyer et al.,* 2000). Modern stellar models with full nuclear reaction networks confirm that narrow zones with neutron burst signatures are produced in Type II supernovae (e.g., *Rauscher et al.,* 2002). Of additional interest is the fact that

sufficiently large quantities of the short-lived radioisotopes ^{60}Fe and ^{182}Hf are produced in the neutron bursts in He shells to explain their abundances in the ESS (*Meyer et al.,* 2003, 2004). The contribution of these neutron bursts to the bulk galactic supply of the heavy elements is small, so traditional astronomical observations or decompositions of SS abundances would not detect this nucleosynthetic component. To date, its signal is only apparent in isotopic anomalies in presolar grains and primitive solar system minerals!

2.2.7. The r-process. *B^{2}FH* recognized that a high-temperature, high-neutron-density explosive process was responsible for many of the heavy elements (Fig. 1). They termed this the r-process since the neutron captures are more *rapid* than the β decays. Unlike the s-process, which is a *secondary* nucleosynthesis process since seed nuclei must already exist, the r-process is *primary* since it assembles its own seed nuclei. The seed nuclei capture neutrons rapidly and establish an (n,γ)–(γ,n) equilibrium for each isotope. Beta decay allows nuclei to increase their charge and thus continue to capture neutrons. This process persists until the supply of neutrons is exhausted.

Since the early 1960s, attention has focused on ejection of neutron-rich matter from SN cores as the likely site for the r-process, but difficulties in ejecting the right amount of such matter plagued the models. In the early 1990s, researchers began to recognize the importance of neutrino-heated ejecta for formation of the r-process isotopes (*Woosley and Hoffman,* 1992; *Meyer et al.,* 1992). The neutrino-energized "hot bubble" that develops near the SN mass cut provides a high-entropy setting in which inefficient assembly of heavy seed nuclei lessens the neutron richness required for formation of the heavy r-process nuclei. *Takahashi et al.* (1994) and *Woosley et al.* (1994) performed detailed SN calculations and found good production of the r-process nuclei but only when they artificially enhanced the entropy of the models by a factor of roughly 3. Subsequently, *Qian and Woosley* (1996) followed neutrino driven wind calculations and found that conditions necessary for the r-process were not obtained. Also posing a problem for the r-process in this setting was the finding that strong neutrino-nucleus interactions during the r-process would severely limit production of heavy nuclei (*Meyer,* 1995; *Fuller and Meyer,* 1995; *Meyer et al.,* 1998b). The problem of too low an entropy (or too low a neutron richness) continues to plague the idea of the r-process in neutrino-driven ejecta unless the proto-neutron star is quite massive (e.g., *Thompson et al.,* 2001) or, perhaps, highly magnetic or rapidly rotating (e.g., *Thompson,* 2003).

Despite the lack of success of the neutrino-driven wind models in explaining the r-process abundances, those models led to several advances in our understanding of the r-process. In particular, we better understand the role of neutrinos in the r-process (e.g., *Meyer,* 1995; *Meyer et al.,* 1998b), the nature and role of statistical equilibria that arise in the r-process (e.g., *Meyer et al.,* 1998b), and the requirements for a successful r-process (*Hoffman et al.,* 1996a; *Meyer and Brown,* 1997). The unsuccessful neutrino-driven models also motivated further work on the r-process in other settings such as directly ejected core matter (*Wheeler et al.,* 1998; *Wanajo et al.,* 2003) or neutron-star collisions (*Freiburghaus et al.,* 1999). While galactic chemical evolution arguments favor supernovae over neutron-star collisions (*Argast et al.,* 2004), a proper understanding of the site of the r-process remains elusive. Nevertheless, the 1990s and early 2000s have seen advances in r-process theory.

The other significant recent advance in understanding the r-process came from observations of heavy-element abundances in metal-poor stars. These observations show that these very old stars have nearly pure and highly enriched r-process heavy-element abundances (*Sneden et al.,* 1996) that match the solar r-process abundance distribution. The principal conclusions from this work are that (1) the r-process dominated the s-process early in the galaxy's history and (2) the r-process, at least for nuclei with mass number greater than 140, is a unique event in that it always gives the same abundance pattern. This second conclusion does not seem to hold for lower-mass r-process elements, which show real star-to-star abundance variations in metal-poor stars (*Sneden et al.,* 2003). Such observations support the notion of diverse r-process events, as inferred from the extinct radioisotopes ^{129}I and ^{182}Hf (*Wasserburg et al.,* 1996; *Qian et al.,* 1998). As discussed further in section 4, the idea is that one type of r-process event is responsible for ^{129}I and a second type of r-process, which occurs about 10 times more frequently than the first, produces ^{182}Hf and the actinides. The challenge to our astrophysical model is to understand how the easier-to-produce low-mass isotopes are made less often than the harder-to-produce heavier isotopes.

2.2.8. Neutron-rich quasi-statistical equilibrium. The neutron-rich Fe-peak isotopes ^{48}Ca, ^{50}Ti, ^{54}Cr, ^{58}Fe, ^{62}Ni, and ^{66}Zn do not seem to have been made in mainline stellar evolution since the main reaction pathways largely bypass them. *Hartmann et al.* (1985) explained the synthesis of the neutron-rich Fe-peak isotopes as a freezeout from a neutron-rich NSE, and cosmochemists embraced that model as an explanation for the isotopic anomalies in ^{48}Ca, ^{50}Ti, ^{54}Cr, ^{58}Fe, and ^{66}Zn in the FUN inclusions (see section 3). The difficulty with this idea, however, is that in the models ^{66}Zn (produced as ^{66}Ni in the NSE) is always more overabundant than ^{48}Ca. This made it difficult to understand how nature in fact could have produced ^{48}Ca.

Subsequently, *Meyer et al.* (1996) showed that expanding and cooling neutron-rich matter would evolve from NSE to a quasi-statistical equilibrium (QSE). The reason is that the three-body reactions that assemble heavier nuclei from α particles, namely, $^4\mathrm{He} + {}^4\mathrm{He} + {}^4\mathrm{He} \rightarrow {}^{12}\mathrm{C}$ and the reaction sequence $^4\mathrm{He} + {}^4\mathrm{He} + \mathrm{n} \rightarrow {}^9\mathrm{Be}$ followed by $^9\mathrm{Be} + {}^4\mathrm{He} \rightarrow {}^{12}\mathrm{C} + \mathrm{n}$, become slower than the expansion at temperatures of roughly 6×10^9 K. This means that the number of heavy nuclei deviates from that required by NSE. Other reactions continue to be fast, and a new equilibrium develops that has one additional constraint, namely, a fixed number of heavy nuclei. These authors also showed that a low-entropy QSE tends to have too many heavy nuclei compared to NSE while

a high-entropy QSE tends to have too few. In the former case, ^{48}Ca, ^{50}Ti, and ^{54}Cr are favored over the heavier neutron-rich Fe-peak isotopes, and their synthesis may be understood.

The fact that low-entropy expansions are favored for ^{48}Ca production pointed to deflagrations of near Chandrasekhar-mass WD stars as the likely nucleosynthetic site. The Chandrasekhar mass is the maximum mass a hydrodynamically stable WD star may have, and is typically about 1.4 $M_\odot$. Such WD stars have high central densities so that, when they explode, nuclei capture electrons, and the matter becomes sufficiently neutron rich to make ^{48}Ca and the other neutron-rich Fe-peak isotopes. Detailed models of such explosions by *Woosley* (1997) show robust production of ^{48}Ca and the other neutron-rich Fe-peak isotopes. These events likely comprise only about 2% of all Type Ia events; thus, ^{48}Ca is produced only rarely in the galaxy but, when it is, in huge quantities.

2.2.9. The p-processs. A number of proton-rich heavy isotopes, collectively known as the p-process nuclei, are completely bypassed by neutron-capture pathways. *B^{2}FH* envisioned them to be the result of proton captures in a H-rich environment. It now seems clear that this idea was wrong and that they were more likely produced in the "γ process" (*Woosley and Howard,* 1978). In this process, pre-existing r- and s-process isotopes are suddenly heated. A sequence of disintegration reactions then begins to strip off first neutrons then protons and α particles. If this processing quenches before the nuclei "melt" all the way down to Fe, an abundance of p-process isotopes results. Such processing occurs in the shock-heated O-rich layers of a core-collapse supernova (*Rayet et al.,* 1995; *Rauscher et al.,* 2002), although it may also occur on the outer layers of a deflagrating C/O WD, a Type Ia supernova (*Howard et al.,* 1991). The important radioisotope ^{146}Sm is made in the γ process.

Two puzzles still surround production of the p-process isotopes. First, the overall yields from the models of explosions of massive stars are a factor of 2 or 3 too low to explain the SS abundances (Fig. 1b). Perhaps production in Type Ia supernovae contributes the missing amount. Second is the fact that all models tend to drastically underproduce the light p-process isotopes ^{92,94}Mo and ^{96,98}Ru. Unlike in heavier elements, the p-process isotopes of Mo and Ru are nearly as abundant as their s- and r-process counterparts. This suggests that some other site is responsible for the bulk of their production. A Type Ia supernova initially seemed a plausible site, but nucleosynthesis calculations done in the context of realistic astrophysical models showed the same underabundances as before (*Howard and Meyer,* 1993). Another possible source is neutrino-heated ejecta in core collapse supernovae that undergo neutron-rich, α-rich freeze-outs (*Fuller and Meyer,* 1995; *Hoffman et al.,* 1996b). Those models showed robust production of the light p-process isotopes, but other isotopes were made in greater quantities. New calculations of these α-rich freezeouts that include interactions of the copious neutrinos with nuclei during the nucleosynthesis show that ^{92,94}Mo can be the most produced isotopes (*Meyer,* 2003), but it remains to be seen whether the SN models can actually achieve the high neutrino fluxes re-quired for this model. In any event, these neutrino-heated ejecta models produce abundant ^{92}Nb, a radioisotope of great interest for cosmochemistry.

3. SURVIVAL OF NUCLEOSYNTHETIC COMPONENTS IN METEORITES

Although it is clear from nuclear systematics that three different nucleosynthetic processes (p, r, and s) must have contributed to the synthesis of the heavy elements (Fig. 1b), these components as well as the products of other nuclear burning stages and processes were apparently thoroughly mixed during the formation of the SS and, until 30 years ago, it was not possible to detect their separate signatures. The p-process, and certain r-process, nuclides are removed from the s-process path, thus their abundances in the SS are well determined. So are those of s-only nuclides, which are shielded by isobars from r-process contributions. However, there are isotopes that are produced by both the s- and the r-process. The classical approach to determine the respective contributions of these two processes is to calculate their s-process abundances from those of s-only isotopes of the same elements and the requirement of a steady s-process flow, i.e., that the s-process abundances are inversely proportional to the neutron capture cross sections of the s-process isotopes of a given element (*Käppeler et al.,* 1989; *Woolum,* 1988). The r-process abundances (the "residuals") of the isotopes that have both s- and r-process contributions are then obtained by subtracting the calculated s-process from the observed SS abundances. Increasingly detailed astrophysical models now allow r-process residuals to be computed from realistic s-process calculations rather than from the requirement of steady s-process flow (*Straniero et al.,* 1995; *Gallino et al.,* 1998; *Arlandini et al.,* 1995).

The preservation of different nucleosynthetic components had been proposed by Clayton (e.g., *Clayton,* 1975a, 1978; *Clayton and Ward,* 1978), who argued that, because of their distinct stellar sources, these components were transported into the SS by chemically distinct carriers that might have remained separated during SS formation ("cosmic chemical memory" model). It thus created great excitement when in 1978 a CAI from the carbonaceous chondrite Allende, EK 1-4-1, was discovered that exhibited excesses in the r-process isotopes of the elements Ba, Nd, and Sm (*McCulloch and Wasserburg,* 1978a; *McCulloch and Wasserburg,* 1978b) and a depletion in p-only ^{84}Sr (*Papanastassiou and Wasserburg,* 1978). The same year saw the discovery of a Xe component in a chemical separate that exhibited an almost pure s-process pattern (*Srinivasan and Anders,* 1978). The CAI EK 1-4-1 is one of a series of refractory inclusions that exhibit mass-dependent fractionation (F) in the elements O, Mg, and Si together with (at that time UNknown) nuclear anomalies in a large number of elements, and were therefore named "FUN" inclusions. The nuclear anomalies in these inclusions consist of p-, r- and

s-process effects in the heavy elements and in excesses and/or depletion in the n-rich isotopes of the Fe-peak elements.

3.1. FUN Inclusions and the Heavy Elements

Two other FUN inclusions, C1 from Allende, and 1623-5 from the CV3 chondrite Vigarano (*Loss et al.,* 1994), show essentially identical anomalies in Sr, Ba, Nd, and Sm [and in many other elements (see *Loss et al.,* 1994)] but the isotopic abundance patterns in these elements are very different from those exhibited by EK 1-4-1. These two different types of patterns have been discussed in detail by *Lee* (1988) in terms of the p-, r-, and s-processes for the production of the heavy elements and we do not want to repeat this discussion here. It is instructive, however, to compare the r-process patterns found in EK 1-4-1 with the s-process patterns found in presolar SiC (see section 5). It was found that SiC is the carrier of the s-process Xe component discovered by *Srinivasan and Anders* (1978) and that SiC is the carrier of s-process Ba, Nd, and Sm as well. Figure 2, adopted from *Begemann* (1993), shows the excesses in the r-process isotopes in EK 1-4-1 and the large depletions of the same isotopes in presolar SiC. These almost perfect complementary patterns give clear evidence of the separate nature of the r- and s-process.

One dramatic difference between the CAI and SiC is the size of the anomalies, which are more than 100-fold larger in SiC than in EK 1-4-1. The reason is that the SiC is true stardust and condensed in the expanding atmosphere of stars whereas the CAIs formed in the SS. Their isotopic anomalies are a memory of presolar material that was not completely homogenized during SS formation and was incorporated into the inclusions. Evidence for a SS system origin of CAIs, even the FUN CAIs, is provided not only by the size of the anomalies, which are much smaller than the expected pure nucleosynthetic components, but also by the fact that, except for mass-dependent fractionation, the major elements such as O, Mg, and Si are isotopically normal. These fractionation effects must be the result of evaporation during the formation of the inclusions, and while part of the small nonlinear deviations in Mg and Si (*Clayton and Mayeda,* 1977; *Wasserburg et al.,* 1977; *Molini-Velsko et al.,* 1986) probably derived from the fact that evaporation does not produce strictly linear mass fractionation, some deviations cannot be explained in this way. It is still a puzzle why in FUN inclusions nuclear anomalies are associated with large mass fractionation effects but, as will be seen in section 3.2, this association of F and UN effects is not the rule.

3.2. FUN and Hibonite Inclusions and the Iron-Peak Elements

The FUN inclusion EK 1-4-1 has large excesses in the n-rich isotopes ^{48}Ca (*Lee et al.,* 1978), ^{50}Ti (*Niederer et al.,* 1980), ^{54}Cr (*Papanastassiou,* 1986), ^{58}Fe (*Völkening and Papanastassiou,* 1989), and ^{66}Zn (*Völkening and Papanastassiou,* 1990). On the other hand, the Allende inclusions

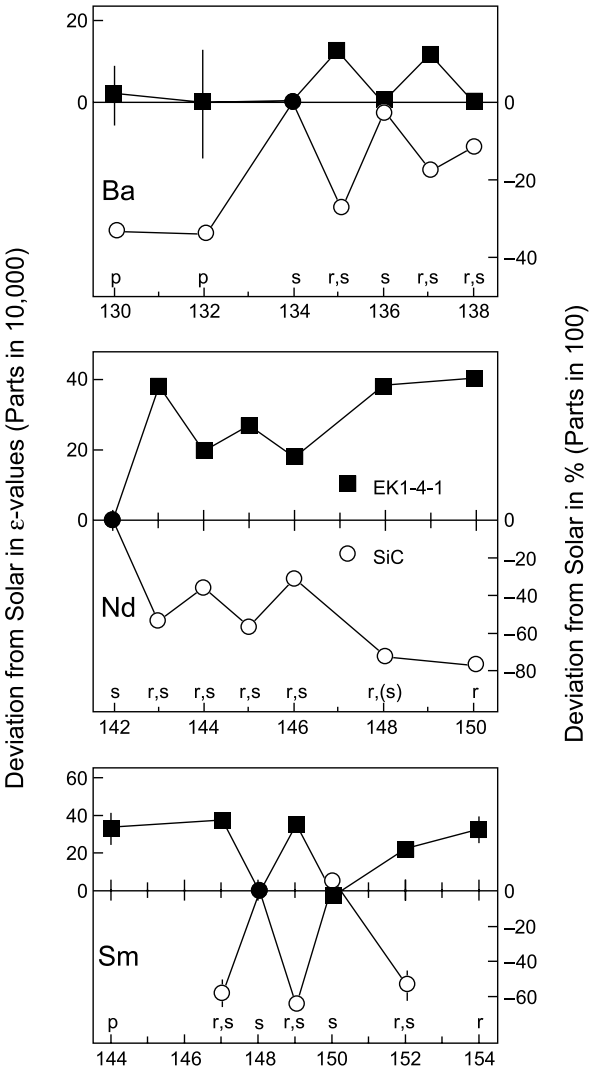

Fig. 2. The isotopic patterns of Ba, Nd, and Sm measured in the FUN inclusion EK 1-4-1 are compared with those measured in presolar SiC. The patterns were normalized to the s-process isotopes ^{134}Ba, ^{142}Nd, and ^{148}Sm. For the EK 1-4-1 data a second normalization was made, requiring that there be no anomalies in ^{138}Ba and ^{150}Ba and equal excesses in ^{143}Nd and ^{148}Nd (*McCulloch and Wasserburg,* 1978a,b). The EK 1-4-1 patterns show excesses in the r-process isotopes; in the case of Sm, also in the p-only isotope ^{144}Sm. The SiC patterns are complementary and are characteristic of the s-process. Adapted from *Begemann* (1993).

C1 and BG82HB1 and the Vigarano inclusion 1623-5 (all FUN) have large deficiencies in ^{48}Ca (*Lee et al.,* 1978; *Papanastassiou and Brigham,* 1989; *Loss et al.,* 1994), ^{50}Ti (*Niederer et al.,* 1980; *Papanastassiou and Brigham,* 1989; *Loss et al.,* 1994), and ^{54}Cr (*Papanastassiou,* 1986; *Papanastassiou and Brigham,* 1989; *Loss et al.,* 1994). However, this is where the complementarity ends; C1 and BG82HB1 have no clear deficits in ^{58}Fe (*Völkening and Papanastassiou,* 1989) and C1 has normal ^{66}Zn (*Völkening and Papanastassiou,* 1990). There are also minor anomalies in other isotopes such as ^{42}Ca, ^{46}Ca, ^{47}Ti, ^{49}Ti, ^{53}Cr, and ^{70}Zn, and

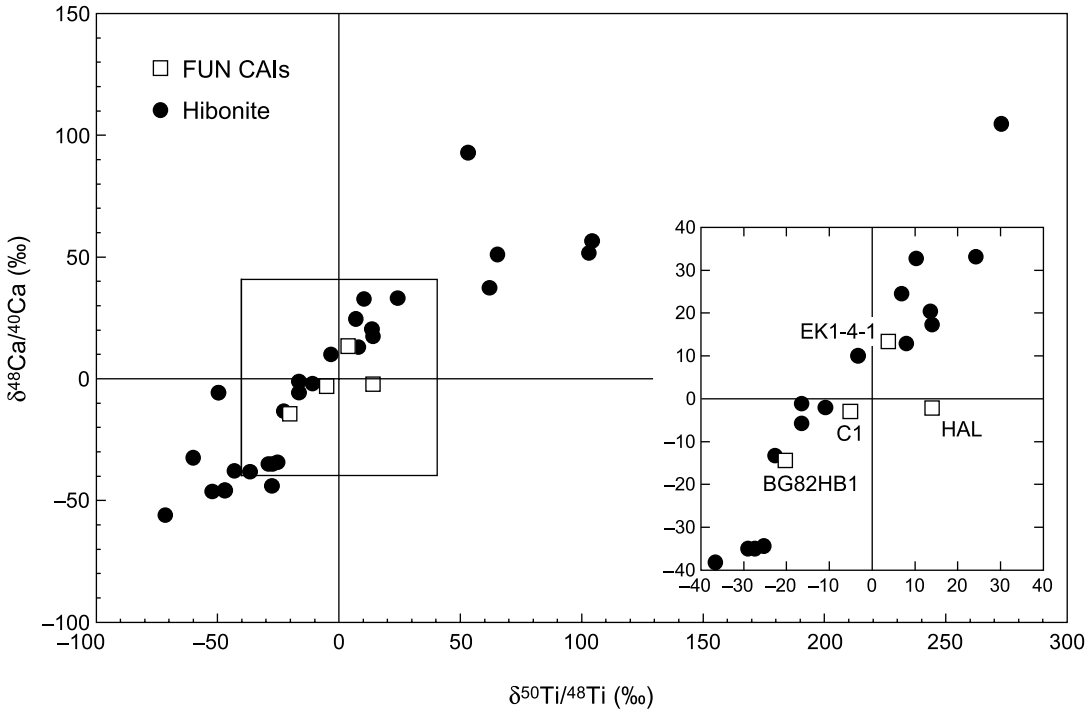

Fig. 3. Isotopic anomalies in the neutron-rich isotopes ^{48}Ca and ^{50}Ti measured in FUN and hibonite-bearing inclusions. The isotopic ratios are expressed as δ values; deviations from the normal ratios are in permil (‰). Isotopic anomalies are qualitatively correlated in that most inclusions with ^{48}Ca excesses have ^{50}Ti excesses and vice versa. Data from *Lee et al.* (1978), *Niederer et al.* (1980), *Fahey et al.* (1987), *Papanastassiou and Brigham* (1989), *Ireland* (1990), and *Sahijpal et al.* (2000).

the exact size of these anomalies depends on the choice of the isotope pair used for internal calibration [see *Lee* (1988) for a detailed discussion]. However, the anomalies in the above-listed n-rich isotopes are so dominant that, even if their exact magnitude is uncertain, their nature cannot be in doubt. Another source of uncertainty is the chemical behavior of the elements involved. For example, Ca and Ti are much more refractory than Zn and partial isotopic equilibration of the latter cannot be excluded (*Völkening and Papanastassiou,* 1990).

Even larger isotopic anomalies than in the FUN inclusions are observed for the elements Ca and Ti in single hibonite grains. While the FUN inclusions have sizes on the order of 1 cm, these hibonite grains are 100 μm or smaller. However, they should be distinguished from presolar hibonite grains discussed in section 5.5. While presolar hibonites have highly anomalous O-isotopic compositions, the hibonites described here have O-isotopic ratios similar to those of other CAIs and are undoubtedly of SS origin. In general, they do not have any pronounced fractionation effects (*Ireland et al.,* 1992), thus they can be termed UN inclusions. For completeness it should be mentioned that there exist also mostly F inclusions such as Allende TE with large fractionations in O, Mg, and Si (*Clayton et al.,* 1984) but only small anomalies in Ca and Ti. Figure 3 shows the anomalies in ^{48}Ca and ^{50}Ti in FUN inclusions and hibonite grains (*Fahey et al.,* 1987; *Papanastassiou and Brigham,* 1989; *Ireland,* 1990; *Sahijpal et al.,* 2000). While there is no perfect linear correlation, with very few exceptions the inclusions and hibonite grains have either excesses or depletions in these two isotopes. Because chemical fractionation between Ca and Ti is possible between the nucleosynthetic source and incorporation into CAIs, a strictly linear correlation is not to be expected.

The general correlation is clear evidence that nucleosynthetic components with large preferential enhancements of the n-rich Fe-peak isotopes and lacking these isotopes were incompletely mixed in the early SS. In the standard Type II SN models (*Woosley and Weaver,* 1995; *Rauscher et al.,* 2002) both ^{48}Ca and ^{50}Ti are underproduced. As discussed below, certain rare Type Ia supernovae are likely responsible for the production of the bulk of the n-rich Fe-group isotopes; thus, the CAIs with depletions in these two isotopes probably formed from collections of SS dust with a lower than average complement of the n-rich component. While components with excesses or depletions in the n-rich isotopes dominate, more detailed analysis of the isotopic data revealed that there are more than only two nucleosynthetic components for Ca and Ti. For example, since Ti has five stable isotopes and two of them (^{46}Ti and ^{48}Ti) are used for making corrections for isotopic mass fractionation, either intrinsic or due to the analysis procedure, we are left

with three independent ratios (^{47}Ti/^{48}Ti, ^{49}Ti/^{48}Ti, and ^{50}Ti/^{48}Ti). If only two components were present, the data would lie on a straight line connecting these components in the three-dimensional space spanned by the three independent ratios. In case of three components, the data would lie on a plane. This kind of analysis showed that for Ti at least four and for Ca at least three components are required to account for the variations in the isotopic ratios (*Jungck et al.,* 1984; *Ireland,* 1990).

Possible nuclear processes that would produce the component with large excesses in the n-rich isotopes were discussed in detail by *Lee* (1988), and the reader is referred to that chapter for the status of the field at that time. Subsequent discovery of ^{58}Fe and ^{66}Zn excesses in EK 1-4-1 seemed to confirm the n-rich nuclear statistical equilibrium (NSE) process (*Hartmann et al.,* 1985) and to exclude n-rich Si burning (*Cameron,* 1979). Neutron-rich NSE burning, even in a multizone mixing model, predicts much larger ^{66}Zn excesses relative to ^{48}Ca than observed (*Völkening and Papanastassiou,* 1990). Chemical fractionation may be responsible for this discrepancy, but it is more likely that the appropriate nucleosynthesis model for the n-rich Fe-peak isotopes is that of a QSE with too many heavy nuclei. As discussed in section 2, matter expanding and cooling from high temperature and density in very low-entropy, neutron rich explosive environments establishes QSEs with too many heavy nuclei relative to NSE, which, in turn, leads to enhanced synthesis of ^{48}Ca, ^{50}Ti, and ^{54}Cr relative to ^{66}Zn (*Meyer et al.,* 1996). Ejection of very-low-entropy, neutron-rich matter arises in deflagrations of near-Chandrasekhar-mass WD stars, and models confirm strong production of ^{48}Ca in these settings (*Woosley,* 1997). Interestingly, such supernovae probably comprise only ~2% of all Type Ia events; therefore, the n-rich Fe-group isotopes are apparently produced infrequently but in prodigious quantities. This is likely to lead to strong inhomogeneities in their abundances distributions in interstellar dust, which, in turn, likely plays an important role in the origin of their anomalies in UN inclusions.

3.3. Other Nuclear Anomalies

In addition to the large and striking anomalies exhibited by FUN and hibonite-bearing inclusions, endemic effects in "normal" CAIs have been found for Ti (*Niederer et al.,* 1980, 1981, 1985; *Niemeyer and Lugmair,* 1981, 1984), Ca (*Jungck et al.,* 1984; *Niederer and Papanastassiou,* 1984), Cr (*Birck and Allègre,* 1984, 1985; *Birck and Lugmair,* 1988) and Ni (*Birck and Lugmair,* 1988). These effects are much smaller than those found in FUN and hibonite inclusions. They are mostly excesses in the n-rich isotopes of these elements and again indicate incomplete mixing of an n-rich component in the ESS.

Improvement in laboratory and instrumental capabilities of mass spectrometry [thermal ionization mass spectrometry (TIMS) and inductively-coupled plasma mass spectrometry (ICP-MS)] has led to further discovery of isotopic anomalies in a series of elements. The isotopic measurements were made either on bulk samples of various meteorites or on different chemical separates (leachates and residues). *Rotaru et al.* (1992) and *Podosek et al.* (1997) have found deficits and large excesses of ^{54}Cr in certain leach fractions from carbonaceous chondrites, the largest effects (excesses of more than 20%) being exhibited by the CI chondrite Orgueil. Although this indicates the presence of the n-rich component of FUN inclusions, no effects in other Fe-peak elements have been detected. Also, no carriers of the ^{54}Cr have yet been detected. Another example is anomalies in the Mo isotopes (*Dauphas et al.,* 2002a,b; *Yin et al.,* 2002a). The dominating pattern found in these measurements is excesses in the r-process isotopes ^{95}Mo, ^{97}Mo, and ^{100}Mo, but also in the p-process isotopes ^{92}Mo and ^{94}Mo. This pattern is the inverse of the s-process pattern present in mainstream SiC grains (see section 5). However, an s-process pattern was also observed in a leachate from Orgueil (*Dauphas et al.,* 2002a). There might be still questions of unresolved interferences but there is no doubt that endemic isotopic anomalies exist not only in CAIs and primitive carbonaceous chondrites but also in planetary differentiates (*Chen et al.,* 2004; *Yin and Jacobsen,* 2004) and the finding of uniform Mo-isotopic compositions (*Becker and Walker,* 2003) seems unfounded. Endemic anomalies are also found for Ru (*Papanastassiou et al.,* 2004). The pattern of these anomalies depends on the normalization scheme used and at the moment it is not clear which nucleosynthetic components can be distinguished. No evidence for the presence of short-lived ^{97}Tc ($T_{1/2} = 2.6 \times 10^6$ yr) or ^{99}Tc ($T_{1/2} = 2.1 \times 10^5$ yr) has been found. Several experimental groups have measured Zr-isotopic ratios in a large variety of meteorites and have found mostly excesses but also some deficits in ^{96}Zr (*Harper,* 1993; *Sanloup et al.,* 2000; *Yin et al.,* 2001; *Schönbächler et al.,* 2003). These patterns are similar to what is found in presolar graphite and SiC grains (section 5) and indicate the presence (or absence) of an r-process component. The isotope ^{92}Zr shows also anomalies but these could be due to the decay of short-lived ^{92}Nb ($T_{1/2} = 3.5 \times 10^7$ yr). Evidence for its presence in the ESS will be discussed in section 4. The Ba-isotopic ratios are also potentially affected by contribution from a radioisotope, ^{135}Cs ($T_{1/2} = 2.3 \times 10^6$ yr) (see section 4). However, Ba-isotopic analyses of leaching fractions from different meteorites (*Hidaka et al.,* 2001, 2003) show excesses as well as deficits in both ^{135}Ba and ^{137}Ba. The patterns with excesses are similar to the r-process pattern exhibited by the FUN inclusion EK 1-4-1, while the pattern with depletions is reminiscent of the s-process pattern found in presolar SiC (see section 5). This again provides evidence that contributions from both nucleosynthetic processes were not perfectly homogenized in the ESS.

There have been many more attempts to detect isotopic anomalies in meteorites (e.g., *Podosek et al.,* 1999) but data need to be on a firmer basis to be discussed here. In some cases, as for example for Cu (*Luck et al.,* 2003; *Russell et al.,* 2003), which has only two stable isotopes, it is not possible to assign any nucleosynthetic pattern to an isotopic anomaly.

TABLE 2. Short-lived radioisotopes for which evidence has been found in meteorites.

Radioisotope*	Half-life (m.y.)	Daughter Isotope	Reference Isotope	Initial Abundance	Reference
^{41}Ca	0.10	^{41}K	^{40}Ca	1.5×10^{-8}	[1]
^{26}Al	0.74	^{26}Mg	^{27}Al	5×10^{-5}	[2]
^{10}Be	1.5	^{10}B	^{9}Be	$\sim 5 \times 10^{-4}$	[3]
^{60}Fe	1.5	^{60}Ni	^{56}Fe	$\sim 1.5 \times 10^{-6}$	[4]
^{53}Mn	3.7	^{53}Cr	^{55}Mn	$\sim 2 \times 10^{-5}$	[5]
^{107}Pd	6.5	^{107}Ag	^{108}Pd	4.5×10^{-5}	[6]
^{182}Hf	9	^{182}W	^{180}Hf	2×10^{-4}	[7]
^{129}I	16	^{129}Xe	^{127}I	10^{-4}	[8]
^{244}Pu	81	Fission Xe	^{238}U	$(4–7) \times 10^{-3}$	[9]
^{146}Sm	103	^{142}Nd	^{144}Sm	8×10^{-3}	[10]
^{7}Be	53 d	^{7}Li	^{9}Be	5×10^{-3}	[11]
^{36}Cl	0.3	^{36}Ar, ^{36}S	^{35}Cl	$(0.14–1) \times 10^{-5}$	[12]
^{135}Cs	2.3	^{135}Ba	^{133}Cs	$(1–5) \times 10^{-4}$	[13]
^{205}Pb	15	^{205}Tl	^{204}Pb	10^{-4}	[14]
^{92}Nb	35	^{92}Zr	^{93}Nb	$\sim 1.5 \times 10^{-5}$	[15]

*For the five isotopes in the lower panel, only hints exist that need confirmation.

References: [1] *Srinivasan et al.* (1994, 1996); [2] *Lee et al.* (1976, 1977); [3] *McKeegan et al.* (2000); [4] *Shukolyukov and Lugmair* (1993), *Tachibana and Huss* (2003), *Mostefaoui et al.* (2005); [5] *Birck and Allègre* (1985), *Lugmair and Shukolyukov* (1998); [6] *Kelly and Wasserburg* (1978); [7] *Lee and Halliday* (1995), *Harper and Jacobsen* (1996), *Kleine et al.* (2002), *Yin et al.* (2002); [8] *Jeffery and Reynolds* (1961); [9] *Rowe and Kuroda* (1965); [10] *Lugmair and Marti* (1977), *Lugmair and Galer* (1992); [11] *Chaussidon et al.* (2004); [12] *Murty et al.* (1997), *Lin et al.* (2005); [13] *McCulloch and Wasserburg* (1978), *Hidaka et al.* (2001); [14] *Nielsen et al.* (2004); [15] *Harper* (1996), *Schönbächler et al.* (2002).

4. SHORT-LIVED NUCLEI

Short-lived radioisotopes have lifetimes (up to 10^8 yr) that are too short for them to have survived for the age of the SS. However, there is evidence that some interesting isotopes were "live" during the early stages of the SS. This evidence comes from excesses in the daughter isotopes above their normal SS abundance. The initial presence of short-lived isotopes (SLI) in ESS materials is a dramatic demonstration of stellar nucleosynthesis occurring as recently as 1 m.y. before SS formation. They thus connect the birth of the SS to the presence of nearby stars.

Short-lived isotopes in the ESS have many important implications. One of them is that the decay of nuclei such as ^{26}Al and ^{60}Fe could have provided the heat for the melting of small planetary bodies (*Urey,* 1955; *Fish et al.,* 1960; *Schramm et al.,* 1970). Another is that SLI can serve as fine-scale chronometers for ESS events (e.g., *Lugmair and Shukolyukov,* 2001; *Gilmour,* 2002). These questions will be treated in other chapters (*Halliday and Kleine,* 2006; *Nichols,* 2006; *Russell et al.,* 2006; *Wadhwa et al.,* 2006) and will not be discussed here. Rather we concentrate on the question of what information SLI can provide about stellar nucleosynthesis. A detailed review of SLI in the ESS greatly exceeds the scope of the present chapter. The interested reader is therefore directed to some recent reviews (*MacPherson et al.,* 1995; *Podosek and Nichols,* 1997; *Goswami and Vanhala,* 2000; *Busso et al.,* 2003; *Nittler and Dauphas,* 2006). Our emphasis will be on recent developments.

Table 2 gives a list of the SLI for which there is clear evidence that they were present and live in the ESS. Hints exist for several other SLI, but these still need confirmation. Positive evidence for the one-time presence of a SLI requires demonstration that the excess of the daughter isotope is linearly correlated with the parent element abundance. In the case of ^{129}I it has been shown that excesses in the decay product ^{129}Xe are correlated with the stable isotope of I, ^{127}I (*Jeffery and Reynolds,* 1961). After the discovery of ^{26}Al in CAIs, a linear correlation was demonstrated between excesses in ^{26}Mg and the stable ^{27}Al in several minerals with different Al/Mg ratios (*Lee et al.,* 1976, 1977). Arguments for a "fossil" origin of ^{26}Mg excesses (*Clayton,* 1986), i.e., ^{26}Al decay long before SS formation and introduction of "fossil" ^{26}Mg into refractory inclusions in the ESS, have not been accepted [see discussion and references in *MacPherson et al.* (1995)]. Presently, there is little doubt that the SLI listed in Table 2 were present in the ESS.

In Table 2 we give the half-lives of the SLI, their daughter isotopes, and the ratios relative to a stable isotope observed in ESS objects. Plutonium has no isotope that still exists today and ^{238}U is used instead. Because these ratios change with time as the different radioisotopes decay at different rates, ratios should be given at the same time. In Table 2 the reference time is the formation time of CAIs

that had a $^{26}Al/^{27}Al$ ratio of 5×10^{-5} [the "canonical ratio" (see *MacPherson et al.,* 1995). Recent high-precision inductively-coupled plasma mass spectrometry and high-precision SIMS measurements of low-Al/Mg phases in CAIs (*Galy et al.,* 2004; *Liu et al.,* 2005; *Young et al.,* 2005) have indicated an initial $^{26}Al/^{27}Al$ ratio in CAIs as high as 7×10^{-5}. However, for the time being we use 5×10^{-5} as the canonical ratio.]. For such CAIs there exists an absolute age of 4567.2 ± 0.6 m.y. based on the U-Pb system ("Pb/Pb" age) (*Amelin et al.,* 2002). Another advantage of using CAIs as a reference is that they contain evidence and reliable initial ratios also for ^{41}Ca and ^{10}Be (*Srinivasan et al.,* 1994, 1996; *McKeegan et al.,* 2000; see also *Goswami and Vanhala,* 2000). Hints for the initial presence of ^{53}Mn, ^{60}Fe, and ^{129}I have also been reported for CAIs, but it is not clear whether the inferred parent/daughter ratios refer to the same time as those for the above three isotopes (e.g., *Goswami et al.,* 2001).

A fundamental problem is that not all SLI can be measured in the same ESS objects. The reason is that the determination of excesses in the daughter isotopes requires a reasonably (sometimes very) large ratio of the parent to daughter element. While this is the case for ^{41}Ca, ^{26}Al, and ^{10}Be in CAIs, there are simply no samples in which this is the case for all SLI. If absolute ages could be obtained for objects in which SLI ratios have been measured, these ratios can be extrapolated to the reference time, but even this is not possible in all cases. It should therefore be realized that uncertainties are involved in the ratios for the SLI ^{60}Fe, ^{53}Mn, and ^{107}Pd given in Table 2. In the case of ^{60}Fe, *Birck and Lugmair* (1988) inferred an $^{60}Fe/^{56}Fe$ ratio of 1.6×10^{-6} from their Fe-Ni measurements in CAIs, but because of possible nuclear anomalies in the Ni isotopes, no firm conclusion on the initial presence of ^{60}Fe in the ESS was reached. Subsequently, evidence for ^{60}Fe was found in eucrites, which are differentiated meteorites, and from bulk samples in the eucrite Chervony Kut a $^{60}Fe/^{56}Fe$ ratio of 4×10^{-9} was derived (*Shukolyukov and Lugmair,* 1993). If we adopt the age based on ^{53}Mn for Chervony Kut (*Lugmair and Shukolyukov,* 1998) and the above-cited Pb/Pb age for CAIs, then this ratio extrapolates to only 2×10^{-8} at the time of CAI formation. Recently, much higher values have been obtained from the analysis of sulfides from unequilibrated ordinary chondrites and enstatite chondrites (*Tachibana and Huss,* 2003a; *Mostefaoui et al.,* 2003, 2004a, 2005; *Guan et al.,* 2003). *Mostefaoui et al.* (2005) reported a $^{60}Fe/^{56}Fe$ ratio of 9.2×10^{-7} for troilite from the unequilibrated ordinary chondrite Semarkona, and *Guan et al.* (2003) obtained ratios from various sulfides in enstatite chondrites ranging all the way up to 8.5×10^{-7}. If we assume that these sulfides have ages comparable to those of chondrules and thus are about 2 m.y. younger than CAIs, then these ratios are consistent with the CAI value obtained by *Birck and Lugmair* (1988).

Similarly, considerable uncertainties exist about the $^{53}Mn/^{52}Mn$ ratio. *Birck and Allègre* (1985) inferred a ratio of 4.4×10^{-5} from the analysis of an Allende CAI. However, the Mn/Cr ratio in CAIs is not high and CAIs contain nucleosynthetic anomalies in several elements, including the Cr isotopes, making the $^{53}Mn/^{52}Mn$ ratio in CAIs suspect (*Lugmair and Shukolyukov,* 1998, 2001). Another approach is to extrapolate the ratio measured in the angrite Lewis Cliff 85010 (*Nyquist et al.,* 1994; *Lugmair and Shukolyukov,* 1998) by using the difference in the Pb/Pb ages obtained for the angrites Lewis Cliff 85010 and Angra dos Reis (*Lugmair and Galer,* 1992) and for CAIs (*Amelin et al.,* 2002). In fact, the angrite age has been used as an anchor point for a Mn-Cr chronology (*Lugmair and Shukolyukov,* 2001; *Nyquist et al.,* 2001). However, extrapolation of the Lewis Cliff 85010 ratio to the CAI Pb/Pb formation time gives a $^{53}Mn/^{52}Mn$ ratio of only $\sim 8 \times 10^{-6}$ and higher ratios have been obtained for Kaidun carbonates (*Hutcheon et al.,* 1999), chondrules from the ordinary chondrites Bishunpur and Chainpur (*Nyquist et al.,* 2001), and in samples from CI and CM carbonaceous chondrites (*Rotaru et al.,* 1992; *Birck et al.,* 1999), that range up to 2×10^{-5}. In Table 2 we adopt this as a compromise value.

A $^{107}Pd/^{108}Pd$ ratio of 2×10^{-5} has been obtained in iron meteorites (*Kelly and Wasserburg,* 1978; *Kaiser and Wasserburg,* 1983) and extrapolation to the time of CAI formation gives a value of $\sim 4.5 \times 10^{-5}$ (*Goswami and Vanhala,* 2000). Recently, a consistent value of 1.1×10^{-4} has been obtained for the $^{182}Hf/^{180}Hf$ ratios from samples of the H4 chondrites Ste. Marguerite and Forest Vale (*Kleine et al.,* 2002) and from whole-rock samples of several carbonaceous and ordinary chondrites and an Allende CAI (*Yin et al.,* 2002b). For discussions and references of the ratios for the longer-lived SLI we refer to the literature (*Goswami and Vanhala,* 2000; *Busso et al.,* 2003).

Hints for the presence of several other short-lived isotopes in the ESS exist but they need confirmation. Chlorine-36 can β^--decay into ^{36}Ar (98.1%) or turn into ^{36}S (1.9%) by β^+-decay or electron capture. *Murty et al.* (1997) inferred a $^{36}Cl/^{35}Cl$ ratio of 1.4×10^{-6} from ^{36}Ar excesses, whereas *Lin et al.* (2005) obtained ratios as high as 10^{-5} from ^{36}S excesses that are correlated with Cl/S ratios in Cl-rich sodalite and nepheline in a CAI. Because these phases are secondary and were most likely formed later than the CAI, the $^{36}Cl/^{35}Cl$ ratio at the time of CAI formation could be as high as 4×10^{-4}. Uncertainty also exists about the initial abundance of ^{135}Cs (*Hidaka et al.,* 2001, 2003; *Nichols et al.,* 2002) and inferred $^{135}Cs/^{133}Cs$ ratios range from $\sim 10^{-4}$ to 5×10^{-4}. One complication in these measurements is that ^{135}Ba excesses can also have an r-process origin, which must be corrected for; another is the volatile nature of Cs so that no samples with high Cs/Ba ratios are found. Niobium-92 represents an interesting case because, in contrast to the other short-lived isotopes, it is produced by the p-process. Inferred $^{92}Nb/^{93}Nb$ ratios in the ESS range from $\sim 1.5 \times 10^{-5}$ (*Harper,* 1996; *Schönbächler et al.,* 2002) to $\sim 10^{-3}$ (*Sanloup et al.,* 2000; *Münker et al.,* 2000; *Yin et al.,* 2000). A possible problem is the presence of nucleosynthetic effects in ^{92}Zr, and only the study by *Schönbächler et al.* (2002) obtained an internal isochron. The high ratio would imply a very high production ratio, which is not achieved by the

standard explosive processing in shells in Type II SN models (*Rauscher et al.,* 2002). As discussed in section 2, ^{92}Nb is likely made in the same, but as yet mysterious, environment as the light p-process isotopes ^{92,94}Mo and ^{96,98}Ru. Neutrino-driven winds from proto-neutron stars can produce these isotopes (e.g., *Hoffman et al.,* 1996b), perhaps with a necessary boost from the copious neutrinos that drive the wind (*Meyer,* 2003). Such wind scenarios robustly produce ^{92}Nb, at a level ^{92}Nb/^{93}Nb ≈ 1.0. *Nielsen et al.* (2004) reported evidence for the initial presence of ^{205}Pb in the ESS from ^{205}Tl excesses in two group IA iron meteorites. Lead-205 is an s-process isotope and decays by electron capture. The inferred ^{205}Pb/^{204}Pb ratio is 10^{-4}, but the possibility that the ^{205}Tl excesses are due to mass-dependent isotopic fraction of Tl, which has only two stable isotopes, has yet to be excluded. Finally, ^{7}Li excesses in an Allende CAI have been interpreted as evidence for the existence of ^{7}Be (*Chaussidon et al.,* 2004, 2005). What makes this finding so interesting is that ^{7}Be can be produced only by energetic particle irradiation and decays by electron capture with a half-life of only 53 d. This sets a severe constraint on the formation time of CAIs and requires an extremely high particle flux from the early Sun.

4.1. Galactic Production of Short-lived Isotopes

As had been proposed early for ^{129}I (*Wasserburg et al.,* 1960), the abundances of ^{244}Pu, ^{146}Sm, ^{182}Hf, and ^{129}I (and possibly ^{53}Mn) seen in the ESS can be explained by the steady-state concentrations of these isotopes in the galaxy at the time of SS formation (*Cameron et al.,* 1995; *Wasserburg et al.,* 1996; *Meyer and Clayton,* 2000). Plutonium-244, ^{182}Hf, and ^{129}I are produced by the r-process and thus have a SN origin. Hafnium-182 can also be produced by the neutron burst in the He shell of an exploding massive star (*Meyer et al.,* 2003, 2004). Samarium-146 is produced by the p-process, also in supernovae, whereas ^{53}Mn has also such an origin but is the result of explosive Si burning. For all these SLI, a steady state is established between SN production throughout galactic history and radioactive decay, and the SS apparently inherited them with the steady-state concentrations they had at the time of SS formation. For all the above SLI except ^{129}I, the abundances in the ESS are consistent with one another if SN production essentially lasted until SS formation; however, in such a case ^{129}I would be overproduced by a large factor (*Wasserburg et al.,* 1996). In fact, a decay interval of ~10^8 yr had been inferred earlier (*Wasserburg et al.,* 1960). This discrepancy prompted *Qian et al.* (1998) to propose different r-process sources for the heavy nuclei including ^{182}Hf and for nuclei around mass 130 including ^{129}I. According to this proposal the second process would occur much less frequently and would thus explain the observed relative abundances of ^{182}Hf and ^{129}I in the ESS (see also *Qian and Wasserburg,* 2000, 2003). A more detailed treatment of the galactic production of SLI can be found in *Nittler and Dauphas* (2006).

4.2. Production of the Short-lived Isotopes Calcium-41, Aluminum-27, Beryllium-10, Iron-60, and Palladium-107

Galactic steady-state production cannot account for the ESS abundances of ^{41}Ca, ^{27}Al, ^{10}Be, ^{60}Fe, and ^{107}Pd. For ^{26}Al this has been clear from its present-day abundance in the galaxy as inferred from the 1.8 MeV γ-ray line (*Mahoney et al.,* 1984). Gamma-ray data, mostly from COMPTEL (*Diehl et al.,* 1995), show that the abundance of ^{26}Al in the galaxy is at least a factor of 10 lower than that in the ESS (*Clayton and Leising,* 1987; *Knödlseder,* 1999). The presence of ^{26}Al and the other SLI in the above list thus require either a stellar source closely preceding SS formation or production by energetic particles from the early Sun.

4.2.1. Production by solar energetic particles. The original proposal of ^{26}Al production by charged particle irradiation from an early active sun by *Fowler et al.* (1962) has received its most recent detailed expression in the X-wind model put forward by Frank Shu and coworkers (*Shu et al.,* 1996, 2001; *Gounelle et al.,* 2001). These authors postulated not only that ^{26}Al, ^{41}Ca, and ^{53}Mn are produced by local irradiation in the X-wind region of the early Sun but also that CAIs and chondrules are produced in this region but at different distances from the Sun. This would explain that initial ^{26}Al/^{27}Al ratios in chondrules are systematically lower than in CAIs. The X-wind model of SLI production received a boost by the discovery in CAIs of initial ^{10}Be (*McKeegan et al.,* 2000), because this radionuclide is only produced by energetic particle irradiation and not by stellar nucleosynthesis. In their model, *Gounelle et al.* (2001) and *Leya et al.* (2003) could produce the ESS abundances of ^{10}Be, ^{26}Al, ^{41}Ca, and ^{53}Mn. However, these predictions required very special assumptions about target composition and structure and rather extreme assumptions about the energy and composition (extremely high ^{3}He abundance) of the solar cosmic rays. In addition, the X-wind model cannot account for ^{107}Pd, ^{60}Fe (see below), and the high ^{36}Cl/^{35}Cl obtained by *Lin et al.* (2004).

Additional evidence against the X-wind model has been provided by recent measurements. *Marhas et al.* (2002) found evidence for ^{10}Be in hibonite grains devoid of ^{41}Ca and ^{26}Al that indicated that the production of ^{10}Be is decoupled from that of these two SLI. Lack of a correlation between ^{10}Be and ^{26}Al was also seen in other measurements (*MacPherson et al.,* 2003). While ^{10}Be, which is not produced by stellar nucleosynthesis, could have been produced by energetic particles in the ESS, a stellar source seems to be needed for the other SLI. Manganese-53 can be made by proton bombardment of solids in the ESS (*Wasserburg and Arnould,* 1987), but its presence in samples from differentiated parent bodies (*Lugmair and Shukolyukov,* 1998) argues against the X-wind model. It was known all along that ^{60}Fe cannot be produced by energetic particle irradiation and the high ^{60}Fe/^{56}Fe inferred from recent studies (*Guan et al.,* 2003; *Mostefaoui et al.,* 2003, 2004a, 2005; *Tachibana and Huss,* 2003a,b) indicates a recent stellar

source. Further evidence against the contention of the X-wind model that the short-lived isotopes, specifically ^{26}Al, had much higher abundances in CAIs than other materials has been provided by two recent studies that found consistency between the Al-Mg and U-Pb clock (*Gilmour,* 2002) for CAIs and chondrules (*Amelin et al.,* 2002) and for CAIs and feldspar from H4 chondritic meteorites (*Zinner and Göpel,* 2002).

In summary, an origin by energetic particle irradiation in the ESS appears to be valid only for ^{10}Be. Even for this SLI other production mechanisms have been suggested. *Cameron* (2002) has proposed production in so-called r-process jets associated with core-collapse supernovae, but the lack of ^{26}Al and ^{41}Ca, which would also be produced by this mechanism, in samples with ^{10}Be seems to rule it out. A more promising alternative has been proposed by *Desch et al.* (2004), who considered ^{10}Be production by spallation from galactic cosmic rays in the ISM and trapping of the cosmic-ray ^{10}Be in the molecular cloud from which the SS formed. The authors estimate that a major portion of the initial ^{10}Be found in CAIs could originate from this source.

4.2.2. Production in a nearby stellar source. Ever since the proposal that a SN explosion triggered the formation of the SS (*Cameron and Truran,* 1977), various stellar sources have been investigated that could have produced and injected the SLI into the protosolar cloud just before its collapse (*Goswami and Vanhala,* 2000). In addition to a supernova (*Cameron et al.,* 1995), an AGB star (*Cameron,* 1993; *Wasserburg et al.,* 1994; *Busso et al.,* 1999, 2003) and a Wolf-Rayet (WR) star (*Arnould et al.,* 1997b) have been proposed as a source for the SLI in the ESS. The question is whether any of these sources can produce the SLI in sufficient amounts and in the proper ratios so that after a certain free decay time between production and formation of CAIs, the abundances of the SLI in the ESS are reproduced. While the free decay time is an adjustable parameter, because of the short half-life of ^{41}Ca, it cannot be much larger than 10^6 yr. While each of these sources can produce some of the SLI, they all have problems with accounting for all of the SLI or accounting for their correct ratios.

The problem with core-collapse supernovae is not that they cannot produce the SLI but that they produce too much of some of them. *Wasserburg et al.* (1998) and *Busso et al.* (2003) have investigated the production of the SLI theoretically predicted from a variety of SN models (*Woosley and Weaver,* 1995; *Rauscher et al.,* 2002). While the models can account for the right proportions of ^{26}Al, ^{41}Ca, and ^{60}Fe, they produce too much ^{53}Mn and far too much ^{107}Pd (*Wasserburg et al.,* 1998; *Meyer et al.,* 2004). A possible solution to this problem has been proposed by Meyer and coworkers (*Meyer and Clayton,* 2000; *Meyer et al.,* 2003). These authors assumed that only the outer layers of the supernova (the layers above the so-called mass cut) held responsible for the SLI were injected into the protosolar cloud and not the inner layers where ^{53}Mn (and also ^{60}Fe to a certain extent) is produced. Various theoretical studies have been devoted to triggered star formation and the injection of SLI into the presolar cloud (*Boss and Foster,* 1997, 1998; *Foster and Boss,* 1997; *Vanhala and Boss,* 2002), and they show that it appears possible to introduce and mix the SLI from a stellar source. There is also astronomical evidence for triggered star formation, most likely from the shock wave associated with SN explosions (*Preibisch,* 1999), and SN remnants are observed close to dense molecular clouds. Injection of only the outer layers of a supernova may require fine-tuning of the mass cut. No detailed quantitative investigations of different SN models have been made to see whether the correct ESS abundances of the SLI are obtained this way. Conclusions on this issue must await detailed models of the evolution of the ejecta from an exploding massive star and their interaction with the surrounding medium.

Wasserburg et al. (1994) and *Busso et al.* (1999, 2003) considered production of the SLI in an AGB star and mixing of its stellar wind or the ejected planetary nebula with the presolar cloud. They have found that the ESS abundances of ^{26}Al, ^{41}Ca, and ^{107}Pd can be produced by a low-mass (1.5 $M_\odot$) star of solar metallicity. This assumes that most of the ^{26}Al is produced during cool bottom processing (*Nollett et al.,* 2003) because production in the H-burning shell is insufficient. Asymptotic giant branch stars do not make ^{53}Mn but, as pointed out above, steady-state galactic production can account for this SLI. The major problem with an AGB source is ^{60}Fe. This SLI can be produced by neutron capture on ^{58}Fe and the unstable ^{59}Fe ($T_{1/2}$ = 44.5 d), but this requires fairly high neutron densities. This excludes low-mass AGB stars if the recent high values of ~10^{-6} obtained for the ^{60}Fe/^{56}Fe are correct. Models of AGB stars of 5 $M_\odot$ and solar metallicity or 3 $M_\odot$ but much lower metallicity can produce sufficient amounts of ^{60}Fe but run into problems matching the abundance ratios of the other SLI (*Busso et al.,* 2003). Non-exploding WR stars (*Arnould et al.,* 1997b) can produce the right abundances of ^{26}Al, ^{41}Ca, and ^{107}Pd but fail completely when it comes to the production of ^{60}Fe.

If we exclude a WR star as the source for the SLI, we are still left with the question of whether a supernova or an AGB star produced them. An issue that is often discussed in connection with this question is the probability of a close stellar source, be it a supernova or an AGB star, immediately before SS formation (see, e.g., *Busso et al.,* 2003). We do not deem such discussions to be very fruitful. The SS did form endowed with SLI and there is overwhelming evidence that a stellar source provided these SLI. As with any singular event (the presence of intelligent life on Earth is another example), it is of little use to consider the *a priori* probability of this event.

What is most important is to find out whether a supernova or an AGB did produce the SLI from their abundances in the ESS. Any stellar source that injected the SLI into the presolar cloud would also have injected other, stable isotopes (*Wasserburg et al.,* 1998; *Nichols et al.,* 1999). While such contributions would not be detectable if the injected and cloud material has been thoroughly mixed, a heterogeneous distribution of the injected stellar material would

show up in the form of isotopic anomalies and these anomalies would be very distinct and thus diagnostic for a SN or AGB source. But even in the absence of such fingerprints we can only hope that more experimental measurements (e.g., Fe-Ni studies), discovery of other SLI in ESS materials, experimental determination of important cross sections (e.g., only theoretical values exist for the neutron-capture cross sections of ^{59}Fe and ^{60}Fe), and improved models of stellar nucleosynthesis and of the dynamics of stellar ejecta and their interaction with cloud material will provide an answer.

5. PRESOLAR GRAINS

5.1. Introduction

Although the study of presolar grains is a relatively new field of astrophysics (the first presolar grains were isolated from meteorites and identified in 1987), it has grown to such an extent that not all aspects of presolar grains can be treated here. These grains provide information on stellar nucleosynthesis and evolution, mixing in supernovae, galactic chemical and isotopic evolution, physical and chemical conditions in stellar atmospheres and supernova and nova ejecta, and conditions in the ESS and in the parent bodies of the meteorites in which the grains are found. The study of these grains allows us to obtain information about individual stars, complementing astronomical observations of elemental and isotopic abundances in stars (e.g., *Lambert,* 1991), by extending measurements to elements that cannot be measured astronomically. Rather than giving a detailed review we will concentrate on elemental and isotopic features of the grains that provide information and constraints on nucleosynthesis and stellar evolution. For more information the interested reader is referred to some reviews (*Anders and Zinner,* 1993; *Ott,* 1993; *Zinner,* 1998a,b, 2004; *Hoppe and Zinner,* 2000; *Nittler,* 2003; *Clayton and Nittler,* 2004) and to the compilation of papers found in *Bernatowicz and Zinner* (1997).

5.2. Types of Presolar Grains

Table 3 shows a list of the presolar grain types identified to date and lists the sizes, approximate abundances, and stellar sources. The carbonaceous phases diamond, SiC, and graphite were discovered because they carry exotic noble gas components that led to their isolation from meteorites. Diamond carries Xe-HL, Xe enriched in the light and heavy isotopes (*Lewis et al.,* 1987; *Anders and Zinner,* 1993; *Huss and Lewis,* 1994a,b); SiC carries Xe-S, Xe with an s-process isotopic signature (*Srinivasan and Anders,* 1978; *Clayton and Ward,* 1978), and Ne-E(H), almost pure ^{22}Ne released at high temperature (*Tang and Anders,* 1988b; *Lewis et al.,* 1994); graphite carries Ne-E(L), released at low temperatures (*Amari et al.,* 1990, 1995b).

Because noble gases are trace elements, their isotopic compositions have mostly been measured in so-called "bulk samples," collections of large numbers of grains. Bulk measurements have also been made for many other elements (C, N, Mg, Si, Ca, Ti, Cr, Fe, Sr, Ba, Nd, Sm, and Dy) (*Ott and Begemann,* 1990; *Zinner et al.,* 1991; *Prombo et al.,* 1993; *Richter et al.,* 1993, 1994; *Russell et al.,* 1996, 1997; *Amari et al.,* 2000; *Podosek et al.,* 2004). However, because presolar grains come from different stellar sources, information on individual stars is obtained by the study of single

TABLE 3. Presolar grain types.

Grain Type	Abundance* (ppm)	Size (μm)	Stellar Sources	Nucleosynthetic Processes† Exhibited by Grains
Silicates in IDPs	900	≤1	RG, AGB and SN	Core H, He
Silicates in meteorites	150	≤0.5	RG and AGB	Core H, CBP
Spinel‡	1.5	0.15–2	RG, AGB, SNe	Core H, CBP, Shell H
Corundum‡	100	0.15–3	RG, AGB, SNe	Core H, CBP, HBB, Shell H, He, s
Nanodiamonds	1400	0.002	SNe	r, p
Mainstream SiC	14	0.3–20	AGB	Core H, Shell H, Shell He, s
SiC type A + B	0.2	0.5–5	J stars?	Shell He and H
SiC type X	0.06	0.3–5	SNe	H, He, O, e, s, n-burst
Graphite	1	1–20	SNe, AGB	H, He, O, e, s, n-burst; Core H, Shell He
Nova grains	0.001	~1	Novae	Ex H
Si nitride	0.002	≤1	SNe	He, O
TiC	~0.001	0.01-0.5	SNe, AGB	He, O, e

*Abundances vary with meteorite type. Shown here are maximum values.

†*In low-to-intermediate-mass stars:* Core H: Core H burning followed by first (and second) dredge-up. Shell H: Shell H burning during the RG and AGB phase. Shell He: He burning during thermal pulses of AGB phase followed by third dredge-up. CBP: Cool bottom processing. HBB: Hot bottom burning. s: s-process, neutron capture at low neutron density, followed by third dredge-up. *In supernovae:* H, He, O: H, He, and O burning in different stellar zones in the massive star before explosion. s: s-process taking place in several zones. e: equilibrium process, leading to the Fe-Ni core. n-burst: Neutron capture at intermediate neutron density. r: Neutron capture at high neutron density. p: p-process, photo disintegration and proton capture. *In novae:* Ex H: Explosive H burning.

‡Here and in the text we refer to grains with elemental compositions close to $MgAl_2O_4$ and Al_2O_3 as spinel and corundum, respectively, as has been done in many publications. However, it should be emphasized that it has been shown that presolar Al_2O_3 occurs both as the mineral corundum and in amorphous form (*Stroud et al.,* 2004). The same is probably the case for $MgAl_2O_4$.

TABLE 4. Isotopic measurements on presolar grains.

Grain Type	Analysis Type	Element	Grain Size	Analysis Technique
SiC	Bulk	Noble gases, C, N, Mg, Ca, Fe, Sr, Ba, Nd, Sm, Dy		Gas MS, TIMS, ion probe
	Single grain	C, Si, N, Mg, K, Ca, Ti, Fe, Ba	≥0.25 μm	Ion probe
		Fe, Sr, Zr, Mo, Ru, Ba	>1 μm	Laser RIMS
		He, Ne	>3 μm	Laser evap. + gas MS
Graphite	Bulk	Noble gases		Gas MS
	Single grain	C, N, O, Mg, Si, K, Ca, Ti	≥1 μm	Ion probe
		Zr, Mo	>1 μm	Laser RIMS
		He, Ne	>3 μm	Laser evap. + Gas MS
Nanodiamonds	Bulk	Noble gases, N, Sr, Te, Ba		Gas MS, TIMS
Oxides	Single grain	O, Mg, K, Ca, Ti, Cr	≥0.1 μm	Ion probe
Si_3N_4	Single grain	N, Si, C	≥0.5 μm	Ion probe
TiC	Single grain	O, Ti	~0.1 μm	Ion probe

grains. For isotopic analysis secondary ion mass spectrometry (SIMS) with the ion microprobe has become the method of choice and by far most single grain measurements have been made with this instrument. Resonance ionization mass spectrometry (RIMS) has distinct advantages of high sensitivity and elimination of isobaric interferences for analysis of trace elements, albeit at some cost in precision and data acquisition rate compared to the ion probe. While most SIMS measurements to date have been on grains 1 μm in size or larger, a new type of ion probe, the NanoSIMS, allows measurements of grains an order of magnitude smaller (e.g., *Zinner et al.,* 2003b, 2005b). Ion probe analysis of individual grains has led to the discovery of new types of presolar grains such as corundum, spinel, hibonite, and titanium oxide (*Hutcheon et al.,* 1994; *Nittler et al.,* 1994, 2005; *Nittler and Alexander,* 1999; *Choi et al.,* 1998, 1999; *Zinner et al.,* 2003b), Si_3N_4 (*Nittler et al.,* 1995), and silicates (*Messenger et al.,* 2003; *Nguyen and Zinner,* 2004). Finally, Ti-, Zr-, and Mo-rich carbides, cohenite (Fe-Ni)C), kamacite (Fe-Ni), and elemental Fe were found as tiny subgrains in TEM studies of graphite spheres (*Bernatowicz et al.,* 1991, 1996; *Croat et al.,* 2003). While TiC inside a SiC grain (*Bernatowicz et al.,* 1992) could have formed by exsolution, there can be little doubt that interior grains in graphite must have formed prior to the condensation of the spherules.

5.3. Elemental and Isotopic Compositions of Presolar Grains

With the exception of Si_3N_4, kamacite, and elemental Fe (which constitute only a tiny fraction of presolar grains discovered to date), all presolar grains identified so far are either C, carbides, or oxides, demonstrating the importance of the elements C and O in the formation of high-temperature phases from stellar atmospheres. These elements also dominate the chemistry of the envelopes of low-to-intermediate mass stars and the outer layers of presupernova stars. Because of the tight bond of these elements in the CO molecule, it is the excess of one over the other that determines whether carbonaceous (C > O) or O-rich (O > C) phases will be formed. *Clayton et al.* (1999) and *Deneault et al.* (2003) suggested condensation of carbonaceous phases in Type II SN ejecta even while C < O because of the limitation of CO buildup in the high-radiation environment of the ejecta (see section 5.6.1).

Table 4 gives a list of the elements for which isotopic ratios have been measured in presolar grains, on bulk samples with gas, thermal ionization, or secondary ion mass spectrometry (GMS, TIMS, or SIMS) and on individual grains by laser GMS, with the ion microprobe (SIMS), or by resonance ionization mass spectrometry (RIMS). Most valuable are isotopic analyses of as many elements as possible on a single grain because the results provide the most information on the parent star of this grain and set the tightest constraints on the nuclear processes that determined the composition of this stellar source.

One fundamental problem in interpreting information obtained from a given grain is that its stellar source is unknown and has to be inferred from the elemental and isotopic composition of the grain. Fortunately, this is possible for most of the grains. For example, there is little doubt that the majority of SiC grains come from low-mass AGB stars that had become carbon stars. Another example are SiC grains of type X (see below), Si_3N_4, and low-density graphite grains whose isotopic compositions, especially the initial presence of short-lived ^{44}Ti, provide clear evidence that these grains have a SN origin. There are also grains whose stellar origin cannot (yet) be determined with certainty. Silicon carbide grains of type A + B have low $^{12}C/^{13}C$ ratios in the range observed in type J and a few other types of carbon stars (*Amari et al.,* 2001c). However, the nucleosynthesis and mixing processes that would lead to the observed surface compositions are not well understood, and the A + B grains cannot be unambiguously assigned to such stars.

5.4. Silicon Carbide and Graphite Grains from Asymptotic Giant Branch Stars

Although most SiC grains are less than 0.5 μm in diameter, some grains are as large as 20 μm. The availability of a large number of grains in the size range of a few micrometers and the fact that SiC is relatively rich in trace elements

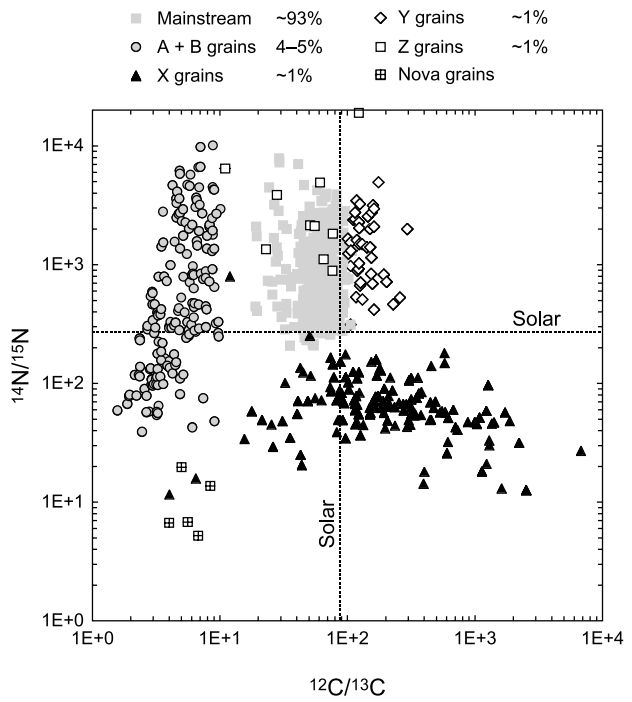

Fig. 4. Nitrogen and C-isotopic ratios of individual presolar SiC grains. Different grain types can be distinguished on the basis of their C, N, and Si isotopic ratios. Because rare grain types were located by automatic ion imaging, the numbers of grains of different types do not correspond to their relative abundances in the meteorites; these abundances are given in the legend. Data are from *Alexander* (1993), *Hoppe et al.* (1994, 1996a, 1997, 2000), *Nittler et al.* (1995), *Huss et al.* (1997), *Amari et al.* (2001a–c), and *Nittler and Hoppe* (2004a).

(*Amari et al.,* 1995a; *Kashiv et al.,* 2002) is the reason that SiC is the best studied presolar grain type (see Table 4). Ion microprobe isotopic analysis has revealed huge variations in many elements. This has led to the classification into different populations (Figs. 4–6) on the basis of C-, N-, and Si-isotopic ratios and inferred $^{26}Al/^{27}Al$ ratios: mainstream grains (~93% of the total), and the minor subtypes A, B, X, Y, Z, and nova grains (*Hoppe and Ott,* 1997; *Amari et al.,* 2001a). It should be noted that the numbers of data points for different grain populations plotted in Figs. 4–6 do not correspond to the abundance of these grains in primitive meteorites because most grains of rare types have been identified through specific searches by ion imaging (*Nittler et al.,* 1995; *Hoppe et al.,* 1996b, 2000; *Lin et al.,* 2002; *Besmehn and Hoppe,* 2003).

Mainstream grains constitute ~93% of all presolar SiC. They have $^{12}C/^{13}C$ ratios between 10 and 100, and mostly ^{14}N, ^{29}Si, and ^{30}Si excesses relative to solar (*Zinner et al.,* 1989, 2003a; *Stone et al.,* 1991; *Virag et al.,* 1992; *Alexander,* 1993; *Hoppe et al.,* 1994, 1996a; *Nittler et al.,* 1995; *Huss et al.,* 1997; *Amari et al.,* 2002; *Nittler and Alexander,* 2003). On a δ-value Si three-isotope plot the data fall along a line with slope of 1.35, which is shifted slightly to the right of the SS composition (Fig. 5 inset). Type Y grains have $^{12}C/^{13}C > 100$ and Si-isotopic compositions that lie to the right of the mainstream correlation line (*Hoppe et al.,* 1994; *Amari et al.,* 2001b). Type Z grains have even larger ^{30}Si excesses relative to ^{29}Si and, on average, lower $\delta^{29}Si$ values than Y grains but have $^{12}C/^{13}C < 100$ (*Alexander,* 1993; *Hoppe et al.,* 1997).

There is abundant evidence that mainstream grains, and very likely also Y and Z grains, originated from carbon stars of low mass (1–3 $M_\odot$). Dust from such stars has been proposed already before identification of presolar SiC to be a minor constituent of primitive meteorites (*Clayton and Ward,* 1978; *Srinivasan and Anders,* 1978; *Clayton,* 1983). Mainstream grains have $^{12}C/^{13}C$ ratios similar to those found in carbon stars (*Lambert et al.*, 1986), which are considered to be the most prolific injectors of carbonaceous dust grains into the ISM (*Tielens,* 1990). Many carbon stars show the 11.3-μm emission feature typical of SiC (*Treffers and Cohen,* 1974; *Speck et al.,* 1997). The presence of Ne-E(H) and the s-process isotopic patterns of the heavy elements exhibited by mainstream SiC provide the most convincing argument for their origin in carbon stars.

5.4.1. Light and intermediate mass elements. Of the elements whose isotopic compositions have been measured in SiC grains, nucleosynthesis occurring in the core during the main sequence of the parent stars affects only C and N. Their isotopic ratios in mainstream, Y, and Z grains are the result of core H burning in the CN cycle followed by the first (and second) dredge-up, and those of C also that of shell He burning and the third dredge-up (TDU) during the thermally pulsing AGB (TP-AGB) phase (*Busso et al.,* 1999). Whereas the first process enriches the star's surface in ^{13}C and ^{14}N, the TDU adds ^{12}C to the envelope, increases the $^{12}C/^{13}C$ ratio from the low values resulting from the first dredge-up, and, by making C > O, causes the star to become a carbon star.

Envelope $^{12}C/^{13}C$ ratios are predicted by canonical stellar evolution models to range from ~20 after the first dredge-up in the RG phase to ~300 in the late TP-AGB phases (*El Eid,* 1994; *Gallino et al.,* 1994; *Amari et al.,* 2001b) and agree with those observed in the above three types of SiC grains (see Fig. 4). The predicted $^{14}N/^{15}N$ ratios of 600–1600 (*Becker and Iben,* 1979; *El Eid,* 1994) fall short of the range observed in the grains. However, the assumption of deep mixing ("cool bottom processing," or CBP) of envelope material to deep hot regions in $M < 2.5\ M_\odot$ stars during their RG and AGB phases (*Charbonnel,* 1995; *Wasserburg et al.,* 1995; *Langer et al.,* 1999; *Nollett et al.,* 2003) results in partial H burning, producing higher $^{14}N/^{15}N$ and lower $^{12}C/^{13}C$ ratios in the envelope than canonical models (see also *Huss et al.,* 1997). Such a process has originally been proposed to explain the low (as low as 3) $^{12}C/^{13}C$ ratios in K giants and early AGB stars (*Gilroy,* 1989; *Gilroy and Brown,* 1991) and the low $^{18}O/^{16}O$ ratios in certain presolar oxide grains (see below). The high $^{14}N/^{15}N$ ratios observed in many SiC grains provide a confirmation that this process occurs in low-mass stars.

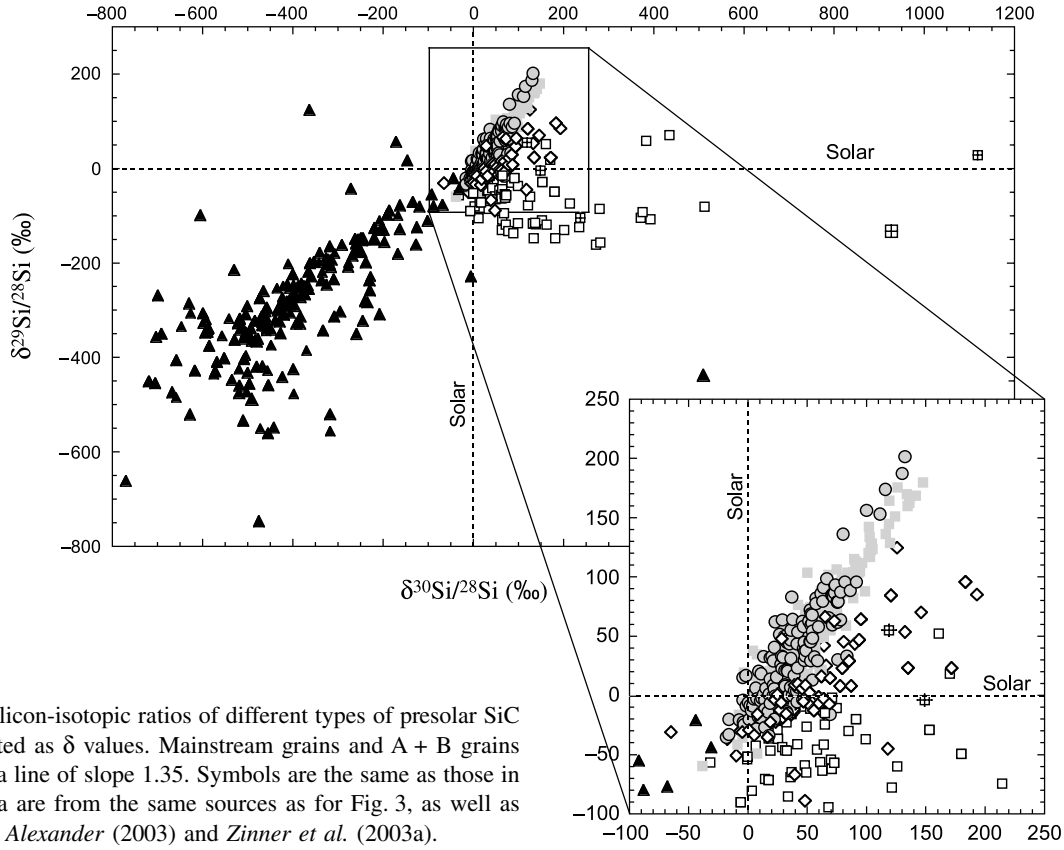

Fig. 5. Silicon-isotopic ratios of different types of presolar SiC grains plotted as δ values. Mainstream grains and A + B grains plot along a line of slope 1.35. Symbols are the same as those in Fig. 4. Data are from the same sources as for Fig. 3, as well as *Nittler and Alexander* (2003) and *Zinner et al.* (2003a).

Two other isotopes that are a signature of AGB stars are ^{26}Al and ^{22}Ne. Figure 6 shows inferred ^{26}Al/^{27}Al ratios in different types of SiC grains. Aluminum-26 is produced in the H shell by proton capture on ^{25}Mg and mixed to the surface by the third dredge-up (*Forestini et al.,* 1991; *Karakas and Lattanzio,* 2003). It can also be produced during "hot bottom burning" (HBB) when the convective envelope extends into the H-burning shell (*Lattanzio et al.,* 1997; *Karakas and Lattanzio,* 2003), but this process is believed to prevent carbon-star formation (*Frost and Lattanzio,* 1996). Neon-22, the main component in Ne-E, is produced in the He shell by ^{14}N + 2α. The Ne-isotopic ratios measured in SiC bulk samples (*Lewis et al.,* 1990, 1994) are very close to those expected for He-shell material (*Gallino et al.,* 1990) without much dilution with envelope material, indicating a special implantation mechanism by an ionized wind during the planetary nebula phase of the parent star (*Verchovsky et al.,* 2004). Evidence that the Ne-E(H) component originated from the He shell of AGB stars and not from ^{22}Na decay (*Clayton,* 1975b) is provided by the fact that in individual grains, of which only ~5% carry ^{22}Ne, it is always accompanied by ^{4}He (*Nichols et al.,* 1995). Excesses in ^{21}Ne in SiC relative to the predicted He-shell composition have been interpreted as being due to spallation by galactic cosmic rays (*Tang and Anders,* 1988a; *Lewis et al.,* 1990, 1994), which allows the determination of grain lifetimes in the ISM. Inferred exposure ages depend on grain size and range from 10 to 130 m.y. (*Lewis et al.,* 1994). However, this interpretation has been challenged (*Ott and Begemann,* 2000), and the question of IS ages of SiC is not settled.

In contrast to the light elements C, N, Ne, and Al and the heavy elements (see below), the Si-isotopic ratios of mainstream grains cannot be explained by nuclear processes

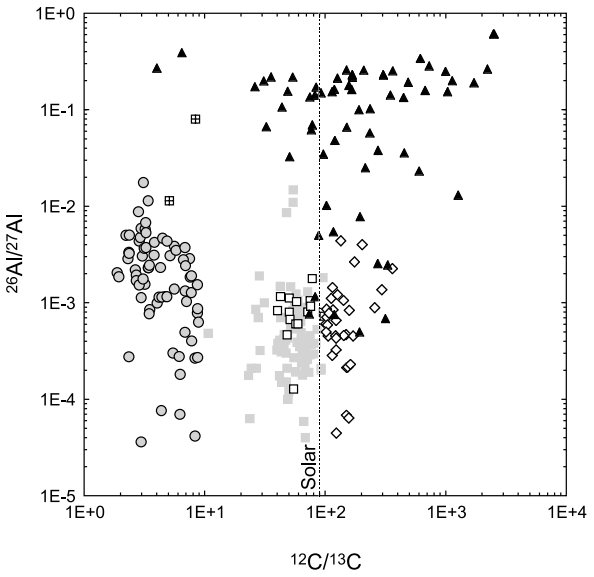

Fig. 6. Aluminum and C-isotopic ratios of individual presolar SiC grains. Symbols and sources for the data are the same as those for Figs. 4 and 5 and *Zinner et al.* (2005a).

taking place within their parent stars. In AGB stars the Si isotopes are affected by neutron capture in the He shell, leading to excesses in ^{29}Si and ^{30}Si along a line with slope 0.1–0.8 (depending on model parameters such as mass, metallicity, mass loss rate, and n-capture cross sections chosen) in a δ-value Si three-isotope plot (*Gallino et al.,* 1990, 1994; *Brown and Clayton,* 1992; *Lugaro et al.,* 1999; *Amari et al.,* 2001b; *Guber et al.,* 2003). Depending on the adopted cross sections (*Bao et al.,* 2000; *Guber et al.,* 2003), predicted excesses are only on the order of 20% for ^{29}Si and 40% for ^{30}Si in low-mass AGB stars of close-to-solar metallicity. This led to the proposal that many stars with varying initial Si-isotopic compositions contributed SiC grains to the SS (*Clayton et al.,* 1991; *Alexander,* 1993) and that neutron-capture nucleosynthesis in these stars only plays a secondary role in modifying these compositions. One explanation for the initial Si ratios in the parent stars of SiC grains is the evolution of the Si-isotopic ratios through galactic history as different generations of supernovae produced Si with increasing ratios of the secondary isotopes ^{29}Si and ^{30}Si to the primary ^{28}Si (*Gallino et al.,* 1994; *Timmes and Clayton,* 1996; *Clayton and Timmes,* 1997a,b). Another is based on local heterogeneities in the galaxy caused by the stochastic nature of the admixture of the ejecta from supernovae of varying type and mass (*Lugaro et al.,* 1999). *Clayton* (1997) has addressed the problem that most SiC grains have higher-than-solar ^{29}Si/^{28}Si and ^{30}Si/^{28}Si ratios by considering the possibility that the mainstream grains originated from stars that were born in central, more metal-rich regions of the galaxy and moved to the molecular cloud from which our Sun formed. *Alexander and Nittler* (1999), on the other hand, suggested that the Sun has an atypical Si-isotopic composition. Recently, *Clayton* (2003) has invoked a merger of our galaxy (high metallicity) with a satellite galaxy (low metallicity) some time before SS formation to explain the Si-isotopic ratios of mainstream grains. A more detailed treatment of the role of GCE on Si-isotopic ratios in SiC grains from AGB stars is found in *Nittler and Dauphas* (2006).

The Si-isotopic compositions of Y and Z grains have been explained by lower-than-solar metallicities for the parent stars of these grains, approximately half the solar metallicity (Z = 0.01 instead of $Z_\odot$ = 0.02) for Y grains (*Amari et al.,* 2001b) and about a third the solar metallicity (Z = 0.006) for Z grains (*Hoppe et al.,* 1997). [This value for the solar metallicity was used for the models in the cited papers. Recently, the solar metallicity has been revised downward to $Z_\odot$ = 0.0122, based on the newly determined solar abundances of C and O by *Asplund et al.* (2005).] Such stars are predicted to have larger isotopic shifts in the Si isotopes in agreement with the deviations of the Si-isotopic ratios of the Y and Z grains to the right of the mainstream correlation line (Fig. 5). If one projects the Si ratios measured in these grains back onto the galactic evolution line $\delta^{29}Si = \delta^{30}Si$ along lines predicted for neutron capture, the average ^{29}Si/^{28}Si (or δ^{29}Si) value of all Y grains is lower than the average of the mainstream grains and the Z grain average is even lower, in agreement with a continuous increase of the Si-isotopic ratios with metallicity during galactic evolution (*Zinner et al.,* 2001; *Nittler and Alexander,* 2003). The larger ^{12}C/^{13}C ratios of Y grains agree with an origin from low-metallicity parent stars, which during their TP-AGB phase dredge up more ^{12}C relative to that in the envelope, whose composition is depleted in C, and elements that experienced neutron capture, from the He shell (see also *Lugaro et al.,* 1999). However, for Z grains, which have ^{12}C/^{13}C ratios in the range of mainstream grains, one has to invoke cool bottom processing (*Wasserburg et al.,* 1995; *Nittler and Alexander,* 2003; *Nollett et al.,* 2003) during the red giant and AGB phase of their parent stars.

Titanium-isotopic ratios in single mainstream and Y grains (*Ireland et al.,* 1991; *Hoppe et al.,* 1994; *Alexander and Nittler,* 1999; *Amari et al.,* 2001b) and in bulk samples (*Amari et al.,* 2000) usually show excesses in all isotopes relative to ^{48}Ti, a result expected of neutron capture in AGB stars. Titanium ratios are correlated with those of Si, and, as for Si, theoretical models (*Lugaro et al.,* 1999) cannot explain the range of Ti ratios in single grains, indicating that the Ti-isotopic compositions are also dominated by galactic evolution effects (*Alexander and Nittler,* 1999; *Nittler and Dauphas,* 2006; *Nittler,* 2005). This interpretation is corroborated by Ti-isotopic data recently obtained for Z grains (*Zinner et al.,* 2005a). These grains show depletions in all isotopes relative to ^{48}Ti, analogous to ^{29}Si depletions in Z grains, except for ^{50}Ti where relative excesses are roughly correlated with ^{30}Si excesses. Apparently, for Ti the secondary isotopes ^{46}Ti, ^{47}Ti, ^{49}Ti, and ^{50}Ti increase in abundance relative to the α-isotope ^{48}Ti with galactic time and excesses in ^{50}Ti because of n-capture in AGB stars are larger in low-metallicity stars.

Calcium-isotopic data for ^{40,42,43,44}Ca have been obtained only in bulk samples (*Amari et al.,* 2000), but ^{44}Ca/^{40}Ca ratios have been measured in many individual SiC grains (see section 5.6.1). Excesses of ^{42}Ca and ^{43}Ca relative to ^{40}Ca agree with predictions for neutron capture. Large ^{44}Ca excesses are apparently due to the presence of type X grains (see section 5.6.1). Measurements of Fe-isotopic ratios have been reported by *Marhas et al.* (2004), who did not find any significant anomalies.

5.4.2. Heavy elements and the s-process. Heavy elements measured in bulk SiC samples, clearly dominated by mainstream grains, include the noble gases Kr and Xe (*Lewis et al.,* 1990; 1994) and the elements Sr (*Podosek et al.,* 2004), Ba (*Ott and Begemann,* 1990; *Zinner et al.,* 1991; *Prombo et al.,* 1993), Nd and Sm (*Zinner et al.,* 1991; *Richter et al.,* 1993), and Dy (*Richter et al.,* 1994). Resonance ionization mass spectrometry has made it possible to measure the isotopic composition of heavy elements in individual grains, and analyses of Sr (*Nicolussi et al.,* 1998b), Zr (*Nicolussi et al.,* 1997), Mo (*Nicolussi et al.,* 1998a), Ru (*Savina et al.,* 2004a), and Ba (*Savina et al.,* 2003a) have been reported (see also *Lugaro et al.,* 2003; *Savina et al.,* 2003b). Secondary ion mass spectrometry isotopic meas-

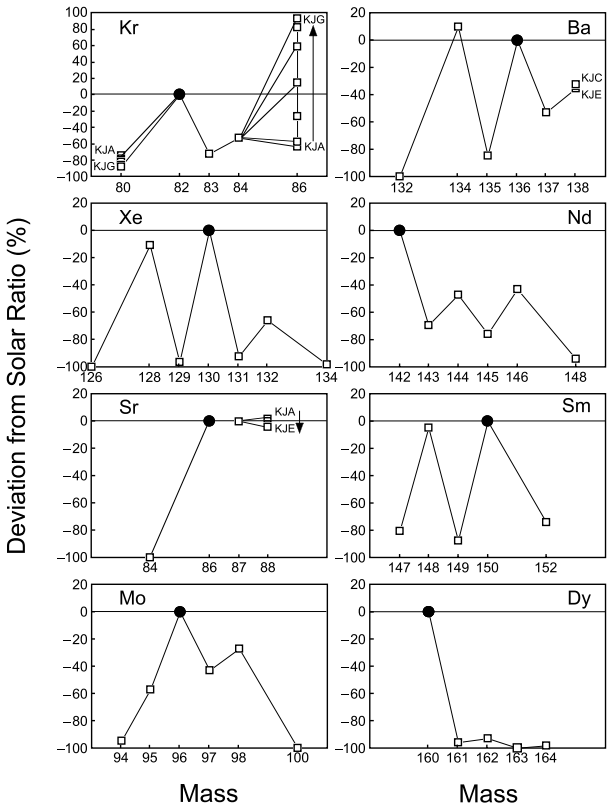

Fig. 7. Isotopic patterns of heavy elements derived from measurements of bulk samples of SiC extracted from the Murchison meteorite. What is plotted are the extrapolated s-process components [the so-called G-components (see *Hoppe and Ott,* 1997)]. Isotopic ratios are relative to the reference isotope plotted as a solid circle and are normalized to the solar isotopic ratios. Data are from *Lewis et al.* (1994) (Kr and Xe), *Podosek et al.* (2004) (Sr), *Prombo et al.* (1993) (Ba), *Richter et al.* (1993) (Nd and Sm), *Richter et al.* (1994) (Dy), and *Lugaro et al.* (2003) (Mo). For ^{80}Kr, ^{86}Kr, ^{138}Ba, and ^{88}Sr the isotopic ratios vary with grain size and the names of different grain size fractions of SiC from the Murchison meteorite (*Amari et al.,* 1994) are indicated in the figure. Grain sizes increase from KJA (average diameter 0.38 μm) to KJG (3.0 μm).

urements of Ba in single grains have also been reported (*Marhas et al.,* 2003). All these elements show the signature of the s-process.

The s-process isotopic patterns of Xe, Kr, Sr, Mo, Ba, Nd, Sm, and Dy are shown in Fig. 7. The isotopic compositions of SiC grains from AGB stars are a mixture of a component with close-to-solar ratios (the so-called N-component) that apparently represents the original composition of the parent star(s) and a pure s-process component that results from nucleosynthesis in the He intershell and TDU. The s-process patterns in Fig. 7 are obtained by extrapolating the measured ratios on three-isotope plots to zero contributions of either p-only or r-only isotopes. It should be mentioned that these patterns are averages obtained from the analysis of many grains. Individual grain analysis shows large variations among grains. One reason is the fact that in a given star SiC grains condense while more and more s-process nuclei are dredged up, enriching the envelope in these and thereby changing the isotopic ratios of the heavy elements. However, individual grains have a wider range in their isotopic ratios than would be expected from a single combination of stellar mass, metallicity, and ^{13}C pocket, confirming multiple stellar sources for presolar SiC.

For all elements listed above (except for Dy) there is good agreement with theoretical models of the s-process in low-mass (mostly <3 $M_\odot$) AGB stars (*Gallino et al.,* 1993, 1997; *Lugaro et al.,* 2003; *Savina et al.,* 2004a). Discrepancies with earlier model calculations were caused by incorrect nuclear cross sections and could be resolved by improved experimental determinations (e.g., *Guber et al.,* 1997; *Wisshak et al.,* 1997; *Koehler et al.,* 1998). The s-process isotopic patterns observed from grains allow the determination of different parameters such as neutron exposure, temperature, and neutron density (*Hoppe and Ott,* 1997). These parameters depend in turn on stellar mass and metallicity, as well as on the neutron source operating in AGB stars. Comparisons of isotopic patterns in grains and composition predictions from stellar models thus allow information to be obtained about the parent stars of the grains. For example, the Ba-isotopic ratios indicate a neutron exposure that is only half that required to explain the bulk s-process element abundances in the SS, and also indicate that most grains come from stars of less than 3 $M_\odot$ (*Ott and Begemann,* 1990; *Gallino et al.,* 1993). Another example is provided by the abundance of ^{96}Zr in single grains, which is sensitive to neutron density because of the relatively short half-life of ^{95}Zr (~64 d). While the ^{13}C(α,n) source with its low neutron density does not significantly produce ^{96}Zr, production by activation of the ^{22}Ne(α,n) source during later thermal pulses in AGB stars depends sensitively on stellar mass. Some grains have very low ^{96}Zr/^{94}Zr ratios, indicating that the ^{22}Ne(α,n) source was weak in their parent stars and points to low-mass AGB stars as the source of mainstream grains (*Lugaro et al.,* 2003). An exciting new result is evidence for the initial presence of extinct ^{99}Tc in presolar SiC grains (*Savina et al.,* 2004a). The Ru isotopes measured by RIMS display an s-process isotopic pattern and show good agreement with theoretical prediction for low-mass AGB stars except for an excess in ^{99}Ru. This excess is well explained by the decay of ^{99}Tc ($T_{1/2}$ = 0.21 m.y.). It is fitting that signatures of this element, whose presence in stars (*Merrill,* 1952) was the first direct astronomical evidence for stellar nucleosynthesis, are now found in stardust analyzed in the laboratory.

5.4.3. High-density graphite grains. Graphite grains of four different density fractions have been isolated from the Murchison meteorite (*Amari et al.,* 1995b,d). Low-density (1.6–2.05 g cm^{-3}) graphite grains have isotopic signatures indicating a SN origin (see section 5.6). Noble gas measurements have revealed two different s-process components of

Kr in the four graphite fractions (*Amari et al.,* 1995b). The three lower-density fractions have Kr-isotopic compositions consistent with a massive-star origin. In contrast, Kr in the highest density (2.15–2.20 g cm^{-3}) fraction, KFC1, indicates an AGB origin. Such an origin is also indicated by the high Zr, Mo, and Ru contents of these grains (*Bernatowicz et al.,* 1996); these s-process elements are expected to be enhanced in the envelope of carbon stars (*Lodders and Fegley,* 1997). *Nicolussi et al.* (1998c) have reported RIMS measurements of Zr- and Mo-isotopic ratios in KFC1 grains in which no other isotopic ratios had been measured. Several grains show s-process patterns for Zr and Mo, similar to those exhibited by mainstream SiC grains, although two grains with a distinct s-process pattern for Zr have normal Mo. Two grains have extreme ^{96}Zr excesses, indicating an origin in SNe or in low-metallicity AGB stars (*Davis et al.,* 2003), but the Mo isotopes in one are almost normal. Molybdenum, like N, might have suffered isotopic equilibration in graphite. High-density graphite grains apparently come from AGB stars as well as from supernovae. They have a wide range of $^{12}C/^{13}C$ ratios with peaks around 10 and around 300–400 in the distribution (*Hoppe et al.,* 1995). If the grains with isotopically light C have a carbon-star origin, they must originated from low-metallicity or intermediate-mass AGB stars, which are expected to have higher $^{12}C/^{13}C$ ratios than the low-mass solar-metallicity AGB stars that produced the mainstream grains (*Amari et al.,* 2001b).

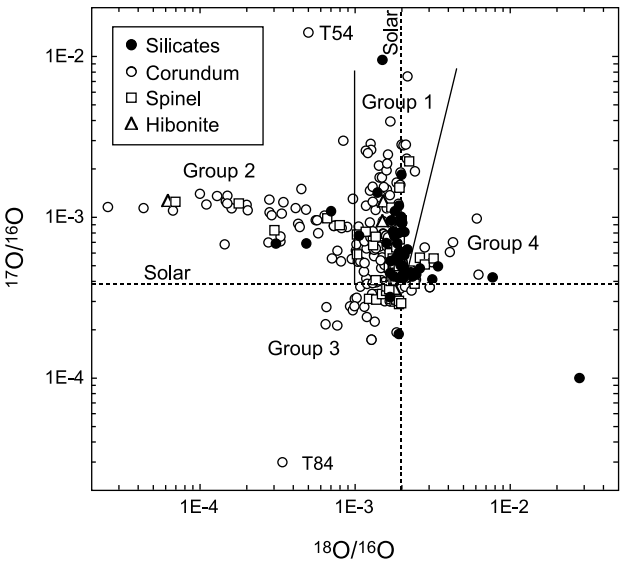

Fig. 8. Oxygen-isotopic ratios in individual oxide grains. Data are from *Nittler et al.* (1997, 1998), *Choi et al.* (1998, 1999), *Krestina et al.* (2002), *Zinner et al.* (2003b, 2004), *Messenger et al.* (2003), *Nguyen and Zinner* (2004), *Floss and Stadermann* (2004), and unpublished data from N. Krestina (2003), L. Nittler (2005), and R. Strebel (2003).

5.5. Oxide Grains from Red Giant and Asymptotic Giant Branch Stars

Presolar oxide grains identified to date include Al oxide (Al_2O_3) (*Huss et al.,* 1994; *Hutcheon et al.,* 1994; *Nittler et al.,* 1994, 1997, 1998; *Nittler and Alexander,* 1999; *Strebel et al.,* 1996; *Choi et al.,* 1998, 1999; *Krestina et al.,* 2002), spinel (*Nittler et al.,* 1997; *Choi et al.,* 1998; *Nguyen et al.,* 2003; *Zinner et al.,* 2003b), hibonite (*Choi et al.,* 1999; *Krestina et al.,* 2002; *Nittler et al.,* 2005), and silicates (*Messenger et al.,* 2003; *Floss and Stadermann,* 2004; *Nguyen and Zinner,* 2004; *Mostefaoui et al.,* 2004b; *Mostefaoui and Hoppe,* 2004; *Nagashima et al.,* 2004). In contrast to SiC grains in meteorites, all of which are of presolar origin, presolar oxides constitute only a small fraction of all oxides and have been identified by O-isotopic measurements in the ion microprobe.

The O-isotopic ratios of presolar oxide and silicate grains are shown in Fig. 8. Because different search techniques were used to locate these grains, the numbers of grains of different mineral phases does not reflect their abundances in meteorites (see also Table 3). Nor does the distribution of isotopic ratios accurately describe the actual distribution among presolar oxide grains. The reason is that searches by direct isotopic imaging (*Nittler et al.,* 1997) discriminate against grains with close-to-normal $^{18}O/^{16}O$ ratios, while raster imaging of tightly packed grains (*Nguyen et al.,* 2003) tends to dilute anomalous isotopic ratios.

Nittler et al. (1997) have classified presolar oxide grains into four different groups according to their O-isotopic ratios (see Fig. 8). The isotopic composition of grains is the result of the original compositions of the parent stars and several different episodes of H burning during the evolution of these stars. Group 1 grains have O-isotopic ratios similar to those observed in red giant and AGB stars (*Harris and Lambert,* 1984; *Harris et al.,* 1987; *Smith and Lambert,* 1990), indicating such an origin also for the grains. These compositions can be explained by H burning in the core of low-to-intermediate mass stars followed by mixing of core material into the envelope during the first dredge-up (also second dredge-up in low-metallicity stars with $M > 3\ M_\odot$) (*Boothroyd et al.,* 1994; *Boothroyd and Sackmann,* 1999). Variations in $^{17}O/^{16}O$ ratios mainly correspond to differences in stellar mass, while those in $^{18}O/^{16}O$ correspond to differences in the metallicity of the parent stars. According to galactic chemical evolution models, $^{17}O/^{16}O$ and $^{18}O/^{16}O$ ratios are expected to increase as a function of stellar metallicity (*Timmes et al.,* 1995). Group 3 grains could thus come from low-mass stars (producing only small ^{17}O enrichments) with lower-than-solar metallicity (originally having lower-than solar $^{17}O/^{16}O$ and $^{18}O/^{16}O$ ratios). Group 2 grains have ^{17}O excesses and large ^{18}O depletions ($^{18}O/^{16}O < 0.001$). Such depletions cannot be produced by the first and second dredge-up but have been successfully explained by extra mixing (cool bottom processing) of low-mass ($M < 1.65\ M_\odot$) stars during the AGB phase that circulates mate-

rial from the envelope through regions close to the H-burning shell (*Wasserburg et al.,* 1995; *Denissenkov and Weiss,* 1996; *Nollett et al.,* 2003). Group 4 grains have both ^{17}O and ^{18}O excesses. If they originated from AGB stars they could either come from low-mass stars, in which ^{18}O produced by He burning of ^{14}N during early pulses was mixed into the envelope by third dredge-up (*Boothroyd and Sackmann,* 1988), or from stars with high metallicity. The O-isotopic ratios of the unusual grain T54 (*Nittler et al.,* 1997) has been interpreted to have an origin in a star with >5 $M_\odot$ that experienced hot bottom burning, a condition during which the convective envelope extends into the H-burning shell (*Boothroyd et al.,* 1995; *Lattanzio et al.,* 1997).

The Mg isotopes and Al have been measured in corundum (*Nittler et al.,* 1997; *Choi et al.,* 1998; 1999; *Krestina et al.,* 2002), spinel (*Nittler et al.,* 2003; *Zinner et al.,* 2005b), hibonite (*Nittler et al.,* 2005), and a silicate grain (*Nguyen and Zinner,* 2004). Because Mg in corundum is very low, with the exception of one grain that has a ^{25}Mg excess of ~25% (*Choi et al.,* 1998), only ^{26}Mg excesses due to ^{26}Al decay have been seen. Some but not all grains in the four groups show evidence for initial ^{26}Al. Because ^{26}Al is produced in the H-burning shell (*Forestini et al.,* 1991; *Mowlavi and Meynet,* 2000; *Karakas and Lattanzio,* 2003), dredge-up of material during the TP-AGB phase is required, and grains without ^{26}Al must have formed before their parent stars reached this evolutionary stage. Initial $^{26}Al/^{27}Al$ ratios are highest in Group 2 grains (*Nittler et al.,* 1997; *Choi et al.,* 1998), which is explained if these grains formed in the later stages of the AGB phase when more ^{18}O had been destroyed by cool bottom processing and more ^{26}Al dredged up (*Choi et al.,* 1998). The high Mg content of spinel and hibonite grains also provides the opportunity to obtain more precise $^{25}Mg/^{24}Mg$ ratios (*Nittler et al.,* 2003, 2005; *Zinner et al.,* 2005b). Oxygen and Mg isotopes in grains from RG and AGB stars are affected by nucleosynthesis occurring at different stages of the parent stars' evolution. Oxygen-isotopic ratios are mostly determined by core H burning during the main-sequence phase followed by the first (and second) dredge-up, but can also be affected by CBP and HBB during the RG and AGB phases. In contrast, Mg isotopes and ^{26}Al are changed during the AGB phase as well as by CBP and HBB (*Karakas and Lattanzio,* 2003). In addition, both O and Mg carry the original isotopic signatures of the parent stars. The O- and Mg-isotopic ratios of the grains appear to show the effects of all these processes. In particular, one spinel with large ^{25}Mg and ^{26}Mg excesses and a large ^{18}O depletion must come from an intermediate-mass AGB star that experienced HBB (*Nittler et al.,* 2003). One presolar pyroxene grain with ^{18}O depletion has a ^{26}Mg excess, most likely indicating CBP (*Nguyen and Zinner,* 2004).

Mostefaoui and Hoppe (2004) have measured Si-isotopic ratios in eight presolar silicate grains. The data points lie close to a line that is parallel to the mainstream correlation line of presolar SiC grains but shifted to the left on a δ-value three-isotope plot. The authors interpreted this to indicate that the parent stars of the silicate grains had not experienced TDU of s-processed material that shifted the Si-isotopic compositions of SiC grains to the right.

Titanium-isotopic ratios have been determined in a few presolar corundum grains (*Choi et al.,* 1998; *Hoppe et al.,* 2003). The observed ^{50}Ti excesses agree with those predicted to result from neutron capture in AGB stars. The depletions in all Ti isotopes relative to ^{48}Ti found in two grains indicate that, just as for SiC grains, galactic evolution affects the isotopic compositions of the parent stars of oxide grains. Several hibonite grains were found to have large ^{41}K excesses (*Choi et al.,* 1998; *Nittler et al.,* 2005), corresponding to a $^{41}Ca/^{40}Ca$ ratio of 2×10^{-4}, within the range of values predicted for the envelope of AGB stars (*Wasserburg et al.,* 1994).

5.6. Grains from Supernovae

5.6.1. Silicon carbide, silicon nitride, and graphite. According to their isotopic compositions SiC grains of type X, Si_3N_4, and low-density graphite grains are believed to have a SN origin. The smoking gun is the initial presence of short-lived ^{44}Ti ($T_{1/2}$ = 60 yr) inferred from large ^{44}Ca excesses in many grains (*Amari et al.,* 1992, 1995c; *Hoppe et al.,* 1996b, 2000; *Nittler et al.,* 1996; *Besmehn and Hoppe,* 2003). This isotope is only produced in supernovae (*Timmes et al.,* 1996). Another smoking gun is the presence of even shorter-lived ^{49}V ($T_{1/2}$ = 330 d) inferred from large ^{49}Ti excesses (*Hoppe and Besmehn,* 2002).

Type X grains are characterized by mostly ^{12}C and ^{15}N excesses relative to solar (Fig. 4), excesses in ^{28}Si (Fig. 5), and very large $^{26}Al/^{27}Al$ ratios, ranging up to 0.6 (Fig. 6) (*Amari et al.,* 1995c; *Hoppe et al.,* 1996b, 2000; *Nittler et al.,* 1995; *Lin et al.,* 2002). In ~15% of the grains evidence for ^{44}Ti has been found. Other isotopic signatures also point to a SN origin. In Type II supernovae ^{44}Ti is produced in the Ni zone that experienced an α-rich freezeout and the Si/S zone that experienced explosive O or incomplete Si burning. Silicon in the latter consists of almost pure ^{28}Si and substantial contributions must come from this zone to explain the large ^{28}Si excesses in the X grains. High $^{12}C/^{13}C$ and low $^{14}N/^{15}N$ ratios are the signatures of He burning and are predicted for the He/C zone; and high $^{26}Al/^{27}Al$ ratios can be reached in the He/N zone by H burning. Some SiC X grains also show large excesses in ^{49}Ti (*Amari et al.,* 1992; *Nittler et al.,* 1996; *Hoppe and Besmehn,* 2002). The correlation of these excesses with the V/Ti ratio (*Hoppe and Besmehn,* 2002) indicates that they come from the decay of short-lived ^{49}V ($T_{1/2}$ = 330 d) and that the grains must have formed within a few months of the explosion. Like ^{44}Ti, ^{49}V is produced in the Si/S zone. Resonance ionization mass spectrometry isotopic measurements of Fe, Sr, Zr, Mo, and Ba have been made on X grains (*Pellin et al.,* 1999, 2000a; *Davis et al.,* 2002). The most complete are the Mo measurements, which reveal large excesses in ^{95}Mo and ^{97}Mo

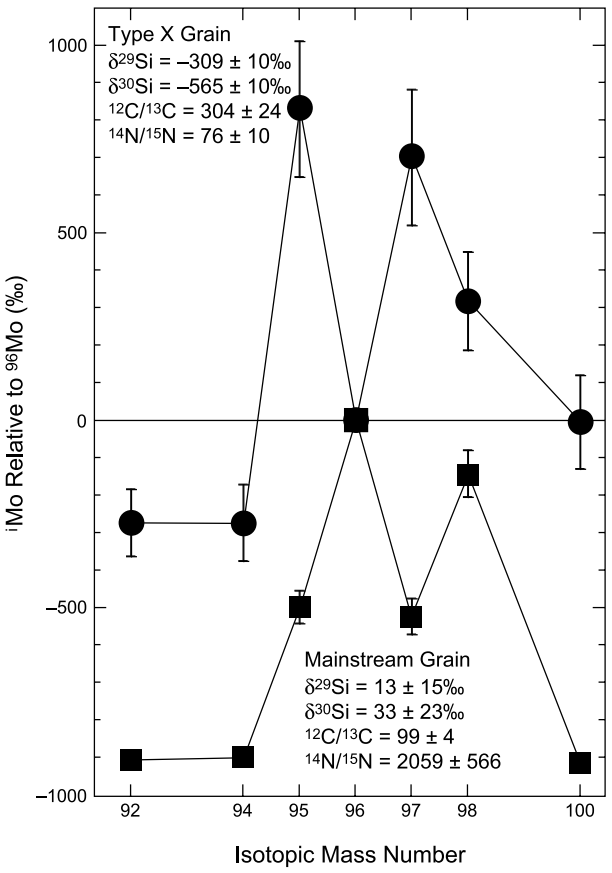

Fig. 9. Molybdenum-isotopic patterns measured by RIMS in a type X and mainstream SiC grain. Figure is from *Pellin et al.* (1999), courtesy of A. Davis.

(Fig. 9). Whereas the mainstream grain shown in Fig. 9 has a typical s-process pattern, in agreement with bulk measurements of other heavy elements such as Xe, Ba, and Nd (Fig. 7), the Mo pattern of the X grain is completely different and indicates neutron capture at much higher neutron densities. It is successfully explained by a neutron-burst model (*Meyer et al.,* 2000). In the Type II SN models by *Rauscher et al.* (2002), an intense neutron burst is predicted to occur when the SN shock heats the He-burning shell and liberates neutrons by the $^{22}Ne(\alpha,n)^{25}Mg$ reaction (see section 2.2.6). This neutron burst can account for the Mo-isotopic patterns observed in X grains.

Presolar Si_3N_4 grains are extremely rare (in Murchison SiC-rich separates ~5% of SiC of type X) but automatic ion imaging has been successfully used to detect those with large ^{28}Si excesses (*Nittler et al.,* 1998; *Besmehn and Hoppe,* 2001; *Lin et al.,* 2002; *Nittler and Alexander,* 2003). The C-, N-, Al-, and Si-isotopic signatures of these grains are the same as those of SiC grains of type X (see Figs. 4–6). Although no resolvable ^{44}Ca excesses have been detected so far (*Besmehn and Hoppe,* 2001), the similarity with X grains implies a SN origin for these grains.

Low-density (LD) graphite grains have in general higher trace-element concentrations than those with higher densities and for this reason have been studied in detail for their isotopic compositions (*Travaglio et al.,* 1999). Many LD grains have ^{15}N and large ^{18}O excesses (*Amari et al.,* 1995e) and high $^{26}Al/^{27}Al$ ratios. Excesses in ^{18}O are correlated with $^{12}C/^{13}C$ ratios. Many grains for which Si-isotopic ratios could be determined with sufficient precision show ^{28}Si excesses, although large ^{29}Si and ^{30}Si excesses are also seen. The similarities of the isotopic signatures with those of SiC X point to a SN origin of LD graphite grains. The ^{18}O excesses are compatible with such an origin. Helium burning produces ^{18}O from ^{14}N, which dominates the CNO isotopes in material that had undergone H burning via the CNO cycle. As a consequence, the He/C zone in pre-SNII massive stars, which experienced partial He burning, has a high ^{18}O abundance (*Woosley and Weaver,* 1995). Wolf-Rayet stars during the WN-WC transitions are predicted to also show ^{12}C, ^{15}N, and ^{18}O excesses and high $^{26}Al/^{27}Al$ ratios (*Arnould et al.,* 1997a) but also large excesses in ^{29}Si and ^{30}Si and are therefore excluded as parent stars of LD graphite grains with ^{28}Si excesses.

Additional features that indicate a SN origin of LD graphite grains are evidence for ^{44}Ti (*Nittler et al.,* 1996) and large excesses of ^{41}K, which must be due to the decay of the radioisotope ^{41}Ca ($T_{1/2} = 1.05 \times 10^5$ yr) (*Amari et al.,* 1996). Inferred $^{41}Ca/^{40}Ca$ ratios are much higher (0.001 to 0.01) than those predicted for the envelopes of AGB stars (*Wasserburg et al.,* 1994) but are predicted to be the result of neutron capture in the C- and O-rich zones of Type II supernovae (*Woosley and Weaver,* 1995). Measurements of Ca-isotopic ratios in grains without evidence for ^{44}Ti show excesses in ^{42}Ca, ^{43}Ca, and ^{44}Ca, with ^{43}Ca having the largest excess (*Amari et al.,* 1996; *Travaglio et al.,* 1999). This pattern is best explained by neutron capture in the He/C and O/C zones of Type II supernovae. Titanium-isotopic ratios show large excesses in ^{49}Ti and smaller ones in ^{50}Ti (*Amari et al.,* 1996; *Nittler et al.,* 1996; *Travaglio et al.,* 1999). This pattern also indicates neutron capture and is well matched by predictions for the He/C zone (*Amari et al.,* 1996). However, large ^{49}Ti excesses in grains with relatively low (10–100) $^{12}C/^{13}C$ ratios can only be explained by the decay of ^{49}V (*Travaglio et al.,* 1999).

The isotopic compositions of SN grains pose the most serious challenge to nuclear astrophysicists. The reason is that the isotopic signatures found in the grains occur in massive stars in very different stellar zones, which experienced different stages of nuclear burning before the SN explosion (e.g., *Woosley and Weaver,* 1995; *Rauscher et al.,* 2002). The isotopic signatures of the SN grains thus suggest deep and inhomogeneous mixing of matter from these different zones in the SN ejecta. While the Ti- and Si-isotopic signature of the grains requires contributions from the Ni, O/Si, and Si/S zones, which experienced Si-, Ne-, and O-burning, significant contributions must also come from the He/N and He/C zones that experienced H and incomplete He burning in order to achieve C > O, the requirement for SiC or

graphite condensation from a gas under equilibrium conditions (*Larimer and Bartholomay,* 1979; *Lodders and Fegley,* 1997). Also the C-, N-, O-, and Al-isotopic ratios indicate contributions from these zones. Furthermore, addition of material from the intermediate O-rich layers must be severely limited. Astronomical observations indicate extensive mixing of SN ejecta (e.g., *Ebisuzaki and Shibazaki,* 1988; *Hughes et al.,* 2000) and hydrodynamic models of SN explosions predict mixing in the ejecta initiated by the formation of Rayleigh-Taylor instabilities (e.g., *Herant et al.,* 1994). In order to better constrain theoretical models of SN nucleosynthesis, *Travaglio et al.* (1999), *Hoppe et al.* (2000), and *Yoshida and Hashimoto* (2004) tried to match the isotopic compositions of SN grains by performing multizone mixing calculations. While these calculations qualitatively account for the grains' isotopic signatures, they cannot quantitatively reproduce all the measured ratios. One example is that the grains show excesses of ^{29}Si over ^{30}Si compared to solar. This is a long-standing problem: SN models cannot account for the solar ^{29}Si/^{30}Si ratio (*Timmes and Clayton,* 1996). Studies of SiC X grains isolated from the Qingzhen enstatite chondrite (*Lin et al.,* 2002) suggest that there are two population of X grains with different trends in the Si-isotopic ratios, the minor population having lower-than-solar ^{29}Si/^{30}Si ratios. The lowest measured ^{14}N/^{15}N and highest ^{26}Al/^{27}Al and ^{44}Ti/^{48}Ti ratios can only be explained by including substantial contributions from the Ni shell (*Yoshida and Hashimoto,* 2004).

However, it still has to be seen whether mixing can occur on a microscopic scale and whether instabilities allow mixing of matter from non-neighboring zones while excluding large contributions from the intermediate O-rich zones. *Clayton et al.* (1999) and *Deneault et al.* (2003) took an alternative approach by suggesting condensation of carbonaceous phases in Type II SN ejecta even while C < O because of the destruction of CO in the high-radiation environment of the ejecta. This relaxes the chemical constraint on mixing. While it might work for graphite, there are doubts whether SiC and Si_3N_4 can condense from a gas with C < O (*Ebel and Grossman,* 2001). Recently, *Clayton et al.* (2002) and *Deneault et al.* (2003) have tried to account for isotopic signatures from different SN zones by considering implantation into newly condensed grains. When the SN shock interacts with density drops at composition boundaries in the star or with mass lost from the pre-supernova star, reverse shocks are generated and work their way back into the ejecta. The gas is slowed but the newly condensed grains, because of their greater inertia, rush ahead of the gas from which they condensed. As the grains overtake the overlying layers, atoms from those layers may be implanted into the grains.

5.6.2. Diamond. Although diamond is the most abundant presolar grain species in meteorites (see Table 3), it remains the least understood. The only presolar isotopic signatures indicating a SN origin are those of Xe-HL (*Lewis et al.,* 1987) and Te (*Richter et al.,* 1998), and to a marginal extent also those of Sr and Ba (*Lewis et al.,* 1991). Nitrogen shows a ^{15}N depletion of 343%, but isotopically light N is produced by the CN cycle in all stars and is therefore not very diagnostic. Furthermore, while the ^{15}N depletion (corresponding to ^{14}N/^{15}N = 414) is relative to the terrestrial ratio (^{14}N/^{15}N = 272), the diamond ratio is close to the currently preferred solar system ratio of 435 ± 55 (*Owen et al.,* 2001). The C-isotopic composition of bulk diamond is essentially the same as that of the SS (*Russell et al.,* 1991, 1996) and diamonds are too small (the average size is ~2.6 nm, hence the term nanodiamonds) to be analyzed as single grains. Clayton and coworkers (*Clayton,* 1989; *Clayton et al.,* 1995) have tried to also attribute the diamonds and their C- and N-isotopic compositions to a Type II supernova. This requires mixing of contributions from different SN zones. However, because only one diamond grain in a million contains a Xe atom, a solar origin of a large fraction of the nanodiamonds remains a distinct possibility (*Dai et al.,* 2002). The light- and heavy-isotope enrichments in Xe-HL have been interpreted as being due to the p-process (the Xe-L) and a neutron burst (the Xe-H), signaling a SN origin for the diamonds (*Heymann and Dziczkaniec,* 1979, 1980; *Clayton,* 1989). The Xe-H isotopic pattern does not match that expected from the r-process; however, *Ott* (1996) proposed that if r-process Xe is separated from iodine and tellurium precursors on a timescale of a few hours after their production, a Xe-H pattern matching the diamonds results. *Richter et al*. (1997) found that this timescale model also provides a better match to their measured Te-isotopic pattern than the neutron burst model. Still, at present, we do not have an unambiguous identification of the origin of the Xe-HL and Te, and of the diamonds (in case they have a different origin).

5.6.3. Oxide grains. Of the more than 500 presolar oxide grains that have been analyzed to date, only one has the typical isotopic signature expected for SN condensates, namely a large ^{16}O excess (Al-rich oxide grain T84 in Fig. 8) (*Nittler et al.,* 1998). All SN zones dominated by O (O/C, O/Ne, O/Si) are dominated by ^{16}O (*Woosley and Weaver,* 1995; *Thielemann et al.,* 1996; *Rauscher et al.,* 2002) as a result of the ^{12}C(α,γ)^{16}O reaction during the latter stages of He burning in the pre-supernova evolution. The paucity of such grains, whose abundance is expected to dominate that of carbonaceous phases with a SN origin, remains a puzzle. It has been suggested that oxide grains from supernovae are smaller than those from red giant stars but recent measurements of submicrometer grains have not uncovered any additional oxides with large ^{16}O excesses (*Zinner et al.,* 2003b; *Nguyen et al.,* 2003). A SN origin has been proposed by *Choi et al.* (1998) for the oxide grains with the largest ^{18}O excesses. None of the O-rich SN layers have large ^{18}O excesses, but O in the He/C zone is dominated by ^{18}O, thus material from this zone has to be admixed to material from O-rich zones in order to reproduce the compositions of these grains. Recently, *Messenger and Keller* (2004) reported a silicate grain from a cluster IDP whose ^{18}O/^{16}O ratio is much higher than has been observed in any other O-rich grains (see Fig. 8) and is comparable to the ratios found in some LD graphite grains of SN origin. Furthermore, the grain has

a large depletion in ^{17}O. There is little doubt that it originated from a SN and its O-isotopic ratios reflect mixing between zones dominated by ^{16}O (O/C, O/Ne) and ^{18}O (He/C zone).

5.7. Grains from Novae

A few SiC and graphite grains have isotopic ratios that are best explained by a nova origin (*Amari et al.,* 2001a; *Nittler and Hoppe,* 2004a,b). These grains have low $^{12}C/^{13}C$ and $^{14}N/^{15}N$ (the SiC grains) ratios (Fig. 4), large ^{30}Si excesses (Fig. 5), and high $^{26}Al/^{27}Al$ ratios (Fig. 6). All these features are predicted to be produced by explosive H burning taking place in classical novae (e.g., *Kovetz and Prialnik,* 1997; *Starrfield et al.,* 1998; *José et al.,* 1999), but the predicted anomalies are much larger than those found in the grains, and the nova ejecta have to be mixed with material of close-to-solar isotopic compositions. A comparison of the data with the models implicates ONe novae with a WD mass of at least 1.25 $M_\odot$ as the most likely sources (*Amari et al.,* 2001a; *José et al.,* 2004). A nova origin of some graphite grains (with densities 2.1–2.2 g cm^{-3}) is also indicated by their Ne-isotopic ratios. Laser extraction gas mass spectrometry of single grains show that, like SiC grains, only a small fraction of them contains evidence for Ne-E. Two of these grains have $^{20}Ne/^{22}Ne$ ratios that are lower than ratios predicted to result from He burning in any known stellar sources, implying decay of ^{22}Na (*Nichols et al.,* 2004). Furthermore, their ^{22}Ne is not accompanied by ^{4}He, which is expected if Ne was implanted. The $^{12}C/^{13}C$ ratios of these two grains are 4 and 10.

5.8. Silicon Carbide Grains of Type A + B

Grains of type A + B have $^{12}C/^{13}C < 10$ but their Si-isotopic ratios plot along the mainstream line (Figs. 4 and 5). In contrast to mainstream grains, many A + B grains have lower than solar $^{14}N/^{15}N$ ratios (*Hoppe et al.,* 1995, 1996a; *Huss et al.,* 1997; *Amari et al.,* 2001c). While the isotopic ratios of mainstream, Y, and Z grains find an explanation in nucleosynthetic models of AGB stars, a satisfactory explanation of the isotopic ratios of A + B grains has not been achieved. The low $^{12}C/^{13}C$ ratios of these grains combined with the requirement for a C-rich environment during their formation indicate He burning followed by limited H burning in their stellar sources. Astrophysical sites for this process are not well known. Candidates for the parent stars of grains with no s-process enhancements (*Amari et al.,* 1995a; *Pellin et al.,* 2000b; *Savina et al.,* 2003c) are J-type carbon stars, which have low $^{12}C/^{13}C$ ratios (*Lambert et al.,* 1986). Unfortunately, J stars are not well understood and there are essentially no astronomical observations of N-isotopic ratios in such stars. The only exception, the observation of $^{14}N/^{15}N > 70$ (*Wannier et al.,* 1991), does not provide much of a constraint. Furthermore, the low $^{14}N/^{15}N$ ratios observed in some of the grains as well as the C-rich nature of their parent stars appear to be incompatible with the consequences of H burning in the CNO cycle, which seems to be responsible for the low $^{12}C/^{13}C$ ratios of J stars and the grains. A + B grains with s-process enhancements might come from post-AGB stars that undergo a very late thermal pulse. An example of such a star is Sakurai's object (e.g., *Asplund et al.,* 1999; *Herwig,* 2001). However, grains with low $^{14}N/^{15}N$ ratios pose a problem. *Huss et al.* (1997) proposed that the currently used $^{18}O(p,\alpha)^{15}N$ reaction rate is too low by a factor of 1000. This would result in low $^{12}C/^{13}C$ and $^{14}N/^{15}N$ ratios if an appropriate level of CBP is considered. Savina and coworkers (*Savina et al.,* 2003c, 2004b) have analyzed Mo and Ru isotopes in several A + B SiC grains by RIMS. Most grains have close-to-solar isotopic ratios, indicating no neutron exposure. However, one grain shows a Mo pattern similar to those shown by X grains (see Fig. 9), indicating a neutron burst, and another grain exhibits a p-process signature in the form of ^{92}Mo, ^{94}Mo, ^{96}Ru, and ^{98}Ru excesses. While these findings seems to indicate a SN origin, it is difficult to reconcile the C- and Si-isotopic ratios with such an origin. The authors suggested the transfer of material in a binary system.

6. CONCLUSION AND OUTLOOK

Astronomy, as an observational science, requires us to glean information about stars from any relevant source nature provides. Traditionally, this source has been electromagnetic radiation, but, as we have seen in this review, novel techniques in chemistry and advances in mass spectrometry have initiated an entirely new type of astronomy, the astronomy of presolar meteoritic grains, or stardust. The detailed isotopic abundances available from stardust are heretofore undreamt-of probes of stellar nucleosynthesis, which, as apparent from this review, already challenge our understanding of stellar astrophysics. It is certain that new isotopic measurements and discovery of new stardust grains will be major forces in driving stellar models to the next level of sophistication.

As our understanding of the production and survival of stardust grows, so too will our understanding of the formation of the SS. The nuclear anomalies in primitive solar system minerals are no doubt inherited in a complicated way from their anomalous precursor dust. Unraveling the complex history of these samples from their initial building blocks to their incorporation into meteorite parent bodies will certainly help us decipher the principal aggregation processes in the ESS. Further isotopic measurements and characterization of new samples will be key in this effort. Equally important will be further insights into the short-lived radioisotopes. As the initial abundances of those isotopes in the ESS become better known, the constraints they provide will increasingly challenge our scenarios for the Sun's birth and early history.

Auguste Comte, in the nineteenth century, opined that we would never know much about the stars given their great distance from us. The capabilities of astronomy from atomic spectroscopy, beginning in the late nineteenth century, certainly demolished that view. Today, as we directly study isotopic anomalies in meteoritic samples in our laboratories on Earth, we begin to understand our connection to the stars in

a new, more tangible way. And it is inspiring to know that our appreciation of this connection will grow in the coming decades!

Acknowledgments. Detailed reviews by A. Davis, P. Hoppe, and L. Nittler greatly helped in improving this chapter and are deeply appreciated. We thank L. Nittler for providing unpublished data.

REFERENCES

Alexander C. M. O'D. (1993) Presolar SiC in chondrites: How variable and how many sources? *Geochim. Cosmochim. Acta, 57,* 2869–2888.

Alexander C. M. O'D. and Nittler L. R. (1999) The galactic evolution of Si, Ti and O isotopic ratios. *Astrophys. J., 519,* 222–235.

Amari S., Anders E., Virag A., and Zinner E. (1990) Interstellar graphite in meteorites. *Nature 345,* 238–240.

Amari S., Hoppe P., Zinner E., and Lewis R. S. (1992) Interstellar SiC with unusual isotopic compositions: Grains from a supernova? *Astrophys. J. Lett., 394,* L43–L46.

Amari S., Lewis R. S., and Anders E. (1994) Interstellar grains in meteorites: I. Isolation of SiC, graphite, and diamond; size distributions of SiC and graphite. *Geochim. Cosmochim. Acta, 58,* 459–470.

Amari S., Hoppe P., Zinner E., and Lewis R. S. (1995a) Trace-element concentrations in single circumstellar silicon carbide grains from the Murchison meteorite. *Meteoritics, 30,* 679–693.

Amari S., Lewis R. S., and Anders E. (1995b) Interstellar grains in meteorites: III. Graphite and its noble gases. *Geochim. Cosmochim. Acta, 59,* 1411–1426.

Amari S., Zinner E., and Lewis R. S. (1995c) ^{41}Ca in circumstellar graphite from supernovae. *Meteoritics, 30,* 480.

Amari S., Zinner E., and Lewis R. S. (1995d) Interstellar graphite from the Murchison meteorite. In *Nuclei in the Cosmos III* (M. Busso et al., eds.), pp. 581-584. American Institute of Physics, New York.

Amari S., Zinner E., and Lewis R. S. (1995e) Large ^{18}O excesses in circumstellar graphite grains from the Murchison meteorite: Indication of a massive star-origin. *Astrophys. J. Lett., 447,* L147–L150.

Amari S., Zinner E., and Lewis R. S. (1996) ^{41}Ca in presolar graphite of supernova origin. *Astrophys. J. Lett., 470,* L101–L104.

Amari S., Zinner E., and Lewis R. S. (2000) Isotopic compositions of different presolar silicon carbide size fractions from the Murchison meteorite. *Meteoritics & Planet. Sci., 35,* 997–1014.

Amari S., Gao X., Nittler L. R., Zinner E., José J., Hernanz M., and Lewis R. S. (2001a) Presolar grains from novae. *Astrophys. J., 551,* 1065–1072.

Amari S., Nittler L. R., Zinner E., Gallino R., Lugaro M., and Lewis R. S. (2001b) Presolar SiC grains of type Y: Origin from low-metallicity AGB stars. *Astrophys. J., 546,* 248–266.

Amari S., Nittler L. R., Zinner E., Lodders K., and Lewis R. S. (2001c) Presolar SiC grains of type A and B: Their isotopic compositions and stellar origins. *Astrophys. J., 559,* 463–483.

Amari S., Jennings C., Nguyen A., Stadermann F. J., Zinner E., and Lewis R. S. (2002) NanoSIMS isotopic analysis of small presolar SiC grains from the Murchison and Indarch meteorites (abstract). In *Lunar and Planetary Science XXXIII,* Abstract #1205. Lunar and Planetary Institute, Houston (CD-ROM).

Amelin Y., Krot A. N., Hutcheon I. D., and Ulyanov A. A. (2002) Lead isotopic ages of chondrules and calcium-aluminum-rich inclusions. *Science, 297,* 1678–1683.

Anders E. and Grevesse N. (1989) Abundances of the elements: Meteoritic and solar. *Geochim. Cosmochim. Acta, 53,* 197–214.

Anders E. and Zinner E. (1993) Interstellar grains in primitive meteorites: Diamond, silicon carbide, and graphite. *Meteoritics, 28,* 490–514.

Argast D., Samland M., Thielemann F.-K., and Qian Y.-Z. (2004) Neutron star mergers versus core-collapse supernovae as dominant r-process sites in the early Galaxy. *Astron. Astrophys., 416,* 997–1011.

Arlandini C., Gallino R., Busso M., and Straniero O. (1995) New calculations of evolution, dredge-up and nucleosynthesis for low mass stars in the TP-AGB phases. In *Stellar Evolution: What Should Be Done* (A. Noels et al., eds.), pp. 447–452. 32nd Liège Intl. Astrophys. Colloquium, Université de Liège, Liège, Belgium.

Arnould M., Meynet G., and Paulus G. (1997a) Wolf-Rayet stars and their nucleosynthetic signatures in meteorites. In *Astrophysical Implications of the Laboratory Study of Presolar Materials* (T. J. Bernatowicz and E. Zinner, eds.), pp. 179–202. American Institute of Physics, New York.

Arnould M., Paulus G., and Meynet G. (1997b) Short-lived radionuclide production by non-exploding Wolf-Rayet stars. *Astron. Astrophys., 321,* 452–464.

Asplund M., Lambert D. L., Kipper T., Pollacco D., and Shetrone M. D. (1999) The rapid evolution of the born-again giant Sakurai's object. *Astron. Astrophys., 343,* 507–518.

Asplund M., Grevesse N., and Sauval A. J. (2005) The solar chemical composition. In *Cosmic Abundances as Records of Stellar Evolution and Nucleosynthesis* (T. G. Barnes and F. N. Bash, eds.), pp. 25–38. ASP Conference Series, Vol. 336, Astronomical Society of the Pacific, San Francisco.

Bao Z. Y., Beer H., Käppeler F., Voss F., Wisshak K., and Rauscher T. (2000) *Atom. Data Nucl. Data Tables, 75,* 1.

Bazan G. and Arnett D. (1998) Two-dimensional hydrodynamics of pre-core collapse: Oxygen shell burning. *Astrophys. J., 496,* 316–332.

Becker H. and Walker R. J. (2003) Efficient mixing of the solar nebula from uniform Mo isotopic composition of meteorites. *Nature, 425,* 152–155.

Becker S. A. and Iben I. Jr. (1979) The asymptotic giant branch evolution of intermediate-mass stars as a function of mass and composition. I. through the second dredge-up phase. *Astrophys. J., 232,* 831–853.

Begemann F. (1993) Isotope abundance anomalies and the early solar system: MuSiC vs. FUN. In *Origin and Evolution of the Elements* (N. Prantzos et al., eds.), pp. 517–526. Cambridge Univ., Cambridge.

Bernatowicz T. J. and Zinner E., eds. (1997) *Astrophysical Implications of the Laboratory Study of Presolar Materials*. American Institute of Physics, New York. 750 pp.

Bernatowicz T., Fraundorf G., Tang M., Anders E., Wopenka B., Zinner E., and Fraundorf P. (1987) Evidence for interstellar SiC in the Murray carbonaceous meteorite. *Nature, 330,* 728–730.

Bernatowicz T. J., Amari S., Zinner E. K., and Lewis R. S. (1991) Interstellar grains within interstellar grains. *Astrophys. J. Lett., 373,* L73–L76.

Bernatowicz T. J., Amari S., and Lewis R. S. (1992) TEM studies of a circumstellar rock (abstract). In *Lunar and Planetary Science XXIII,* pp. 91–92. Lunar and Planetary Institute, Houston.

Bernatowicz T. J., Cowsik R., Gibbons P. C., Lodders K., Fegley B. Jr., Amari S., and Lewis R. S. (1996) Constraints on stellar grain formation from presolar graphite in the Murchison meteorite. *Astrophys. J., 472,* 760–782.

Besmehn A. and Hoppe P. (2001) Silicon- and calcium-isotopic compositions of presolar silicon nitride grains from the Indarch enstatite chondrite (abstract). In *Lunar and Planetary Science XXXII,* Abstract #1188. Lunar and Planetary Institute, Houston (CD-ROM).

Besmehn A. and Hoppe P. (2003) A NanoSIMS study of Si- and Ca-Ti-isotopic compositions of presolar silicon carbide grains from supernovae. *Geochim. Cosmochim. Acta, 67,* 4693–4703.

Bethe H. A. (1939) Energy production in stars. *Phys. Rev., 55,* 103.

Bethe H. A. and Critchfield C. L. (1938) The formation of deuterons by proton capture. *Phys. Rev., 54,* 248–254.

Bethe H. A. and Wilson J. R. (1985) Revival of a stalled supernova shock by neutrino heating. *Astrophys. J., 295,* 14–23.

Birck J.-L. and Allègre C. J. (1984) Chromium isotopic anomalies in Allende refractory inclusions. *Geophys. Res. Lett., 11,* 943–946.

Birck J.-L. and Allègre C. J. (1985) Evidence for the presence of ^{53}Mn in the early solar system. *Geophys. Res. Lett., 12,* 745–748.

Birck J.-L. and Lugmair G. W. (1988) Nickel and chromium isotopes in Allende inclusions. *Earth Planet. Sci. Lett., 90,* 131–143.

Birck J. L., Rotaru M., and Allègre C. J. (1999) ^{53}Mn-^{53}Cr evolution of the early solar system. *Geochim. Cosmochim. Acta, 63,* 4111–4117.

Black D. C. (1972) On the origins of trapped helium, neon and argon isotopic variations in meteorites II. Carbonaceous meteorites. *Geochim. Cosmochim. Acta, 36,* 377–394.

Black D. C. and Pepin R. O. (1969) Trapped neon in meteorites. II. *Earth Planet. Sci. Lett., 6,* 395–405.

Blake J. B. and Schramm D. N. (1976) A possible alternative to the r-process. *Astrophys. J., 209,* 846–849.

Blake J. B., Woosley S. E., and Weaver T. A. (1981) Nucleosynthesis of neutron-rich heavy nuclei during explosive helium burning in massive stars. *Astrophys. J., 248,* 315–320.

Boato G. (1954) The isotopic composition of hydrogen and carbon in the carbonaceous chondrites. *Geochim. Cosmochim. Acta, 6,* 209–220.

Bodansky D., Clayton D. D., and Fowler W. A. (1968) Nuclear quasi-equilibrium during silicon burning. *Astrophys. J., 16,* 299–371.

Bonetti R., Broggini C., Campajola L., Corvisiero P., D'Alessandro A., Dessalvi M., D'Onofrio A., Fubini A., Gervino G., Gialanella L., Grieife U., Guglielmetti A., Gustavino C., Imbriani G., Junker M., Prati P., Roca V., Rolfs C., Romano M., Schuemann F., Strieder F., Terrasi F., Trautvetter H. P., and Zavatarelli S. (1999) First measurement of the ^{3}He (^{3}He, 2p) ^{4}He cross section down to the lower edge of the solar Gamow peak. *Phys. Rev. Lett., 82,* 5205–5208.

Boothroyd A. I. and Sackmann I.-J. (1988) Low-mass stars. III. Low-mass stars with steady mass loss: Up to the asymptotic giant branch and through the final thermal pulses. *Astrophys. J., 328,* 653–670.

Boothroyd A. I. and Sackmann I.-J. (1999) The CNO isotopes: Deep circulation in red giants and first and second dredge-up. *Astrophys. J., 510,* 232–250.

Boothroyd A. I., Sackmann I.-J., and Wasserburg G. J. (1994) Predictions of oxygen isotope ratios in stars and of oxygen-rich interstellar grains in meteorites. *Astrophys. J. Lett., 430,* L77–L80.

Boothroyd A. I., Sackmann I.-J., and Wasserburg G. J. (1995) Hot bottom burning in asymptotic giant branch stars and its effect on oxygen isotopic abundances. *Astrophys. J. Lett., 442,* L21–L24.

Boss A. and Foster P. (1997) Triggering presolar cloud collapse and injecting matrial into the presolar nebula. In *Astrophysical Implications of the Laboratory Study of Presolar Materials* (T. Bernatowicz and E. Zinner, eds.), pp. 649–664. American Institute of Physics, New York.

Boss A. P. and Foster P. N. (1998) Injection of short-lived isotopes into the presolar cloud. *Astrophys. J. Lett., 494,* L103–L106.

Brown L. E. and Clayton D. D. (1992) SiC particles from asymptotic giant branch stars: Mg burning and the s-process. *Astrophys. J. Lett., 392,* L79–L82.

Burbidge E. M., Burbidge G. R., Fowler W. A., and Hoyle F. (1957) Synthesis of the elements in stars. *Rev. Mod. Phys., 29,* 547–650.

Burrows A. (2000) Supernova explosions in the universe. *Nature, 403,* 727–733.

Busso M., Gallino R., and Wasserburg G. J. (1999) Nucleosynthesis in asymptotic giant branch stars: Relevance for galactic enrichment and solar system formation. *Annu. Rev. Astron. Astrophys., 37,* 239–309.

Busso M., Gallino R., and Wasserburg G. J. (2003) Short-lived nuclei in the early solar system: A low mass stellar source? *Publ. Astron. Soc. Australia, 20,* 356–370.

Cameron A. G. W. (1957) Stellar evolution, nuclear astrophysics and nucleogenesis. *Publ. Astron. Soc. Pacific, 69,* 201–222.

Cameron A. G. W. (1962) The formation of the sun and planets. *Icarus, 1,* 13–69.

Cameron A. G. W. (1973) Abundance of the elements in the solar system. *Space Sci. Rev., 15,* 121–146.

Cameron A. G. W. (1979) The neutron-rich silicon-burning and equilibrium processes of nucleosynthesis. *Astrophys. J. Lett., 230,* L53–L57.

Cameron A. G. W. (1993) Nucleosynthesis and star formation. In *Protostars and Planets III* (E. H. Levy and J. Lunine, eds.), pp. 47–73. Univ. of Arizona, Tucson.

Cameron A. G. W. (2002) Meteoritic isotopic abundance effects from r-process jets (abstract). In *Lunar and Planetary Science XXXIII,* Abstract #1112. Lunar and Planetary Institute, Houston (CD-ROM).

Cameron A. G. W. and Truran J. W. (1977) The supernovae trigger for formation of the solar system. *Icarus, 30,* 447–461.

Cameron A. G. W., Höflich P., Myers P. C., and Clayton D. D. (1995) Massive supernovae, orion gamma rays, and the formation of the solar system. *Astrophys. J. Lett., 447,* L53–L57.

Charbonnel C. (1995) A consistent explanation for ^{12}C/^{13}C, ^{7}Li, and ^{3}He anomalies in red giant stars. *Astrophys. J. Lett., 453,* L41–L44.

Chaussidon M. and Gounelle M. (2006) Irradiation processes in the early solar system. In *Meteorites and the Early Solar System II* (D. S. Lauretta and H. Y. McSween Jr., eds.), this volume. Univ. of Arizona, Tucson.

Chaussidon M., Robert F., and McKeegan K. D. (2004) Li and B isotopic variations in Allende type B1 CAI 3529-41: Trace of incorporation of short-lived ^{7}Be and ^{10}Be. In *Lunar and Planetary Science XXXV,* Abstract #1568. Lunar and Planetary Institute, Houston (CD-ROM).

Chaussidon M., Robert F., and McKeegan K. D. (2005) Li and B isotopic variation in an Allende CAI: Evidence for in situ decay of ^{10}Be and for the possible presence of the short-lived nuclide ^{7}Be in the early solar system. *Geochim. Cosmochim. Acta,* in press.

Chen J. H., Papanastassiou D. A., Wasserburg G. J., and Ngo H. H. (2004) Endemic Mo isotopic anomalies in iron and carbonaceous meteorites (abstract). In *Lunar and Planetary Science XXXV,* Abstract #1431. Lunar and Planetary Institute, Houston (CD-ROM).

Choi B.-G., Huss G. R., Wasserburg G. J., and Gallino R. (1998) Presolar corundum and spinel in ordinary chondrites: Origins from AGB stars and a supernova. *Science, 282,* 1284–1289.

Choi B.-G., Wasserburg G. J., and Huss G. R. (1999) Circumstellar hibonite and corundum and nucleosynthesis in asymptotic giant branch stars. *Astrophys. J. Lett., 522,* L133–L136.

Clayton D. D. (1975a) Extinct radioactivities: Trapped residuals of presolar grains. *Astrophys. J., 199,* 765–769.

Clayton D. D. (1975b) Na-22, Ne-E, extinct radioactive anomalies and unsupported Ar-40. *Nature, 257,* 36–37.

Clayton D. D. (1983) Discovery of s-process Nd in Allende residue. *Astrophys. J. Lett., 271,* L107–L109.

Clayton D. D. (1986) Interstellar fossil ^{26}Mg and its possible relationship to excess meteoritic ^{26}Mg. *Astrophys. J., 310,*490–498.

Clayton D. D. (1989) Origin of heavy xenon in meteoritic diamonds. *Astrophys. J., 340,* 613–619.

Clayton D. D. (1997) Placing the sun and mainstream SiC particles in galactic chemodynamic evolution. *Astrophys. J. Lett., 484,* L67–L70.

Clayton D. D. (2003) Presolar galactic merger spawned the SiC grain mainstream. *Astrophys. J., 598,* 313–324.

Clayton D. D. and Leising M. D. (1987) ^{26}Al in the interstellar medium. *Phys. Rept., 144,* 1–50.

Clayton D. D. and Nittler L. R. (2004) Astrophysics with presolar stardust. *Annu. Rev. Astron. Astrophys., 42,* 39–78.

Clayton D. D. and Timmes F. X. (1997a) Implications of presolar grains for galactic chemical evolution. In *Astrophysical Implications of the Laboratory Study of Presolar Materials* (T. J. Bernatowicz and E. Zinner, eds.), pp. 237–264. American Institute of Physics, New York.

Clayton D. D. and Timmes F. X. (1997b) Placing the Sun in galactic chemical evolution: Mainstream SiC particles. *Astrophys. J., 483,* 220–227.

Clayton D. D. and Ward R. A. (1978) s-Process studies: Xenon and krypton isotopic abundances. *Astrophys. J., 224,* 1000–1006.

Clayton D. D., Obradovic M., Guha S., and Brown L. E. (1991) Silicon and titanium isotopes in SiC from AGB stars (abstract). In *Lunar and Planetary Science XXII,* pp. 221–222. Lunar and Planetary Institute, Houston.

Clayton D. D., Meyer B. S., Sanderson C. I., Russell S. S., and Pillinger C. T. (1995) Carbon and nitrogen isotopes in type II supernova diamonds. *Astrophys. J., 447,* 894–905.

Clayton D. D., Liu W., and Dalgarno A. (1999) Condensation of carbon in radioactive supernova gas. *Science, 283,* 1290–1292.

Clayton D. D., Meyer B. S., The L.-S., and El Eid M. F. (2002) Iron implantation in presolar supernova grains. *Astrophys. J. Lett., 578,* L83–L86.

Clayton R. N. (1978) Isotopic anomalies in the early solar system. *Annu. Rev. Nucl. Part. Sci., 28,* 501–522.

Clayton R. N. (2002) Self-shielding in the solar nebula. *Nature, 415,* 860–861.

Clayton R. N. and Mayeda T. K. (1977) Correlated oxygen and magnesium isotope anomalies in Allende inclusions, I: Oxygen. *Geophys. Res. Lett., 4,* 295–298.

Clayton R. N., Grossman L., and Mayeda T. K. (1973) A component of primitive nuclear composition in carbonaceous meteorites. *Science, 182,* 485–488.

Clayton R. N., MacPherson G. J., Hutcheon I. D., Davis A. M., Grossman L., Mayeda T. K., Molini-Velsko C., Allen J. M., and El Goresy A. (1984) Two forsterite-bearing FUN inclusions in the Allende meteorite. *Geochim. Cosmochim. Acta, 48,* 535–548.

Clayton R. N., Hinton R. W., and Davis A. M. (1988) Isotopic variations in the rock-forming elements in meteorites. *Phil. Trans. R. Soc. Lond., A325,* 483–501.

Colgate S. A. and White R. H. (1966) The hydrodynamic behavior of supernovae explosions. *Astrophys. J., 143,* 626–681.

Croat T. K., Bernatowicz T., Amari S., Messenger S., and Stadermann F. J. (2003) Structural, chemical, and isotopic microanalytical investigations of graphite from supernovae. *Geochim. Cosmochim. Acta, 67,* 4705–4725.

Dai Z. R., Bradley J. P., Joswiak D. J., Brownlee D. E., Hill H. G. M., and Genge M. J. (2002) Possible *in situ* formation of meteoritic nanodiamonds in the early solar system. *Nature, 418,* 157–159.

Dauphas N., Marty B., and Reisberg L. (2002a) Molybdenum evidence for inherited planetary scale isotope heterogeneity of the protosolar nebula. *Astrophys. J., 565,* 640–644.

Dauphas N., Marty B., and Reisberg L. (2002b) Molybdenum nucleosynthetic dichotomy revealed in primitive meteorites. *Astrophys. J. Lett., 569,* L139–L142.

Davis A. M., Gallino R., Lugaro M., Tripa C. E., Savina M. R., Pellin M. J., and Lewis R. S. (2002) Presolar grains and the nucleosynthesis of iron isotopes (abstract). In *Lunar and Planetary Science XXXIII,* Abstract #2018. Lunar and Planetary Institute, Houston (CD-ROM).

Davis A. M., Gallino R., Straniero O., Dominguez I., and Lugaro M. (2003) Heavy element nucleosynthesis in low metallicity, low mass AGB stars (abstract). In *Lunar and Planetary Science XXXIV,* Abstract #2034. Lunar and Planetary Institute, Houston (CD-ROM).

Deneault E. A.-N., Clayton D. D., and Heger A. (2003) Supernova reverse shocks and SiC growth. *Astrophys. J., 594,* 312–325.

Denissenkov P. A. and Weiss A. (1996) Deep diffusive mixing in globular-cluster red giants. *Astron. Astrophys., 308,* 773–784.

Desch S. J., Connolly H. C. Jr., and Srinivasan G. (2004) An interstellar origin for the beryllium 10 in calcium-rich, aluminum-rich inclusions. *Astrophys. J., 602,* 528–542.

Diehl R., Dupraz C., Bennett K., Bloemen H., Hermsen W., Knödlseder J., Lichti G., Morris D., Ryan J., Schönfelder V., Steinle H., Strong A., Swanenburg B., Varendorff M., and Winkler C. (1995) COMPTEL observations of galactic ^{26}Al emission. *Astron. Astrophys., 298,* 445–460.

Ebel D. S. and Grossman L. (2001) Condensation from supernova gas made of free atoms. *Geochim. Cosmochim. Acta, 65,* 469–477.

Ebisuzaki T. and Shibazaki N. (1988) The effects of mixing of the ejecta on the hard X-ray emissions from SN 1987A. *Astrophys. J. Lett., 327,* L5–L8.

El Eid M. (1994) CNO isotopes in red giants: Theory versus observations. *Astron. Astrophys., 285,* 915–928.

El Eid M. F., Meyer B. S., and The L.-S. (2004) Evolution of

massive stars up to the end of central oxygen burning. *Astrophys. J., 611,* 452–465.

Fahey A., Goswami J. N., McKeegan K. D., and Zinner E. (1985) Evidence for extreme ^{50}Ti enrichments in primitive meteorites. *Astrophys. J. Lett., 296,* L17–L20.

Fahey A. J., Goswami J. N., McKeegan K. D., and Zinner E. (1987) ^{16}O excesses in Murchison and Murray hibonites: A case against a late supernova injection origin of isotopic anomalies in O, Mg, Ca, and Ti. *Astrophys. J. Lett., 323,* L91–L95.

Filippenko A. V. (1997) Optical spectra of supernovae. *Annu. Rev. Astron. Astrophys., 35,* 309–355.

Fish R. A., Goles G. G., and Anders E. (1960) The record in the meteorites. III. On the development of meteorites in asteroidal bodies. *Astrophys. J., 132,* 243–258.

Floss C. and Stadermann F. J. (2004) Isotopically primitive interplanetary dust particles of cometary origin: Evidence from nitrogen isotopic compositions (abstract). In *Lunar and Planetary Science XXXV,* Abstract #1281. Lunar and Planetary Institute, Houston (CD-ROM).

Forestini M., Paulus G., and Arnould M. (1991) On the production of ^{26}Al in AGB stars. *Astron. Astrophys., 252,* 597–604.

Foster P. N. and Boss A. P. (1997) Injection of radioactive nuclides from the stellar source that triggered the collapse of the presolar nebula. *Astrophys. J., 489,* 346–357.

Fowler W. A., Greenstein J. L., and Hoyle F. (1962) Nucleosynthesis during the early history of the solar system. *Geophys. J., 6,* 148–220.

Freiburghaus C., Rosswog S., and Thielemann F.-K. (1999) R-process in neutron star mergers. *Astrophys. J. Lett., 525,* L121–L124.

Frost C. A. and Lattanzio J. C. (1996) AGB stars: What should be done? In *Stellar Evolution: What Should Be Done* (A. Noel et al., eds.), pp. 307–325. 32nd Liège Intl. Astrophys. Colloquium, Université de Liège, Liège, Belgium.

Fuller G. M. and Meyer B. S. (1995) Neutrino capture and supernova nucleosynthesis. *Astrophys. J., 453,* 792–809.

Gallino R., Busso M., Picchio G., and Raiteri C. M. (1990) On the astrophysical interpretation of isotope anomalies in meteoritic SiC grains. *Nature, 348,* 298–302.

Gallino R., Raiteri C. M., and Busso M. (1993) Carbon stars and isotopic Ba anomalies in meteoritic SiC grains. *Astrophys. J., 410,* 400–411.

Gallino R., Raiteri C. M., Busso M., and Matteucci F. (1994) The puzzle of silicon, titanium and magnesium anomalies in meteoritic silicon carbide grains. *Astrophys. J., 430,* 858–869.

Gallino R., Busso M., and Lugaro M. (1997) Neutron capture nucleosynthesis in AGB stars. In *Astrophysical Implications of the Laboratory Study of Presolar Materials* (T. J. Bernatowicz and E. Zinner, eds.), pp. 115-153. American Institute of Physics, New York.

Gallino R., Arlandini C., Busso M., Lugaro M., Travaglio C., Straniero O., Chieffi A., and Limongi M. (1998) Evolution and nucleosynthesis in low-mass asymptotic giant branch stars. II. Neutron capture and the s-process. *Astrophys. J., 497,* 388–403.

Galy A., Hutcheon I. D., and Grossman L. (2004) $(^{26}Al/^{27}Al)_0$ of the solar nebula inferred from Al-Mg systematics in bulk CAIs from CV3 chondrites (abstract). In *Lunar and Planetary Science XXXV,* Abstract #1790. Lunar and Planetary Institute, Houston (CD-ROM).

Gilmour J. (2002) The solar system's first clocks. *Science, 297,* 1658–1659.

Gilroy K. K. (1989) Carbon isotope ratios and lithium abundances in open cluster giants. *Astrophys. J., 347,* 835–848.

Gilroy K. K. and Brown J. A. (1991) Carbon isotope ratios along the giant branch of M67. *Astrophys. J., 371,* 578–583.

Goswami J. N. and Vanhala H. A. T. (2000) Extinct radionuclides and the origin of the solar system. In *Protostars and Planets IV* (V. Mannings et al., eds.), p. 963. Univ. of Arizona, Tucson.

Goswami J. N., Marhas K. K., and Sahijpal S. (2001) Did solar energetic particles produce the short-lived nuclides present in the early solar system? *Astrophys. J., 549,* 1151–1159.

Gounelle M., Shu F. H., Shang H., Glassgold A. E., Rehm K. E., and Lee T. (2001) Extinct radioactivities and protosolar cosmic rays: Self-shielding and light elements. *Astrophys. J., 548,* 1051–1070.

Grevesse N., Noels A., and Sauval A. J. (1996) Standard abundances. In *Cosmic Abundances* (S. S. Holt and G. Sonneborn, eds.), pp. 117–126. BookCrafters, Inc., San Francisco.

Grossman L. (1972) Condensation in the primitive solar nebula. *Geochim. Cosmochim. Acta, 36,* 597–619.

Guan Y., Huss G. R., Leshin L. A., and MacPherson G. J. (2003) Ni isotope anormalies and ^{60}Fe in sulfides from unequilibrated enstatite chondrites (abstract). *Meteoritics & Planet. Sci., 38,* A138.

Guber K. H., Spencer R. R., Koehler P. E., and Winters R. R. (1997) New ^{142,144}Nd (n,γ) cross sections and the s-process origin of the Nd anomalies in presolar meteoritic silicon carbide grains. *Phys. Rev. Lett., 78,* 2704–2707.

Guber K. H., Koehler P. E., Derrien H., Valentine T. E., Leal L. C., Sayer R. O., and Rauscher T. (2003) Neutron capture reaction rates for silicon and their impact on the origin of presolar mainstream SiC grains. *Phys. Rev. C, 67,* 062802-1 to 062802-4.

Halliday A. N. and Kleine T. (2006) Meteorites and the timing, mechanisms, and conditions of terrestrial planet accretion and early differentiation. In *Meteorites and the Early Solar System II* (D. S. Lauretta and H. Y. McSween Jr., eds.), this volume. Univ. of Arizona, Tucson.

Harper C. L. Jr. (1993) Isotopic astronomy from anomalies in meteorites: Recent advances and new frontiers. *J. Phys. G, 19,* S81–S94.

Harper C. L. Jr. (1996) Evidence for ^{92g}Nb in the early solar system and evaluation of a new p-process cosmochronometer from ^{92g}Nb/^{92}Mo. *Astrophys. J., 466,* 437–456.

Harper C. L. Jr. and Jacobsen S. B. (1996) Evidence for ^{182}Hf in the early solar system and constraints on the timescale of terrestrial accretion and core formation. *Geochim. Cosmochim. Acta, 60,* 1131–1153.

Harris M. J. and Lambert D. L. (1984) Oxygen isotopic abundances in the atmospheres of seven red giant stars. *Astrophys. J., 285,* 674–682.

Harris M. J., Lambert D. L., Hinkle K. H., Gustafsson B., and Eriksson K. (1987) Oxygen isotopic abundances in evolved stars. III. 26 carbon stars. *Astrophys. J., 316,* 294–304.

Hartmann D., Woosley S. E., and El Eid M. F. (1985) Nucleosynthesis in neutron-rich supernova ejecta. *Astrophys. J., 297,* 837–845.

Herant M., Benz W., Hix W. R., Fryer C. L., and Colgate S. A. (1994) Inside the supernova: A powerful convective engine. *Astrophys. J., 435,* 339–361.

Herwig F. (2001) The evolutionary timescale of Sakurai's Object: A test of convection theory? *Astrophys. J. Lett., 554,* L71–L74.

Heymann D. (1983) Barium from a mini r-process in supernovae. *Astrophys. J., 267,* 747–756.

Heymann D. and Dziczkaniec M. (1979) Xenon from intermediate zones of supernovae. *Proc. Lunar Planet. Sci. Conf. 10th,* pp. 1943–1959.

Heymann D. and Dziczkaniec M. (1980) A first roadmap for kryptology. *Proc. Lunar Planet. Sci. Conf. 11th,* pp. 1179–1213.

Hidaka H., Ohta Y., Yoneda S., and DeLaeter J. R. (2001) Isotopic search for live ^{135}Cs in the early solar system and possibility of ^{135}Cs-^{135}Ba chronometer. *Earth Planet. Sci. Lett., 193,* 459–466.

Hidaka H., Ohta Y., and Yoneda S. (2003) Nucleosynthetic components of the early solar system inferred from Ba isotopic compositions in carbonaceous chondrites. *Earth Planet. Sci. Lett., 214,* 455–466.

Hillebrandt W., Kodama T., and Takahashi K. (1976) R-process nucleosynthesis — A dynamical model. *Astron. Astrophys., 52,* 63–68.

Hoffman R. D., Woosley S. E., Fuller G. M., and Meyer B. S. (1996a) Nucleosynthesis in neutrino-driven winds. I. The physical conditions. *Astrophys. J., 460,* 478–488.

Hoffman R. D., Woosley S. E., Fuller G. M., and Meyer B. S. (1996b) Production of the light p-process nuclei in neutrino-driven winds. *Astrophys. J., 460,* 478–488.

Hoppe P. and Besmehn A. (2002) Evidence for extinct vanadium-49 in presolar silicon carbide grains from supernovae. *Astrophys. J. Lett., 576,* L69–L72.

Hoppe P. and Ott U. (1997) Mainstream silicon carbide grains from meteorites. In *Astrophysical Implications of the Laboratory Study of Presolar Materials* (T. J. Bernatowicz and E. Zinner, eds.), pp. 27–58. American Institute of Physics, New York.

Hoppe P. and Zinner E. (2000) Presolar dust grains from meteorites and their stellar sources. *J. Geophys. Res., 105,* 10371–10385.

Hoppe P., Amari S., Zinner E., Ireland T., and Lewis R. S. (1994) Carbon, nitrogen, magnesium, silicon and titanium isotopic compositions of single interstellar silicon carbide grains from the Murchison carbonaceous chondrite. *Astrophys. J., 430,* 870–890.

Hoppe P., Amari S., Zinner E., and Lewis R. S. (1995) Isotopic compositions of C, N, O, Mg, and Si, trace element abundances, and morphologies of single circumstellar graphite grains in four density fractions from the Murchison meteorite. *Geochim. Cosmochim. Acta, 59,* 4029–4056.

Hoppe P., Strebel R., Eberhardt P., Amari S., and Lewis R. S. (1996a) Small SiC grains and a nitride grain of circumstellar origin from the Murchison meteorite: Implications for stellar evolution and nucleosynthesis. *Geochim. Cosmochim. Acta, 60,* 883–907.

Hoppe P., Strebel R., Eberhardt P., Amari S., and Lewis R. S. (1996b) Type II supernova matter in a silicon carbide grain from the Murchison meteorite. *Science, 272,* 1314–1316.

Hoppe P., Annen P., Strebel R., Eberhardt P., Gallino R., Lugaro M., Amari S., and Lewis R. S. (1997) Meteoritic silicon carbide grains with unusual Si-isotopic compositions: Evidence for an origin in low-mass metallicity asymptotic giant branch stars. *Astrophys. J. Lett., 487,* L101–L104.

Hoppe P., Strebel R., Eberhardt P., Amari S., and Lewis R. S. (2000) Isotopic properties of silicon carbide X grains from the Murchison meteorite in the size range 0.5–1.5 μm. *Meteoritics & Planet. Sci., 35,* 1157–1176.

Hoppe P., Nittler L. R., Mostefaoui S., Alexander C. M. O'D., and Marhas K. K. (2003) A NanoSIMS study of titanium-isotopic compositions of presolar corundum grains (abstract). In *Lunar and Planetary Science XXXIV,* Abstract #1570. Lunar and Planetary Institute, Houston (CD-ROM).

Howard W. M. and Meyer B. S. (1993) The p-process and Type Ia supernovae. In *Nuclei in the Cosmos 2* (F. Käppeler and K. Wisshak, eds.), pp. 575–580. Institute of Physics, Bristol and Philadelphia.

Howard W. M., Meyer B. S., and Woosley S. . (1991) A new site for the astrophysical gamma-process. *Astrophys. J. Lett., 373,* L5–L8.

Hoyle F. (1946) The synthesis of the elements from hydrogen. *Mon. Not. R. Astron. Soc., 106,* 343–383.

Hoyle F. (1954) On nuclear reactions occuring in very hot stars. I. The synthesis of elements from carbon to nickel. *Astrophys. J. Suppl., 1,* 121–146.

Hughes J. P., Rakowski C. E., Burrows D. N., and Slane P. O. (2000) Nucleosynthesis and mixing in Cassiopeia A. *Astrophys. J. Lett., 528,* L109–L113.

Huss G. R. and Lewis R. S. (1994a) Noble gases in presolar diamonds I: Three distinct components and their implications for diamond origins. *Meteoritics, 29,* 791–810.

Huss G. R. and Lewis R. S. (1994b) Noble gases in presolar diamonds II: Component abundances reflect thermal processing. *Meteoritics, 29,* 811–829.

Huss G. R., Fahey A. J., Gallino R., and Wasserburg G. J. (1994) Oxygen isotopes in circumstellar Al_2O_3 grains from meteorites and stellar nucleosynthesis. *Astrophys. J. Lett., 430,* L81–L84.

Huss G. R., Hutcheon I. D., and Wasserburg G. J. (1997) Isotopic systematics of presolar silicon carbide from the Orgueil (CI) carbonaceous chondrite: Implications for solar system formation and stellar nucleosynthesis. *Geochim. Cosmochim. Acta, 61,* 5117–5148.

Hutcheon I. D., Huss G. R., Fahey A. J., and Wasserburg G. J. (1994) Extreme ^{26}Mg and ^{17}O enrichments in an Orgueil corundum: Identification of a presolar oxide grain. *Astrophys. J. Lett., 425,* L97–L100.

Hutcheon I. D., Weisberg M. K., Phinney D. L., Zolensky M. E., Prinz M., and Ivanov A. V. (1999) Radiogenic ^{53}Cr in Kaidun carbonates: Evidence for very early aqueous activity (abstract). In *Lunar and Planetary Science XXX,* Abstract #1722. Lunar and Planetary Institute, Houston (CD-ROM).

Imbriani G., Limongi M., Gialanella L., Terrasi F., Straniero O., and Chieffi A. (2001) The $^{12}C(\alpha,\gamma)^{16}O$ reaction rate and the evolution of stars in the mass range $0.8 \le M/M_\odot \le 25$. *Astrophys. J., 558,* 903–915.

Ireland T. R. (1990) Presolar isotopic and chemical signatures in hibonite-bearing refractory inclusions from the Murchison carbonaceous chondrite. *Geochim. Cosmochim. Acta, 54,* 3219–3237.

Ireland T. R., Zinner E. K., and Amari S. (1991) Isotopically anomalous Ti in presolar SiC from the Murchison meteorite. *Astrophys. J. Lett., 376,* L53–L56.

Ireland T. R., Fahey A. J., Zinner E., and Esat T. M. (1992) Evidence for distillation in the formation of HAL and related hibonite inclusions. *Geochim. Cosmochim. Acta, 56,* 2503–2520.

Jeffery P. M. and Reynolds J. H. (1961) Origin of excess Xe^{129} in stone meteorites. *J. Geophys. Res., 66,* 3582–3583.

José J., Coc A., and Hernanz M. (1999) Nuclear uncertainties in the NeNa-MgAl cycles and production of ^{22}Na and ^{26}Al during nova outbursts. *Astrophys. J., 520,* 347–360.

José J., Hernanz M., Amari S., Lodders K., and Zinner E. (2004) The imprint of nova nucleosynthesis in presolar grains. *Astro-*

phys. J., 612, 414–428.

Jungck M. H. A., Shimamura T., and Lugmair G. W. (1984) Ca isotope variations in Allende. *Geochim. Cosmochim. Acta, 48,* 2651–2658.

Kaiser T. and Wasserburg G. J. (1983) The isotopic composition and concentration of Ag in iron meteorites and the origin of exotic silver. *Geochim. Cosmochim. Acta, 47,* 43–58.

Käppeler F., Beer H., and Wisshak K. (1989) s-Process nucleosynthesis — nuclear physics and the classic model. *Rept. Prog. Phys., 52,* 945–1013.

Karakas A. I. and Lattanzio J. C. (2003) Production of aluminium and the heavy magnesium isotopes in asymptotic giant branch stars. *Publ. Astron. Soc. Australia, 20,* 279–293.

Kashiv Y., Cai Z., Lai B., Sutton S. R., Lewis R. S., Davis A. M., Clayton R. N., and Pellin M. J. (2002) Condensation of trace elements into presolar SiC stardust grains (abstract). In *Lunar and Planetary Science XXXIII,* Abstract #2056. Lunar and Planetary Institute, Houston (CD-ROM).

Kelly W. R. and Wasserburg G. J. (1978) Evidence for the existence of ^{107}Pd in the early solar system. *Geophys. Res. Lett., 5,* 1079–1082.

Kerridge J. F. and Matthews M. S., eds. (1988) *Meteorites and the Early Solar System.* Univ. of Arizona, Tucson. 1269 pp.

Kleine T., Münker C., Mezger K., and Palme H. (2002) Rapid accretion and early core formation on asteroids and the terrestrial planets from Hf-W chronometry. *Nature, 418,* 952–955.

Knödlseder J. (1999) Implications of 1.8 MeV gamma-ray observations for the origin of ^{26}Al. *Astrophys. J., 510,* 915–929.

Koehler P. E., Spencer R. R., Guber K. H., Winters R. R., Raman S., Harvey J. A., Hill N. W., Blackmon J. C., Bardayan D. W., Larson D. C., Lewis T. A., Pierce D. E., and Smith M. S. (1998) High resolution neutron capture and transmission measurement on ^{137}Ba and their impact on the interpretation of meteoritic barium anomalies. *Phys. Rev. C, 57,* R1558–R1561.

Kovetz A. and Prialnik D. (1997) The composition of nova ejecta from multicycle evolution models. *Astrophys. J., 477,* 356–367.

Krestina N., Hsu W., and Wasserburg G. J. (2002) Circumstellar oxide grains in ordinary chondrites and their origin (abstract). In *Lunar and Planetary Science XXXIII,* Abstract #1425. Lunar and Planetary Institute, Houston (CD-ROM).

Kunz R., Fey M., Jaeger M., Mayer A., Hammer J. W., Staudt G., Harissopulos S., and Paradellis T. (2002) Astrophysical reaction rate of ^{12}C(a, γ)^{16}O. *Astrophys. J., 2002,* 643–650.

Lambert D. L. (1991) The abundance connection — the view from the trenches. In *Evolution of Stars: The Photospheric Abundance Connection* (G. Michaud and A. Tutukov, eds.), pp. 451–460. Kluwer, Dordrecht.

Lambert D. L., Gustafsson B., Eriksson K., and Hinkle K. H. (1986) The chemical composition of carbon stars. I. Carbon, nitrogen, and oxygen in 30 cool carbon stars in the galactic disk. *Astrophys. J. Suppl., 62,* 373–425.

Langer N., Heger A., Wellstein S., and Herwig F. (1999) Mixing and nucleosynthesis in rotating TP-AGB stars. *Astron. Astrophys., 346,* L37–L40.

Larimer J. W. and Bartholomay M. (1979) The role of carbon and oxygen in cosmic gases: Some applications to the chemistry and mineralogy of enstatite chondrites. *Geochim. Cosmochim. Acta, 43,* 1455–1466.

Lattanzio J. C., Frost C. A., Cannon R. C., and Wood P. R. (1997) Hot bottom burning nucleosynthesis in 6 $M_\odot$ stellar models. *Nucl. Phys., A621,* 435c–438c.

Lee D.-C. and Halliday A. N. (1995) Hafnium-tungsten chronometry and the timing of terrestrial core formation. *Nature, 378,* 771–774.

Lee T. (1979) New isotopic clues to solar system formation. *Rev. Geophys. Space Phys., 17,* 1591–1611.

Lee T. (1988) Implications of isotopic anomalies for nucleosynthesis. In *Meteorites and the Early Solar System* (J. F. Kerridge and M. S. Matthews), pp. 1063–1089. Univ. of Arizona, Tucson.

Lee T., Panastassiou D. A., and Wasserburg G. J. (1976) Demonstration of ^{26}Mg excess in Allende and evidence for ^{26}Al. *Geophys. Res. Lett., 3,* 109–112.

Lee T., Papanastassiou D. A., and Wasserburg G. J. (1977) Aluminum-26 in the early solar system: Fossil or fuel? *Astrophys. J. Lett., 211,* L107–L110.

Lee T., Papanastassiou D. A., and Wasserburg G. J. (1978) Calcium isotopic anomalies in the Allende Meteorite. *Astrophys. J. Lett., 220,* L21–L25.

Lewis R. S., Tang M., Wacker J. F., Anders E., and Steel E. (1987) Interstellar diamonds in meteorites. *Nature, 326,* 160–162.

Lewis R. S., Amari S., and Anders E. (1990) Meteoritic silicon carbide: Pristine material from carbon stars. *Nature, 348,* 293–298.

Lewis R. S., Huss G. R., and Lugmair G. (1991) Finally, Ba & Sr accompanying Xe-Hl in diamonds from Allende (abstract). In *Lunar and Planetary Science XXII*, pp. 807–808. Lunar and Planetary Institute, Houston.

Lewis R. S., Amari S., and Anders E. (1994) Interstellar grains in meteorites: II. SiC and its noble gases. *Geochim. Cosmochim. Acta, 58,* 471–494.

Leya I., Halliday A. N., and Wieler R. (2003) The predictable collateral consequences of nucleosynthesis by spallation reactions in the early solar system. *Astrophys. J., 594,* 605–616.

Lin Y., Amari S., and Pravdivtseva O. (2002) Presolar grains from the Qingzhen (EH3) meteorite. *Astrophys. J., 575,* 257–263.

Lin Y., Guan Y., Leshin L. A., Ouyang Z., and Wang D. (2004) Evidence for live ^{36}Cl in Ca-Al-rich inclusions from the Ninqiang carbonaceous chondrite (abstract). In *Lunar and Planetary Science XXXV,* Abstract #2084. Lunar and Planetary Institute, Houston (CD-ROM).

Lin Y., Guan Y., Leshin L. A., Ouyang Z., and Wang D. (2005) Short-lived chlorine-36 in Ca- and Al-rich inclusion from the Ningqiang carbonaceous chondrite. *Proc. Natl. Acad. Sci., 102,* 1306–1311.

Liu M.-C., Iizuka Y., McKeegan K. D., Tonui E. K., and Young E. D. (2005) Supracanonical ^{26}Al/^{27}Al ratios in an unaltered Allende CAI (abstract). In *Lunar and Planetary Science XXXVI,* Abstract #2079. Lunar and Planetary Institute, Houston (CD-ROM).

Lodders K. (2003) Solar system abundances and condensation temperatures of the elements. *Astrophys. J., 591,* 1220–1247.

Lodders K. and Fegley B. Jr. (1997) Condensation chemistry of carbon stars. In *Astrophysical Implications of the Laboratory Study of Presolar Materials* (T. J. Bernatowicz and E. Zinner, eds.), pp. 391–423. American Institute of Physics, New York.

Loss R. D., Lugmair G. W., Davis A. M., and MacPherson G. J. (1994) Isotopically distinct reservoirs in the solar nebula: Isotope anomalies in vigarano meteorite inclusions. *Astrophys. J. Lett., 436,* L193–L196.

Luck J. M., Ben Othman D., Barrat J. A., and Albarède F. (2003) Coupled ^{63}Cu and ^{16}O excesses in chondrites. *Geochim. Cosmochim. Acta, 67,* 143–151.

Lugaro M., Zinner E., Gallino R., and Amari S. (1999) Si isotopic

ratios in mainstream presolar SiC grains revisited. *Astrophys. J., 527,* 369–394.

Lugaro M., Davis A. M., Gallino R., Pellin M. J., Straniero O., and Käppeler F. (2003) Isotopic compositions of strontium, zirconium, molybdenum, and barium in single presolar SiC grains and asymptotic giant branch stars. *Astrophys. J., 593,* 486–508.

Lugmair G. W. and Galer S. J. G. (1992) Age and isotopic relationships among the angrites Lewis Cliff 86010 and Angra dos Reis. *Geochim. Cosmochim. Acta, 56,* 1673–1694.

Lugmair G. W. and Marti K. (1977) Sm-Nd-Pu timepieces in the Angra dos Reis meteorite. *Earth Planet. Sci. Lett., 35,* 273–284.

Lugmair G. W. and Shukolyukov A. (1998) Early solar system timescales according to ^{53}Mn-^{53}Cr systematics. *Geochim. Cosmochim. Acta, 62,* 2863–2886.

Lugmair G. W. and Shukolyukov A. (2001) Early solar system events and timescales. *Meteoritics & Planet. Sci., 36,* 1017–1026.

MacPherson G. J., Davis A. M., and Zinner E. K. (1995) The distribution of aluminum-26 in the early solar system — A reappraisal. *Meteoritics, 30,* 365–386.

MacPherson G. J., Huss G. R., and Davis A. M. (2003) Extinct ^{10}Be in type A calcium-aluminum-rich inclusions from CV chondrites. *Geochim. Cosmochim. Acta, 67,* 3165–3179.

Mahoney W. A., Ling J. C., Wheaton W. A., and Jacobsen A. S. (1984) HEAO 3 discovery of ^{26}Al in the interstellar medium. *Astrophys. J., 286,* 578–585.

Marhas K. K., Goswami J. N., and Davis A. M. (2002) Short-lived nuclides in hibonite grains from Murchison: Evidence for solar system evolution. *Science, 298,* 2182–2185.

Marhas K. K., Hoppe P., and Ott U. (2003) A NanoSIMS study of C-, Si-, and Ba-isotopic compositions of presolar silicon carbide grains from the Murchison meteorite (abstract). *Meteoritics & Planet. Sci., 38,* A58.

Marhas K. K., Hoppe P., and Besmehn A. (2004) A NanoSIMS study of iron-isotopic compositions in presolar silicon carbide grains (abstract). In *Lunar and Planetary Science XXXV,* Abstract #1834. Lunar and Planetary Institute, Houston (CD-ROM).

McCulloch M. T. and Wasserburg G. J. (1978a) Barium and neodymium isotopic anomalies in the Allende Meteorite. *Astrophys. J. Lett., 220,* L15–L19.

McCulloch M. T. and Wasserburg G. J. (1978b) More anomalies from the Allende meteorite: Samarium. *Geophys. Res. Lett., 5,* 599–602.

McKeegan K. D., Chaussidon M., and Robert F. (2000) Incorporation of short-lived ^{10}Be in a calcium-aluminum-rich inclusion from the Allende meteorite. *Science, 289,* 1334–1337.

Merrill P. W. (1952) Spectroscopic observations of stars of class S. *Astrophys. J., 116,* 21–26.

Messenger S. (2000) Identification of molecular-cloud material in interplanetary dust particles. *Nature, 404,* 968–971.

Messenger S. and Keller L. P. (2004) A supernova silicate from a cluster IDP (abstract). *Meteoritics & Planet. Sci., 39,* A68.

Messenger S. and Walker R. (1997) Evidence for molecular cloud material in meteorites and interplanetary dust. In *Astrophysical Implications of the Laboratory Study of Presolar Materials* (T. Bernatowicz and E. Zinner, eds.), pp. 545–566. American Institute of Physics, New York.

Messenger S., Keller L. P., Stadermann F. J., Walker R. M., and Zinner E. (2003) Samples of stars beyond the solar system: Silicate grains in interplanetary dust. *Science, 300,* 105–108.

Meyer B. S. (1995) Neutrino reactions on ^{4}He and the r-process. *Astrophys. J. Lett., 449,* L55–L58.

Meyer B. S. (2003) Neutrinos, supernovae, molybdenum, and extinct ^{92}Nb. *Nucl. Phys. A, 719,* C13–C20.

Meyer B. S. and Brown J. S. (1997) Survey of r-process models. *Astrophys. J., 112,* 199–220.

Meyer B. S. and Clayton D. D. (2000) Short-lived radioactivities and the birth of the Sun. *Space Sci. Rev., 92,* 133–152.

Meyer B. S., Mathews G. J., Howard W. M., Woosley S. E., and Hoffman R. (1992) The r-process in supernovae. *Astrophys. J., 399,* 656–664.

Meyer B. S., Weaver T. A., and Woosley S. E. (1995) Isotope source table for a 25 $M_\odot$ supernova. *Meteoritics, 30,* 325–334.

Meyer B. S., Krishnan T. D., and Clayton D. D. (1996) ^{48}Ca production in matter expanding from high temperature and density. *Astrophys. J., 462,* 825–838.

Meyer B. S., Krishnan T. D., and Clayton D. D. (1998a) Theory of quasi-equilibrium nucleosynthesis and applications to matter expanding from high temperature and density. *Astrophys. J., 498,* 808–830.

Meyer B. S., McLaughlin G. C., and Fuller G. M. (1998b) Neutrino-capture and r-process nucleosynthesis. *Phys. Rev. C, 58,* 3696–3710.

Meyer B. S., Clayton D. D., and The L.-S. (2000) Molybdenum and zirconium isotopes from a supernova neutron burst. *Astrophys. J. Lett., 540,* L49–L52.

Meyer B. S., Clayton D. D., The L.-S., and El Eid M. F. (2003) Injection of ^{182}Hf into the early solar nebula (abstract). In *Lunar and Planetary Science XXXIV,* Abstract #2074. Lunar and Planetary Institute, Houston (CD-ROM).

Meyer B. S., The L.-S., and Clayton D. D. (2004) Helium-shell nucleosynthesis and extinct radioactivities (abstract). In *Lunar and Planetary Science XXXV,* Abstract #1908. Lunar and Planetary Institute, Houston (CD-ROM).

Molini-Velsko C., Mayeda T. K., and Clayton R. N. (1986) Isotopic composition of silicon in meteorites. *Geochim. Cosmochim. Acta, 50,* 2719–2726.

Mostefaoui S. and Hoppe P. (2004) Discovery of abundant in situ silicate and spinel grains from red giant stars in a primitive meteorite. *Astrophys. J. Lett., 613,* L149–L152.

Mostefaoui S., Lugmair G. W., Hoppe P., and El Goresy A. (2003) Evidence for live iron-60 in Semarkona and Chervony Kut: A NanoSIMS study (abstract). In *Lunar and Planetary Science XXXI,V* Abstract #1585. Lunar and Planetary Institute, Houston (CD-ROM).

Mostefaoui S., Lugmair G. W., and Hoppe P. (2004a) In-situ evidence for live iron-60 in the solar system: A potential heat source for planetary differentiation from a nearby supernova explosion (abstract). In *Lunar and Planetary Science XXXV,* Abstract #1271. Lunar and Planetary Institute, Houston (CD-ROM).

Mostefaoui S., Marhas K. K., and Hoppe P. (2004b) Discovery of an in-situ presolar silicate grain with GEMS-like composition in the Bishunpur matrix (abstract). In *Lunar and Planetary Science XXXV,* Abstract #1593. Lunar and Planetary Institute, Houston (CD-ROM).

Mostefaoui S., Lugmair G. W., and Hoppe P. (2005) Iron-60: A heat source for planetary differentiation from a nearby supernova explosion. *Astrophys. J., 625,* 271–277.

Mowlavi N. and Meynet G. (2000) Aluminum 26 production in asymptotic giant branch stars. *Astron. Astrophys., 361,* 959–976.

Münker C., Weyer S., Mezger K., Rehkämper M., Wombacher F., and Bischoff A. (2000) ^{92}Nb-^{92}Zr and the early differentiation history of planetary bodies. *Science, 289,* 1538–1542.

Murty S. V. S. and Marti K. (1994) Nitrogen isotopic signatures in Cape York: Implications for formation of Group IIIA irons. *Geochim. Cosmochim. Acta, 58,* 1841–1848.

Murty S. V. S., Goswami J. N., and Shukolyukov Y. A. (1997) Excess ^{36}Ar in the Efremovka meteorite: A strong hint for the presence of ^{36}Cl in the early solar system. *Astrophys. J. Lett., 475,* L65–L68.

Nagashima K., Krot A. N., and Yurimoto H. (2004) Stardust silicates from primitive meteorites. *Nature, 428,* 921–924.

Nguyen A. N. and Zinner E. (2004) Discovery of ancient silicate stardust in a meteorite. *Science, 303,* 1496–1499.

Nguyen A., Zinner E., and Lewis R. S. (2003) Identification of small presolar spinel and corundum grains by isotopic raster imaging. *Publ. Astron. Soc. Australia, 20,* 382–388.

Nichols R. H. Jr. (2006) Chronological constraints on planetesimal accretion. In *Meteorites and the Early Solar System II* (D. S. Lauretta and H. Y. McSween Jr., eds.), this volume. Univ. of Arizona, Tucson.

Nichols R. H. Jr., Kehm K., and Hohenberg C. M. (1995) Microanalytic laser extraction of noble gases: Techniques and applications. In *Advances in Analytic Geochemistry, Vol. 2* (M. Hyman and M. Rowe, eds.), pp. 119–140. JAI, Greenwich, Connecticut.

Nichols R. H. Jr., Podosek F. A., Meyer B. S., and Jennings C. L. (1999) Collateral consequences of the inhomogeneous distribution of short-lived radionuclides in the solar nebula. *Meteoritics & Planet. Sci., 34,* 869–884.

Nichols R. H. Jr., Brannon J. C., and Podosek F. A. (2002) Excess 135-barium from live 135-cesium in Orgueil chemical separates (abstract). In *Lunar and Planetary Science XXXIII,* Abstract #1929. Lunar and Planetary Institute, Houston (CD-ROM).

Nicolussi G. K., Davis A. M., Pellin M. J., Lewis R. S., Clayton R. N., and Amari S. (1997) s-process zirconium in presolar silicon carbide grains. *Science, 277,* 1281–1283.

Nicolussi G. K., Pellin M. J., Lewis R. S., Davis A. M., Amari S., and Clayton R. N. (1998a) Molybdenum isotopic composition of individual presolar silicon carbide grains from the Murchison meteorite. *Geochim. Cosmochim. Acta, 62,* 1093–1104.

Nicolussi G. K., Pellin M. J., Lewis R. S., Davis A. M., Clayton R. N., and Amari S. (1998b) Strontium isotopic composition in individual circumstellar silicon carbide grains: A record of s-process nucleosynthesis. *Phys. Rev. Lett., 81,* 3583–3586.

Nicolussi G. K., Pellin M. J., Lewis R. S., Davis A. M., Clayton R. N., and Amari S. (1998c) Zirconium and molybdenum in individual circumstellar graphite grains: New isotopic data on the nucleosynthesis of heavy elements. *Astrophys. J., 504,* 492–499.

Niederer F. R. and Papanastassiou D. A. (1984) Ca isotopes in refractory inclusions. *Geochim. Cosmochim. Acta, 48,* 1279–1293.

Niederer F. R., Papanastassiou D. A., and Wasserburg G. J. (1980) Endemic isotopic anomalies in titanium. *Astrophys. J. Lett., 240,* L73–L77.

Niederer F. R., Papanastassiou D. A., and Wasserburg G. J. (1981) The isotopic composition of Ti in the Allende and Leoville meteorites. *Geochim. Cosmochim. Acta, 45,* 1017–1031.

Niederer F. R., Papanastassiou D. A., and Wasserburg G. J. (1985) Absolute isotopic abundances of Ti in meteorites. *Geochim. Cosmochim. Acta., 49,* 835–851.

Nielsen S. G., Rehkämper M., and Halliday A. N. (2004) First evidence of live ^{205}Pb in the early solar system. *Geochim. Cosmochim. Acta, 68,* A727.

Niemeyer S. and Lugmair G. W. (1981) Ubiquitous isotopic anomalies in Ti from normal Allende inclusions. *Earth Planet. Sci. Lett., 53,* 211–225.

Niemeyer S. and Lugmair G. W. (1984) Titanium isotopic anomalies in meteorites. *Geochim. Cosmochim. Acta, 48,* 1401–1416.

Nittler L. R. (2003) Presolar stardust in meteorites: Recent advances and scientific frontiers. *Earth Planet. Sci. Lett., 209,* 259–273.

Nittler L. R. (2005) Constraints on heterogeneous galactic chemical evolution from meteoritic stardust. *Astrophys. J., 618,* 281–296.

Nittler L. R. and Alexander C. M. O'D. (1999) Automatic identification of presolar Al- and Ti-rich oxide grains from ordinary chondrites (abstract). In *Lunar and Planetary Science XXX*, Abstract #2041. Lunar and Planetary Institute, Houston (CD-ROM).

Nittler L. R. and Alexander C. M. O'D. (2003) Automated isotopic measurements of micron-sized dust: Application to meteoritic presolar silicon carbide. *Geochim. Cosmochim. Acta, 67,* 4961–4980.

Nittler L. R. and Dauphas N. (2006) Meteorites and the chemical evolution of the Milky Way. In *Meteorites and the Early Solar System II* (D. S. Lauretta and H. Y. McSween Jr., eds.), this volume. Univ. of Arizona, Tucson.

Nittler L. R. and Hoppe P. (2004a) High initial ^{26}Al/^{27}Al ratios in presolar SiC grains from novae (abstract). *Meteoritics & Planet. Sci., 39,* A78.

Nittler L. R. and Hoppe P. (2004b) New presolar silicon carbide grains with nova isotope signatures (abstract). In *Lunar and Planetary Science XXXV,* Abstract #1598. Lunar and Planetary Institute, Houston (CD-ROM).

Nittler L. R., Alexander C. M. O'D., Gao X., Walker R. M., and Zinner E. K. (1994) Interstellar oxide grains from the Tieschitz ordinary chondrite. *Nature, 370,* 443–446.

Nittler L. R., Hoppe P., Alexander C. M. O'D., Amari S., Eberhardt P., Gao X., Lewis R. S., Strebel R., Walker R. M., and Zinner E. (1995) Silicon nitride from supernovae. *Astrophys. J. Lett., 453,* L25–L28.

Nittler L. R., Amari S., Zinner E., Woosley S. E., and Lewis R. S. (1996) Extinct ^{44}Ti in presolar graphite and SiC: Proof of a supernova origin. *Astrophys. J. Lett., 462,* L31–L34.

Nittler L. R., Alexander C. M. O'D., Gao X., Walker R. M., and Zinner E. (1997) Stellar sapphires: The properties and origins of presolar Al_2O_3 in meteorites. *Astrophys. J., 483,* 475–495.

Nittler L. R., Alexander C. M. O'D., Wang J., and Gao X. (1998) Meteoritic oxide grain from supernova found. *Nature, 393,* 222.

Nittler L. R., Hoppe P., Alexander C. M. O'D., Busso M., Gallino R., Marhas K. K., and Nollett K. (2003) Magnesium isotopes in presolar spinel (abstract). In *Lunar and Planetary Science XXXIV,* Abstract #1703. Lunar and Planetary Institute, Houston (CD-ROM).

Nittler L. R., Alexander C. M. O'D., Stadermann F. J., and Zinner E. K. (2005) Presolar Al-, Ca-, and Ti-rich oxide grains in the Krymka meteorite (abstract). In *Lunar and Planetary Science XXXVI,* Abstract #2200. Lunar and Planetary Institute, Houston (CD-ROM).

Nollett K. M., Busso M., and Wasserburg G. J. (2003) Cool bottom processes on the thermally pulsing asymptotic giant branch and the isotopic composition of circumstellar dust grains.

Astrophys. J., 582, 1036–1058.

Nuth J. A. III, Charnley S. B., and Johnson N. M. (2006) Chemical processes in the interstellar medium: Source of the gas and dust in the primitive solar nebula. In *Meteorites and the Early Solar System II* (D. S. Lauretta and H. Y. McSween Jr., eds.), this volume. Univ. of Arizona, Tucson.

Nyquist L. E., Bansal B., Wiesmann H., and Shih C.-Y. (1994) Neodymium, strontium and chromium isotopic studies of the LEW86010 and Angra dos Reis meteorites and the chronology of the angrite parent body. *Meteoritics, 29,* 872–885.

Nyquist L., Lindstrom D., Mittlefehldt D., Shih C.-Y., Wiesmann H., Wentworth S., and Martinez R. (2001) Manganese-chromium formation intervals for chondrules from the Bishunpur and Chainpur meteorites. *Meteoritics & Planet. Sci., 36,* 911–938.

Ott U. (1993) Interstellar grains in meteorites. *Nature, 364,* 25–33.

Ott U. (1996) Interstellar diamond xenon and timescales of supernova ejecta. *Astrophys. J., 463,* 344–348.

Ott U. and Begemann F. (1990) Discovery of s-process barium in the Murchison meteorite. *Astrophys. J. Lett., 353,* L57–L60.

Ott U. and Begemann F. (2000) Spallation recoil and age of presolar grains in meteorites. *Meteoritics & Planet. Sci., 35,* 53–63.

Owen T., Mahaffy P. R., Niemann H. B., Atreya S., and Wong M. (2001) Protosolar nitrogen. *Astrophys. J. Lett., 553,* L77–L79.

Palme H. (2000) Are there chemical gradients in the inner solar system? In *From Dust to Terrestrial Planets 9* (W. Benz et al., eds.), pp. 237–262. Kluwer, Dordrecht.

Papanastassiou D. A. (1986) Cr isotopic anomalies in the Allende meteorite. *Astrophys. J. Lett., 308,* L27–L30.

Papanastassiou D. A. and Brigham C. A. (1989) The identification of meteorite inclusions with isotope anomalies. *Astrophys. J. Lett., 338,* L37–L40.

Papanastassiou D. A. and Wasserburg G. J. (1978) Strontium isotopic anomalies in the Allenda meteorite. *Geophys. Res. Lett., 5,* 595–598.

Papanastassiou D. A., Chen J. H., and Wasserburg G. J. (2004) More on Ru endemic isotope anomalies in meteorites (abstract). In *Lunar and Planetary Science XXXV,* Abstract #1828. Lunar and Planetary Institute, Houston (CD-ROM).

Pellin M. J., Davis A. M., Lewis R. S., Amari S., and Clayton R. N. (1999) Molybdenum isotopic composition of single silicon carbide grains from supernovae (abstract). In *Lunar and Planetary Science XXX*, Abstract #1969. Lunar and Planetary Institute, Houston (CD-ROM).

Pellin M. J., Calaway W. F., Davis A. M., Lewis R. S., Amari S., and Clayton R. N. (2000a) Toward complete isotopic analysis of individual presolar silicon carbide grains: C, N, Si, Sr, Zr, Mo, and Ba in single grains of type X (abstract). In *Lunar and Planetary Science XXXI,* Abstract #1917. Lunar and Planetary Institute, Houston (CD-ROM).

Pellin M. J., Davis A. M., Calaway W. F., Lewis R. S., Clayton R. N., and Amari S. (2000b) Zr and Mo isotopic constraints on the origin of unusual types of presolar SiC grains (abstract). In *Lunar and Planetary Science XXXI,* Abstract #1934. Lunar and Planetary Institute, Houston (CD-ROM).

Perlmutter S., Aldering G., Goldhaber G., Knop R. A., Nugent P., Castro P. G., Deustua S., Fabbro S., Goobar A., Groom D. E., Hook I. M., Kim A. G., Kim M. Y., Lee J. C., Nunes N. J., Pain R., Pennypacker C. R., Quimby R., Lidman C., Ellis R. S., Irwin M., McMahon R. G., Ruiz-Lapuente P., Walton N., Schaefer B., Boyle B. J., Filippenko A. V., Matheson T., Fruchter A. S., Panagia N., Newbert H. J. M., and Couch W. J. (1999) Measurements of Ω and Λ from 42 high-redshift supernovae. *Astrophys. J., 517,* 565–586.

Phillips M. (2003) Stellar candles for the extragalactic distance scale. In *Lecture Notes in Physics, Vol. 635* (D. Alloin and W. Gieren, eds.), pp. 175–185. Springer-Verlag, Berlin.

Plewa T., Calder A. C., and Lamb D. Q. (2004) Type Ia supernova explosion: Gravitationally confined detonation. *Astrophys. J. Lett., 612,* L37–L40.

Podosek F. and Nichols R. (1997) Short-lived radionuclides in the solar nebula. In *Astrophysical Implications of the Laboratory Study of Presolar Materials* (T. Bernatowicz and E. Zinner, eds.), pp. 617–648. American Institute of Physics, New York.

Podosek F. A., Ott U., Brannon J. C., Neal C. R., Bernatowicz T. J., Swan P., and Mahan S. E. (1997) Thoroughly anomalous chromium in Orgueil. *Meteoritics & Planet. Sci., 32,* 617–627.

Podosek F. A., Nichols R. H. Jr., Brannon J. C., Meyer B. S., Ott U., Jennings C. L., and Luo N. (1999) Potassium, stardust, and the last supernova. *Geochim. Cosmochim. Acta, 63,* 2351–2362.

Podosek F. A., Prombo C. A., Amari S., and Lewis R. S. (2004) s-process Sr isotopic compositions in presolar SiC from the Murchsion meteorite. *Astrophys. J., 605,* 960–965.

Preibisch T. (1999) The history of low-mass star formation in the upper Scorpius OB association. *Astronom. J., 117,* 2381–2397.

Prombo C. A., Podosek F. A., Amari S., and Lewis R. S. (1993) s-process Ba isotopic compositions in presolar SiC from the Murchison meteorite. *Astrophys. J., 410,* 393–399.

Qian Y.-Z. and Wasserburg G. J. (2000) Stellar abundances in the early galaxy and two r-process components. *Phys. Rept., 333-334,* 77–108.

Qian Y.-Z. and Wasserburg G. J. (2003) Stellar sources for heavy r-process nuclei. *Astrophys. J., 588,* 1099–1109.

Qian Y.-Z. and Woosley S. E. (1996) Nucleosynthesis in neutrino-driven winds from protoneutron stars II. The r-process. *Astrophys. J., 471,* 331–351.

Qian Y.-Z., Vogel P., and Wasserburg G. J. (1998) Diverse supernova sources for the r-process. *Astrophys. J., 494,* 285–296.

Rauscher T., Heger A., Hoffman R. D., and Woosley S. E. (2002) Nucleosynthesis in massive stars with improved nuclear and stellar physics. *Astrophys. J., 576,* 323–348.

Rayet M., Arnould M., Hashimoto M., Prantzos N., and Nomoto K. (1995) The p-process in Type II supernovae. *Astron. Astrophys., 298,* 517–527.

Reynolds J. H. (1960a) Determination of the age of the elements. *Phys. Rev. Lett., 4,* 8–10.

Reynolds J. H. (1960b) Isotopic composition of primordial xenon. *Phys. Rev. Lett., 4,* 351–354.

Richter S., Ott U., and Begemann F. (1993) s-process isotope abundance anomalies in meteoritic silicon carbide: New data. In *Nuclei in the Cosmos 2* (F. Käppeler and K. Wisshak, eds.), pp. 127–132. Institute of Physics, Bristol and Philadelphia.

Richter S., Ott U., and Begemann F. (1994) s-process isotope abundance anomalies in meteoritic silicon carbide: Data for Dy. In *Proceedings of the European Workshop on Heavy Element Nucleosynthesis* (E. Somorjai and Z. Fülöp, eds.), pp. 44–46. Hungarian Academy of Sciences, Debrecen.

Richter S., Ott U., and Begemann F. (1997) Tellurium-H in interstellar diamonds (abstract). In *Lunar and Planetary Science XXVIII,* pp. 1163–1164. Lunar and Planetary Institute, Houston.

Richter S., Ott U., and Begemann F. (1998) Tellurium in pre-solar

diamonds as an indicator for rapid separation of supernova ejecta. *Nature, 391,* 261–263.

Riess A. G., Flippenko A. V., Challis P., Clocchiatti A., Diercks A., Garnavich P. M., Gilliland R. L., Hogan C. J., Jha S., Kirshner R. P., Leibundgut B., Phillips M. M., Reiss D., Schmidt B. P., Schommer R. A., Smith R. C., Spyromilio J., Stubbs C., Suntzeff N. B., and Tonry J. (1998) Observational evidence from supernovae for an accelerating universe and a cosmological constant. *Astron. J., 116,* 1009–1038.

Robert F. (2006) The solar system deuterium/hydrogen ratio. In *Meteorites and the Early Solar System II* (D. S. Lauretta and H. Y. McSween Jr., eds.), this volume. Univ. of Arizona, Tucson.

Rotaru M., Birck J. L., and Allègre C. J. (1992) Clues to early solar system history from chromium isotopes in carbonaceous chondrites. *Nature, 358,* 465–470.

Rowe M. W. and Kuroda P. K. (1965) Fissiogenic xenon from the Pasamonte meteorite. *J. Geophys. Res., 70,* 709–714.

Russell S. S., Arden J. W., and Pillinger C. T. (1991) Evidence for multiple sources of diamond from primitive chondrites. *Science, 254,* 1188–1191.

Russell S. S., Arden J. W., and Pillinger C. T. (1996) A carbon and nitrogen isotope study of diamond from primitive chondrites. *Meteoritics & Planet. Sci., 31,* 343–355.

Russell S. S., Ott U., Alexander C. M. O'D., Zinner E. K., Arden J. W., and Pillinger C. T. (1997) Presolar silicon carbide from the Indarch (EH4) meteorite: Comparison with silicon carbide populations from other meteorite classes. *Meteoritics & Planet. Sci., 32,* 719–732.

Russell S. S., Zhu X., Guo Y., Belshaw N., Gounelle M., Mullane E., and Coles B. (2003) Copper isotope systematics in CR, CH-like, and CB meteorites: A preliminary study (abstract). *Meteoritics & Planet. Sci., 38,* A124.

Russell S. S., Hartmann L., Cuzzi J., Krot A. N., Gounelle M., and Weidenschilling S. (2006) Timescales of the solar protoplanetary disk. In *Meteorites and the Early Solar System II* (D. S. Lauretta and H. Y. McSween Jr., eds.), this volume. Univ. of Arizona, Tucson.

Sahijpal S., Goswami J. N., and Davis A. M. (2000) K, Mg, Ti, and Ca isotopic compositions and refractory trace element abundances in hibonites from CM and CV meteorites: Implications for early solar system processes. *Geochim. Cosmochim. Acta., 64,* 1989–2005.

Sanloup C., Blichert-Toft J., Télouk P., Gillet P., and Albarède F. (2000) Zr isotope anomalies in chondrites and the presence of ^{92}Nb in the early solar system. *Earth Planet. Sci. Lett., 184,* 75–81.

Savina M. R., Davis A. M., Tripa C. E., Pellin M. J., Clayton R. N., Lewis R. S., Amari S., Gallino R., and Lugaro M. (2003a) Barium isotopes in individual presolar silicon carbide grains from the Murchison meteorite. *Geochim. Cosmochim. Acta, 67,* 3201–3214.

Savina M. R., Pellin M. J., Tripa C. E., Veryovkin I. V., Calaway W. F., and Davis A. M. (2003b) Analyzing individual presolar grains with CHARISMA. *Geochim. Cosmochim. Acta, 67,* 3215–3225.

Savina M. R., Tripa C. E., Pellin M. J., Davis A. M., Clayton R. N., Lewis R. S., and Amari S. (2003c) Isotopic composition of molybdenum and barium in single presolar silicon carbide grains of type A + B (abstract). In *Lunar and Planetary Science XXXIV,* Abstract #2079. Lunar and Planetary Institute, Houston (CD-ROM).

Savina M. R., Davis A. M., Tripa C. E., Pellin M. J., Gallino R., Lewis R. S., and Amari S. (2004a) Extinct technetium in presolar silicon carbide grains. *Science, 303,* 649–652.

Savina M. R., Pellin M. J., Tripa C. E., Davis A. M., Lewis R. S., and Amari S. (2004b) Excess p-process molybdenum and ruthenium in a presolar SiC grain. *Nuclei in the Cosmos VIII,* Abstract #C160. TRIUMF, Vancouver.

Schönbächler M., Rehkämper M., Halliday A. N., Lee D.-C., Bourot-Denise M., Zanda B., Hattendorf B., and Günther D. (2002) Niobium-zirconium chronometry and early solar system development. *Science, 295,* 1705–1708.

Schönbächler M., Lee D.-C., Rehkämper M., Halliday A. N., Fehr M. A., Hattendorf B., and Günther D. (2003) Zirconium isotope evidence for incomplete admixing of r-process components in the solar nebula. *Earth Planet. Sci. Lett., 216,* 467–481.

Schramm D. N., Tera F., and Wasserburg G. J. (1970) The isotopic abundance of ^{26}Mg and limits on ^{26}Al in the early solar system. *Earth Planet. Sci. Lett., 10,* 44–59.

Shu F. H., Shang H., and Lee T. (1996) Toward an astrophysical theory of chondrites. *Science, 271,* 1545–1552.

Shu F. H., Shang H., Gounelle M., Glassgold A. E., and Lee T. (2001) The origin of chondrules and refractory inclusions in chondritic meteorites. *Astrophys. J., 548,* 1029–1050.

Shukolyukov A. and Lugmair G. W. (1993) Live iron-60 in the early solar system. *Science, 259,* 1138–1142.

Smith V. V. and Lambert D. L. (1990) The chemical composition of red giants. III. Further CNO isotopic and s-process abundances in thermally pulsing asymptotic giant branch stars. *Astrophys. J. Suppl. Ser., 72,* 387–416.

Sneden C., McWilliam A., Preston G. W., Cowan J. J., Burris D. L., and Armosky B. J. (1996) The ultra — metal-poor, neutron-capture — rich giant star CS 22892-052. *Astrophys. J., 467,* 819–840.

Sneden C., Cowan J. J., Lawler J. E., Ivans I. I., Burles S., Beers T. C., Primas F., Hill V., Truran J. W., Fuller G. M., Pfeiffer B., and Kratz K. (2003) The extremely metal-poor, neutron capture-rich star CS 22892-052: A comprehensive abundance analysis. *Astrophys. J., 591,* 936–953.

Speck A. K., Barlow M. J., and Skinner C. J. (1997) The nature of silicon carbide in carbon star outflows. *Mon. Not. R. Astron. Soc., 234,* 79–84.

Srinivasan B. and Anders E. (1978) Noble gases in the Murchison meteorite: Possible relics of s-process nucleosynthesis. *Science, 201,* 51–56.

Srinivasan G., Ulyanov A. A., and Goswami J. N. (1994) ^{41}Ca in the early solar system. *Astrophys. J. Lett., 431,* L67–L70.

Srinivasan G., Sahijpal S., Ulyanov A. A., and Goswami J. N. (1996) Ion microprobe studies of Efremovka CAIs: II. Potassium isotope composition and ^{41}Ca in the early solar system. *Geochim. Cosmochim. Acta, 60,* 1823–1835.

Starrfield S., Truran J. W., Wiescher M. C., and Sparks W. M. (1998) Evolutionary sequences for Nova V1974 Cygni using new nuclear reaction rates and opacities. *Mon. Not. R. Astron. Soc., 296,* 502–522.

Stone J., Hutcheon I. D., Epstein S., and Wasserburg G. J. (1991) Correlated Si isotope anomalies and large ^{13}C enrichments in a family of exotic SiC grains. *Earth Planet. Sci. Lett., 107,* 570–581.

Straniero O., Gallino R., Busso M., Chiefei A., Raiteri C. M., Limongi M., and Salaris M. (1995) Radiative ^{13}C burning in asymptotic giant branch stars and s-processing. *Astrophys. J. Lett., 440,* L85–L87.

Strebel R., Hoppe P., and Eberhardt P. (1996) A circumstellar Al-

and Mg-rich oxide grain from the Orgueil meteorite (abstract). *Meteoritics, 31,* A136.

Stroud R. M., Nittler L. R., and Alexander C. M. O'D. (2004) Polymorphism in presolar Al_2O_3 grains from asymptotic giant branch stars. *Science, 305,* 1455–1457.

Suess H. E. and Urey H. C. (1956) Abundances of the elements. *Rev. Mod. Phys., 28,* 53–74.

Tachibana S. and Huss G. R. (2003a) The initial abundance of ^{60}Fe in the solar system. *Astrophys. J. Lett., 588,* L41–L44.

Tachibana S. and Huss G. R. (2003b) Iron-60 in troilites from an unequilibrated ordinary chondrite and the initial ^{60}Fe/^{56}Fe in the early solar system (abstract). In *Lunar and Planetary Science XXXIV,* Abstract #1737. Lunar and Planetary Institute, Houston (CD-ROM).

Takahashi K., Witti J., and Janka H.-T. (1994) Nucleosynthesis in neutrino-driven winds from protoneutron stars II. The r-process. *Astron. Astrophys., 286,* 857–869.

Tang M. and Anders E. (1988a) Interstellar silicon carbide: How much older than the solar system? *Astrophys. J. Lett., 335,* L31–L34.

Tang M. and Anders E. (1988b) Isotopic anomalies of Ne, Xe, and C in meteorites. II. Interstellar diamond and SiC: Carriers of exotic noble gases. *Geochim. Cosmochim. Acta, 52,* 1235–1244.

The L.-S., El Eid M. F., and Meyer B. S. (2000) A new study of s-process nucleosynthesis in massive stars. *Astrophys. J., 533,* 998–1015.

Thielemann F.-K., Arnould M., and Hillebrandt W. (1979) Meteoritic anomalies and explosive neutron processing of helium-burning shells. *Astron. Astrophys., 74,* 175–185.

Thielemann F.-K., Nomoto K., and Hashimoto M.-A. (1996) Core-collapse supernovae and their ejecta. *Astrophys. J., 460,* 408–436.

Thiemens M. H. and Heidenreich J. E. I. (1983) The mass independent fractionation of oxygen: A novel isotope effect and its possible cosmochemical implications. *Science, 219,* 1073–1075.

Thompson T. A. (2003) Magnetic protoneutron star winds and r-process nucleosynthesis. *Astrophys. J. Lett., 585,* L33–L36.

Thompson T. A., Burrows A., and Meyer B. S. (2001) The physics of proto-neutron star winds: Implications for r-process nucleosynthesis. *Astrophys. J., 562,* 887–908.

Tielens A. G. G. M. (1990) Carbon stardust: From soot to diamonds. In *Carbon in the Galaxy: Studies from Earth and Space* (J. C. Tarter et al., eds.), pp. 59–111. NASA Conference Publication 3061, U.S. Government Printing Office, Washington DC.

Timmes F. X. and Clayton D. D. (1996) Galactic evolution of silicon isotopes: Application to presolar SiC grains from meteorites. *Astrophys. J., 472,* 723–741.

Timmes F. X., Woosley S. E., and Weaver T. A. (1995) Galactic chemical evolution: Hydrogen through zinc. *Astrophys. J. Suppl. Ser., 98,* 617–658.

Timmes F. X., Woosley S. E., Hartmann D. H., and Hoffman R. D. (1996) The production of ^{44}Ti and ^{60}Co in supernovae. *Astrophys. J., 464,* 332–341.

Travaglio C., Gallino R., Amari S., Zinner E., Woosley S., and Lewis R. S. (1999) Low-density graphite grains and mixing in type II supernovae. *Astrophys. J., 510,* 325–354.

Treffers R. and Cohen M. (1974) High-resolution spectra of cold stars in the 10- and 20-micron regions. *Astrophys. J., 188,* 545–552.

Truran J. W., Cowan J. H., and Cameron A. G. W. (1978) The He-driven r-process in supernovae. *Astrophys. J. Lett., 222,* L63–L67.

Umeda H. and Nomoto K. (2003) First generation black-hole forming supernovae and the metal abundance pattern of a very iron-poor star. *Nature, 422,* 871–873.

Urey H. C. (1955) The cosmic abundances of potassium, uranium and thorium and the heat balances of the Earth, the Moon, and Mars. *Proc. Natl. Acad. Sci., 41,* 127–144.

Vanhala H. A. T. and Boss A. P. (2002) Injection of radioactivities into the forming solar system. *Astrophys. J., 575,* 1144–1150.

Verchovsky A. B., Wright I. P., and Pillinger C. T. (2004) Astrophysical significance of asymptotic giant branch stellar wind energies recorded in meteoritic SiC grains. *Astrophys. J., 607,* 611–619.

Virag A., Wopenka B., Amari S., Zinner E., Anders E., and Lewis R. S. (1992) Isotopic, optical, and trace element properties of large single SiC grains from the Murchison meteorite. *Geochim. Cosmochim. Acta, 56,* 1715–1733.

Völkening J. and Papanastassiou D. A. (1989) Iron isotope anomalies. *Astrophys. J. Lett., 347,* L43–L46.

Völkening J. and Papanastassiou D. A. (1990) Zinc isotope anomalies. *Astrophys. J. Lett., 358,* L29–L32.

Wadhwa M., Srinivasan G., and Carlson R. W. (2006) Timescales of planetesimal differentiation in the early solar system. In *Meteorites and the Early Solar System II* (D. S. Lauretta and H. Y. McSween Jr., eds.), this volume. Univ. of Arizona, Tucson.

Wallerstein G., Iben I. Jr., Parker P., Boesgaard A. M., Hale G. M., Champagne A. E., Barnes C. A., Käppeler F., Smith V. V., Hoffman R. D., Timmes F. X., Sneden C., Boyd R. N., Meyer B. S., and Lambert D. L. (1997) Synthesis of the elements in stars: Forty years of progress. *Rev. Mod. Phys., 69,* 995–1084.

Wanajo S., Tamamura M., Itoh N., Nomoto K., Ishimaru Y., Beers T. C., and Nozawa S. (2003) The r-process in supernova explosions from the collapse of O-Ne-Mg cores. *Astrophys. J., 593,* 968–979.

Wannier P. G., Andersson B. G., Olofsson H., Ukita N., and Young K. (1991) Abundances in red giant stars: Nitrogen isotopes in carbon-rich molecular envelopes. *Astrophys. J., 380,* 593–605.

Wasserburg G. J. (1987) Isotopic abundances: Inferences on solar system and planetary evolution. *Earth Planet. Sci. Lett., 86,* 129–173.

Wasserburg G. J. and Arnould M. (1987) A possible relationship between extinct ^{26}Al and ^{53} Mn in meteorites and early solar activity. In *Nuclear Astrophysics, Vol. 287* (W. Hillebrandt et al., eds.), pp. 262–276. Springer-Verlag, Berlin.

Wasserburg G. J., Fowler W. A., and Hoyle F. (1960) Duration of nucleosynthesis. *Phys. Rev. Lett., 4,* 112–114.

Wasserburg G. J., Huneke J. C., and Burnett D. S. (1969) Correlation between fission tracks and fission type xenon in meteoritic whitlockite. *J. Geophys. Res., 74,* 4221–4232.

Wasserburg G. J., Lee T., and Papanastassiou D. A. (1977) Correlated oxygen and magnesium isotopic anomalies in Allende inclusions: II. Magnesium. *Geophys. Res. Lett., 4,* 299–302.

Wasserburg G. J., Busso M., Gallino R., and Raiteri C. M. (1994) Asymptotic giant branch stars as a source of short-lived radioactive nuclei in the solar nebula. *Astrophys. J., 424,* 412–428.

Wasserburg G. J., Boothroyd A. I., and Sackmann I.-J. (1995) Deep circulation in red giant stars: A solution to the carbon and oxygen isotope puzzles? *Astrophys. J. Lett., 447,* L37–L40.

Wasserburg G. J., Busso M., and Gallino R. (1996) Abundances of actinides and short-lived nonactinides in the interstellar medium: Diverse supernova sources for the r-processes. *Astrophys. J. Lett., 466,* L109–L113.

Wasserburg G. J., Gallino R., and Busso M. (1998) A test of the supernova trigger hypothesis with ^{60}Fe and ^{26}Al. *Astrophys. J. Lett., 500,* L189–L193.

Wheeler J. C., Cowan J. J., and Hillebrandt W. (1998) The r-process in collapsing O/Ne/Mg cores. *Astrophys. J. Lett., 493,* L101–L104.

Wisshak K., Voss F., Käppeler F., and Kazakov L. (1997) Neutron capture in neodymium isotopes: Implications for the s-process. *Nucl. Phys., A621,* 270c–273c.

Woolum D. S. (1988) Solar-system abundances and processes of nucleosynthesis. In *Meteorites and the Early Solar System* (J. F. Kerridge and M. S. Matthews. eds.), pp. 995–1020. Univ. of Arizona, Tucson.

Woosley S. E. (1997) Neutron-rich nucleosynthesis in carbon deflagration supernovae. *Astrophys. J., 476,* 801–810.

Woosley S. E. and Baron E. (1992) The collapse of white dwarfs to neutron stars. *Astrophys. J., 391,* 228–235.

Woosley S. E. and Hoffman R. D. (1992) The alpha-process and the r-process. *Astrophys. J., 395,* 202–239.

Woosley S. E. and Howard W. M. (1978) The p-process in supernovae. *Astrophys. J. Suppl. Ser., 36,* 285–304.

Woosley S. E. and Weaver T. A. (1995) The evolution and explosion of massive stars, II. Explosive hydrodynamics and nucleosynthesis. *Astrophys. J. Suppl. Ser., 101,* 181–235.

Woosley S. E., Wilson J. R., Mathews G. J., Hoffman R. D., and Meyer B. S. (1994) The r-process and neutrino-heated supernova ejecta. *Astrophys. J., 433,* 229–246.

Woosley S. E., Heger A., and Weaver T. A. (2002) The evolution and explosion of massive stars. *Rev. Mod. Phys., 74,* 1015–1071.

Yin Q.-Z. and Jacobsen S. B. (2004) On the issue of molybdenum isotopic anomalies in meteorites: Is it still fun? (abstract). In *Lunar and Planetary Science XXXV,* Abstract #1942. Lunar and Planetary Institute, Houston (CD-ROM).

Yin Q. Z., Jacobsen S. B., McDonough W. F., Horn I., Petaev M. I., and Zipfel J. (2000) Supernova sources and the ^{92}Nb-^{92}Zr p-process chronometer. *Astrophys. J. Lett., 536,* L49–L53.

Yin Q., Jacobsen S. B., Blichert-Toft J., Télouk P., and Albarède F. (2001) Nb-Zr and Hf-W isotope systematics: Applications to early solar system chronology and planetary differentiation (abstract). In *Lunar and Planetary Science XXXII,* Abstract #2128. Lunar and Planetary Institute, Houston (CD-ROM).

Yin Q., Jacobsen S. B., and Yamashita K. (2002a) Diverse supernova sources of pre-solar material inferred from molybdenum isotopes in meteorites. *Nature, 415,* 881–883.

Yin Q., Jacobsen S. B., Yamashita K., Blichert-Toft J., Télouk P., and Albarède F. (2002b) A short timescale for terrestrial planet formation from Hf-W chronometry of meteorites. *Nature, 418,* 949–952.

Yoshida T. and Hashimoto M. (2004) Numerical analyses of isotopic ratios of presolar grains from supernovae. *Astrophys. J., 606,* 592–604.

Young E. D., Simon J. I., Galy A., Russell S. S., Tonui E., and Lovera O. (2005) Supracanonical ^{26}Al/^{27}Al and the residence time of CAIs in the solar protoplanetary disk. *Science, 308,* 223–227.

Zinner E. (1998a) Stellar nucleosynthesis and the isotopic composition of presolar grains from primitive meteorites. *Annu. Rev. Earth Planet. Sci., 26,* 147–188.

Zinner E. (1998b) Trends in the study of presolar dust grains from primitive meteorites. *Meteoritics & Planet. Sci., 33,* 549–564.

Zinner E. (2004) Presolar grains. In *Treatise on Geochemistry, Vol. 1: Meteorites, Comets, and Planets* (A. M. Davis, ed.), pp. 17–39. Elsevier, Oxford.

Zinner E. and Göpel C. (2002) Aluminum-26 in H4 chondrites: Implications for its production and its usefulness as a fine-scale chronometer for early-solar system events. *Meteoritics & Planet. Sci., 37,* 1001–1013.

Zinner E. K., Fahey A. J., Goswami J. N., Ireland T. R., and McKeegan K. D. (1986) Large ^{48}Ca anomalies are associated with ^{50}Ti anomalies in Murchison and Murray hibonites. *Astrophys. J. Lett., 311,* L103–L107.

Zinner E., Tang M., and Anders E. (1989) Interstellar SiC in the Murchison and Murray meteorites: Isotopic composition of Ne, Xe, Si, C, and N. *Geochim. Cosmochim. Acta, 53,* 3273–3290.

Zinner E., Amari S., and Lewis R. S. (1991) s-Process Ba, Nd, and Sm in presolar SiC from the Murchison meteorite. *Astrophys. J. Lett., 382,* L47–L50.

Zinner E., Amari S., Gallino R., and Lugaro M. (2001) Evidence for a range of metallicities in the parent stars of presolar SiC grains. *Nucl. Phys., A688,* 102–105.

Zinner E., Amari S., Guinness R., and Jennings C. (2003a) Si isotopic measurements of small SiC and Si_3N_4 grains from the Indarch (EH4) meteorite (abstract). *Meteoritics & Planet. Sci., 38,* A60.

Zinner E., Amari S., Guinness R., Nguyen A., Stadermann F., Walker R. M., and Lewis R. S. (2003b) Presolar spinel grains from the Murray and Murchison carbonaceous chondrites. *Geochim. Cosmochim. Acta, 67,* 5083–5095.

Zinner E., Amari S., Jennings C., Mertz A. F., Nguyen A. N., Nittler L. R., Hoppe P., Gallino R., and Lugaro M. (2005a) Al and Ti isotopic ratios of presolar SiC grains of type Z (abstract). In *Lunar and Planetary Science XXXVI,* Abstract #1691. Lunar and Planetary Institute, Houston (CD-ROM).

Zinner E., Nittler L. R., Hoppe P., Gallino R., Straniero O., and Alexander C. M. O'D. (2005b) Oxygen, magnesium and chromium isotopic ratios of presolar spinel grains. *Geochim. Cosmochim. Acta, 69,* 4149–4165.